MINISTRY OF EDUCATION AND SCIENCE OF UKRAINE

National Aerospace University
“Kharkiv Aviation Institute”

S. Bezuglyi, F. Sirenko, M. Shevchenko

COMPONENTS OF AIRCRAFT POWER PLANT SYSTEMS

Synopsis

Kharkiv “KhAI” 2016

UDC 629.7.036 (075.8)
BBL 31.76я73
В-44

Розглянуто загальні відомості щодо будови агрегатів систем авіаційних силових установок. Наведено основні дані, описано область застосування, принцип роботи цих агрегатів.

Викладено основні відомості про конструкції й розрахунки деяких агрегатів, що застосовуються у системах живлення паливом і мастилом. Висвітліно особливості конструктивного виконання, принципи роботи об'ємних і відцентрових насосів і паливних форсунок.

Для англомовних студентів, які вивчають системи і агрегати авіаційних силових і енергетичних установок.

Reviewers: Candidate of Technical Science A. Litvyak,
Doctor of Technical Science V. Logynov

Bezuglyi, S.
В-44 Components of Aircraft Power Plant Systems [Text]: lect. summary / S. Bezuglyi, F. Sirenko, M. Shevchenko. – Kharkov: National Aerospace University «Kharkov Aviation Institute», 2016. – 104 p.

ISBN 978-966-662-505-5

The synopsis deals with the general information about the construction of aircraft power plant accessories. The synopsis also contains the technical specifications, application range and operation principle of these accessories.

The synopsis addresses the general information about the construction and analysis of the accessories used in the fuel and oil feeding systems. The specific features of construction and operation of centrifugal pumps, displacement pumps and fuel nozzles are considered.

This synopsis will be interesting for the English-speaking students who study the systems and units of aircraft engines and power plants.

Figs. 65. Tables 2. Bibliogr.: 10 names

UDC 629.7.036 (075.8)
BBL 31.76я73

ISBN 978-966-662-505-5

CONTENT

INTRODUCTION

Aircraft power plant is designed to create thrust and power, it consists of an engine, as well as the systems and units that ensure its operation.

Power plant includes fuel, lubricating, fire, deicing systems, as well as cooling, starting, intake and exhaust systems and others. Units of power plant are engine mount, gondola, power plant control system, propeller (for the piston and turboprop engines), and so on. These systems and units are closely linked to each other in an aircraft.

"System" is the definition of great importance. «System» in the course of “Aircraft Power Plants and Accessories” means a set of «mains», which are combined by a common function and ensure the engine operation. The characteristic feature of such system is a type of used energy and its carriers. Correspondingly the system may be hydraulic, gas, electrical and mechanical. Hydraulic systems depending on the type of liquid may be fuel, oil or water. Gas system may be the air, nitrogen, or other.

The main consists of units, pipelines (lines) and fittings (connectors). A unit is a machine, a device, an assembly, a gear and so on. Units are divided into special items as tanks, cylinders, pumps, filters, radiators, coolers, heaters, controlling and monitoring equipment.

Systems in aircraft power plants can be open and closed (circulating) depending on working substance routing. In open loop operation the substance moves from the source to the consumer via supply (suction, feed) line and then leaves the system. In closed systems the working substance moves from the source to the consumer through supply line, and then returns back to the source or is sent to supply line through the scavenge line. Also there are systems where one part of the working substance returns to the source and the other one directs to the supply line.

The closed systems can be:

– single-loop, if the working substance returns to the source;

– double-loop, if the part of the working substance returns to the source and part goes to the supply line;

– short-closed if the working substance does not come back to the source but again is sent to supply line which comes to the consumer.

In aircraft engines a unit is a part of engine that serves for definite aim, for example: oil supply unit, oil-fuel unit, auxiliary power unit. There are a lot of different units in modern aircraft.

Development of aircraft units is on with the development of aircraft engines and aircraft equipment in general.

The units of jet engines had got particular progress. The list, variety of operating principles and designs of jet engine units has significantly increased recently. Units take a great part in ensuring the safe operation of the engine. Under the conditions of high flight velocities, large rotation speed of rotors and rapid processes in GTE a man is not able to monitor the engine parameters

anymore. If the number of units for piston engines increased gradually, then for jet engines they were needed for immediate design of complex automation systems.

Currently, there is a wide range of units, installed in the engines. The basic units of GTE systems are:

1. *In the gas and air system:*

– anti-stall devices (lines and air bleed valves), compressor guide vane governors;

– actuators of adjustable nozzles and diffusers, thrust reversers and cooling the turbine;

– breathers;

– deicing system;

– air intake and exhaust system

2. *Fuel system*:

– high pressure pumps;

– booster pumps;

– sprayers;

– fuel distributors through sprayer pipelines;

– fuel governors (main and afterburning);

– filters.

3. *Lubricating system*:

– pumping and scavenge pumps;

– oil nozzles;

– filters;

– deaerators;

– radiators (fuel-oil and air-oil);

– bypass and relief valves.

4. *Starting system*:

– starters of different types;

– starting fuel pumps, fuel sprayers, sparks.

– electric and hydromechanical control system.

5. *Propeller system* (for turboprop engines):

– hubs of controllable-pitch propellers;

– units of propeller and engine control (controllable-pitch propeller governors; and automatic fuel-control unit);

– feathering and reversing pumps and relays;

– deicers;

– braking device.

6. *Aircraft units*:

– generators (AC and DC with different frequency);

– compressors (for feeding systems with compressed air);

– vacuum-pumps;

– different hydraulic high pressure pumps;
– drivers of constant rotation speed etc.

Besides above mentioned units there is special-purpose equipment like, for example, turbo-coolers (turbo expanders). Turbo-coolers are necessary when the flight velocity is very high (M>>1) for cooling the oil and sometimes fuel with air, for reducing the temperature in the cockpit, for cooling of individual units and engine parts, as well as for cooling aircraft unit compartments.

The ramjet engines and some gas turbine engines use special air and gas turbines for driving fuel pumps and other engine units (TPA (turbine-pump assembly), turbine drives, aircraft power supplies, generators of compressed air and so on). Some aircraft units use autonomous electric drive or turbine drive (when the power consumption is high), for example, pumps of the gearbox, set of scavenge pumps, actuating cylinder for the adjustable nozzle flaps.

Location of unit is chosen according to the characteristic of this unit (for example pumps, especially scavenge are placed at the lowest point of the engine).

In some cases aircraft units cannot be placed on the engine because of their large quantity. Due to their specific purpose they require installation in a specific point of the plane. Some aircraft units are mounted in a special box that is connected to the engine with drive. There is a tendency to drive aircraft units by the electric drivers, especially when the unit works periodically and consumes low power.

When choosing the place for the unit it is necessary to provide free access to it for service inspection and replacement.

In most cases operating units must be blown-off and cooled, when the engine is running, especially during long range flight at high velocities.

Units should meet the following technical requirements:

1. Long-term reliable operation (unit lifetime is usually longer than that of the engine).
2. Small weight and dimensions, which are achieved by a compact design, the use of light alloys, synthetic materials and composites.
3. Tightness of all joints and connections (tightness of hydraulic assemblies ensures their reliability).
4. Ease of mounting and connection to the engine drive.
5. Ease of tuning on the engine and carrying out routine maintenance.

Reliable operation of units prolongs engine life-time.

1 POSITIVE DISPLACEMENT PUMPS

1.1 Pumps used in aircraft power plants

A pump is the most important unit of the aircraft power plant. A pump is a unit that moves fluids (liquids or gases), or sometimes slurries, by mechanical action. It transforms mechanical energy supplied to the pump into the energy of the fluid motion (pressure and velocity of the fluid increase).

Pumps of the aircraft power plants have numerous missions: fuel supply to the combustion chamber, oil supply for lubricating the friction surfaces and for cooling the hot parts, feeding hydraulic devices with the working substance for driving the movable elements of the engine like movable guide vanes, flaps of the adjustable jet nozzle, a reverser and others.

The positive displacement (volumetric) and rotordynamic (dynamic) pumps are widespread in aviation.

Positive displacement pumps. A positive displacement pump makes fluid move by trapping a fixed portion and forcing (displacing) it to the discharge pipe.

Some positive displacement pumps have an expanding cavity on the suction side and a decreasing cavity on the discharge side. The fluid rushes into the pump as the cavity on the suction side expands (because the pressure in the cavity becomes less than that at the suction side) and breaks out of the discharge as the cavity collapses. The volume is constant through each cycle of operation.

The hydraulic resistance of lines and components, that are located after the pump, determines an outlet pressure. Therefore, the positive displacement pump can theoretically output arbitrary high pressure. The pressure that is generated by the positive displacement pump is limited by the durability and the rigidity of the pump parts and seals of its pumping unit.

A positive displacement pumps differ in the mechanism used to move the fluid:

- *Rotary-type* positive displacement pumps: internal gear (Fig. 1.1, b), screw, shuttle block, vane (Fig. 1.1, d), flexible vane or sliding vane (Fig. 1.1, c), circumferential piston, elastic impeller, helical twisted roots (e.g. the Wendelkolben pump) or liquid-ring pumps.
- *Reciprocating-type* positive displacement pumps: plunger (Fig. 1.1, a), piston or diaphragm pumps.

In the **plunger pump,** a reciprocating plunger pushes the fluid. In the **rotation** pump, a rotating assembly makes the fluid move. That is why, the rotation pump of the same dimensions as the plunger pump provides higher capacity.

The **rotation pump** operates without the fluid distribution elements at the inlet and outlet whereas the plunger pump must contain such elements.

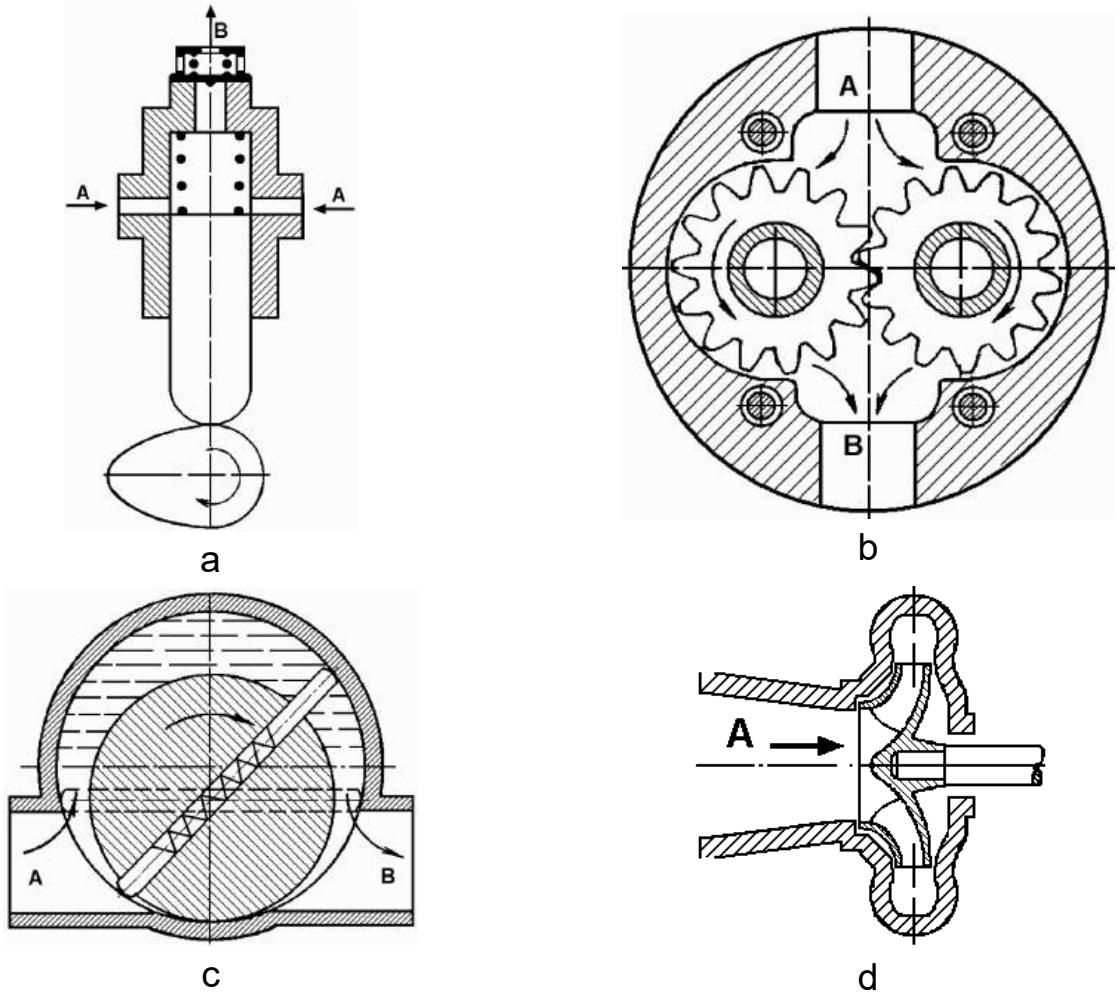

Fig. 1.1 – Pump diagrams:
a – plunger pump; b – gear pump; c – sliding-vane pump; d – centrifugal pump

The **vane pump** (fig. 1.1, d) has a cylindrical rotor encased in a similarly shaped housing. As the rotor is rotating, the vanes trap fluid between the rotor and the casing and draw the fluid through the pump. The pressure head H generated by the vane pump considerably depends on the rotational speed. It is limited by the circumferential velocity of the impeller periphery (Fig. 1.2).

When the volumetric pump operates at the constant rotational speed and its discharge section is variable then it provides theoretically constant volumetric flow rate Q under the variable pressure p (fig. 1.2). Under the same conditions the vane pump operates at the variable pressure and the variable flow rate (fig. 1.3). The advantage of the vane pump is that it can operate at high rotational speed and high circumferential velocity of impeller (>10 m/s) whereas the circumferential velocity of the elements of volumetric pumps cannot exceed 10 m/s.

The cavitation risk limits a rotor circumferential velocity of all pumps, but the vane pump can operate at the higher rotor circumferential velocity than the volumetric pump.

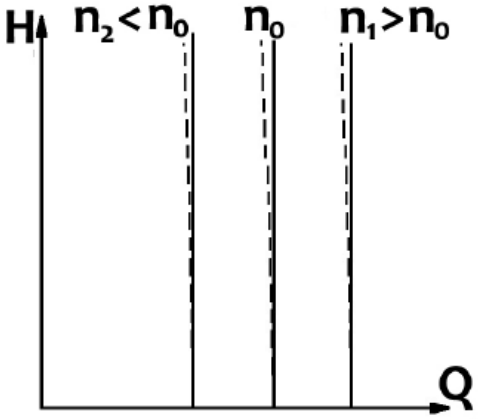

Fig. 1.2 – The pressure head H generated by the volumetric pump depending on volumetric flow rate Q under the different rotational speed

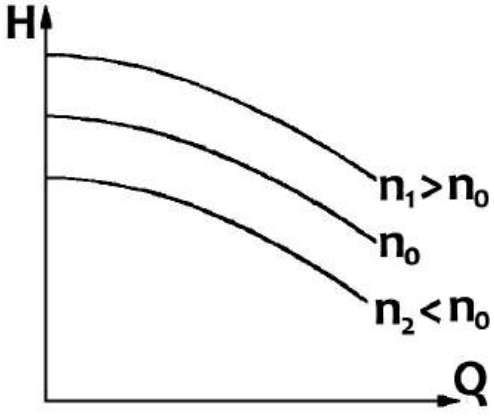

Fig. 1.3 – The pressure head H generated by the vane pump depending on volumetric flow rate Q under the different rotational speed

Opposite to the volumetric pump, the vane one delivers the working substance smoothly, without any pressure fluctuations, which is undoubtedly the advantage of the vane pump.

But the vane pumps have large clearances, therefore they need a priming. Priming the pump means removing all the entrapped air from the suction line and the pump, and filling the same with liquid.

1.2 Main elements of the pump

Casing provides a pressure boundary for the pump and contains channels to direct the suction and discharge flows properly. The pump casing has suction and discharge cavities for the main flow path of the pump and normally has small drain and vent fittings to remove gases trapped in the pump casing or to drain the pump casing for maintenance.

Pumping unit consists of separate pumping elements that consume energy to perform mechanical work by moving the fluid.

Pump drive shaft serves for imparting torque from a power source or prime mover to the pumping unit.

Sealing elements of the pumping unit and the drive shaft reduce internal leakages and isolate the internal pump cavity.

Bypass valve recirculates an excessive fluid back to the pump inlet in case the pump capacity can't be *adjusted*.

The capacity adjuster allows changing the flow rate under the constant rotor speed.

Check valves or *shut-off cocks* prevent fluid backflow in the system through the clearances in the pumping unit of inoperative pump.

1.3 Positive-displacement pump capacity

The capacity and necessary flow uniformity determine the main parameters of pump: the number of pumping elements, their size, and the rotational speed of the pumping unit. The required fluid flow rate Q_c, that is necessary for normal system operation determines the pump capacity.

The rated pump capacity and pressure must be higher than the necessary ones to have a reserve, guaranteeing a reliable pump operation under diverse system failures, at low rotation speed or during the climbing.

For any type of volumetric pump, the ideal (theoretical) capacity is evaluated as

$$Q_{id} = \frac{F \cdot b \cdot z \cdot n}{60}, \text{ m}^3/\text{s},$$

where F - cross-sectional area of each pumping element, m^2;
b - axial size of the pumping element, m;
z - number of pumping elements;
n - rotational speed, rpm.

Ideal capacity can be analytically determined according to the pump geometrical parameters or can be measured by a slow turning of pump (n = 20 - 30 rpm) under the zero pressure drop.

1.4 Displacement pump efficiency

The positive displacement pump of any type has some inner volumetric losses. They result in reduction of the effective pump capacity.

The reduction of the effective capacity Q_p relative to the ideal one occurs because of the internal leakages Q_{leak} over the clearances between the exhaust and inlet cavities and because of the volumetric losses during the suction Q_{in} in case of the cavitation:

$$Q_p = Q_{id} - Q_{leak} - Q_{in}.$$

The volumetric efficiency η_v defines volumetric losses in the pump. The volumetric efficiency is a relation between the effective and ideal capacities:

$$\eta_v = \frac{Q_p}{Q_{id}} = 1 - \frac{Q_{leak}}{Q_{id}} - \frac{Q_{in}}{Q_{id}} = 1 - \delta Q_{leak} - \delta Q_{in}.$$

The volumetric efficiency depends on the pump design and its operational conditions: pumping unit sealing, conditions at the pump inlet, pressure drop, rotational speed and fluid temperature.

The volumetric efficiency cannot get outside the 0 - 1 range. Its magnitude depends on influence of these parameters.

The analysis of the listed above factors influence η_V allowing to make the following conclusions.

1. η_V is greatly affected by the clearances in the pumping unit. Using well-known equation for the fluid flow rate through a narrow (capillary) slot, we get

$$Q_{leak} = \frac{1}{12} \cdot \frac{\Delta p \cdot S^3 \cdot \omega}{\rho \cdot \nu \cdot L},$$

where Δp – pressure drop;

S –slot height;

ω – slot width perpendicularly to the flow direction;

L – slot length in a flow direction;

ρ – flow density;

ν – kinematical viscosity.

Therefore other conditions being equal the leakage considerably depends on the nominal clearance S (the leakage is proportional to S^3). Hence as S grows, so η_V sharply decreases (Fig. 1.4).

2. The fluid leakage is directly proportional to the pressure drop Δp of the pump. Hence η_V linearly decreases with Δp growth (Fig. 1.5).

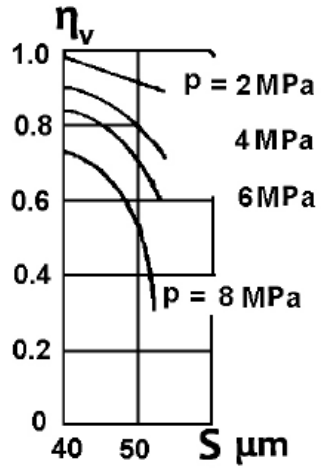

Fig. 1.4 – The volumetric efficiency depending on the clearance

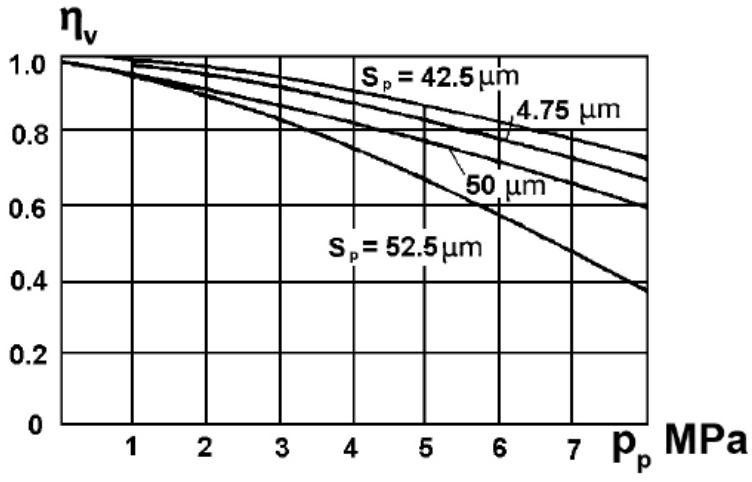

Fig. 1.5 – The volumetric efficiency depending on the pressure drop

3. The rotational speed influences η_v. Let us discuss this effect. During cavitation-free operation the rotational speed is proportional to the volumetric efficiency. It happens because Q_{id} is proportional to the rotational speed n, at the constant leakage rate Δp, ν and ρ. As you already know, the leakages are rotational speed independent. The inlet losses Q_{in} are absent or are so small, that do not affect the capacity.

When rotational speed increases, the losses at the inlet become higher than the leakages over the clearances and η_v falls down.

Thus, the minimal rotational speed is limited by the condition of leak absence, and the maximal rotational speed – by the reliability of filling the working cavities (Fig. 1.6).

4. The fluid temperature influences η_v by means of the fluid viscosity and saturated vapor pressure.

The leakage is inverse to the fluid viscosity, that is why η_v increases when the viscosity increases. However high ν makes a positive effect on η_v so long as the negative influence of this factor on the operating cavities filling does not outweigh a positive effect from the leakage reduction.

Thus, η_v is the highest when the total inner losses are minimal.

According to the considered above, η_v depends on the fluid temperature. In some temperature interval η_v remains within the acceptable limits. If the temperature increases, the volumetric efficiency decreases because of high leakages and cavitation (because of Δp increase). If the temperature decreases, the volumetric efficiency decreases owing to increase a suction line resistance because of under filling of the operating cavities (Fig. 1.7).

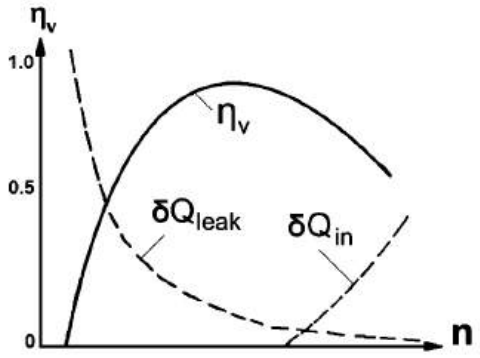

Fig. 1.6 – The volumetric efficiency and losses depending on the rotational speed

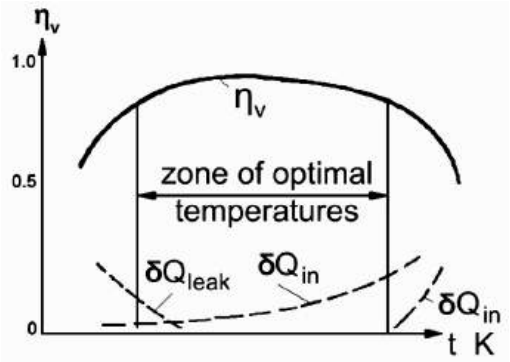

Fig. 1.7 – The volumetric efficiency and losses depending on the temperature

1.5 Power consumption of the pump

The power consumed by any pump is

$$N_c = \frac{\Delta p \cdot Q_p}{\eta_p}, \text{ W},$$

where Δp is a pressure drop, Pa;

Q_p is a pump capacity, m^3/s.

The total pump efficiency η_p is equal to the product of η_v and η_m, which is a mechanical pump efficiency that depends on the pressure drop, the pump design features (clearances in the pumping unit, the conditions of the friction surfaces lubrication etc.). The mechanical efficiency can be evaluated as

$$\eta_m = \frac{\Delta p \cdot Q_p}{\eta_v \cdot N_c} = \frac{\Delta p \cdot Q_{id}}{N_c} = \frac{N_t}{N_c},$$

where N_t is a theoretical power of the pump equal to $N_c - \Delta N_f$, ΔN_f is a friction power. Thus,

$$\eta_m = \frac{N_c - \Delta N_f}{N_c} = 1 - \frac{\Delta N_f}{N_t + \Delta N_f}.$$

As

$$N_t = \Delta p \cdot Q_{id}.$$

so under zero pressure drop, the theoretical power and the mechanical efficiency become also zero. When Δp increases from 0 to some value $\Delta p'$, the mechanical efficiency grows, as the theoretical power of the pump grows faster than the mechanical losses in this range. Outside the considered range the losses grow faster than the power resulting in a η_m drop.

2 GEAR PUMPS

2.1 Structure and operation

At present time, the gear pump is most widespread, because of the following advantages:

1) simple design;
2) small amount of rotating parts and friction pairs;

3) low overall sizes;
4) possibility to increase number of sections and stages in one assembly;
5) high reliability.

The most substantial disadvantage of the gear pump is a gradual increase of the clearances in maintenance due to the pumping unit parts wear out. As a result, the pump capacity turns low.

The pumping unit usually consists of two toothed gears fitted with as small as possible clearances in the special places of the casing. The teeth spaces are in a periodic contact with the inlet (suction) and outlet (exhaust) chambers.

The pump transfers fluid in tooth space from the inlet chamber to the outlet chamber. Next, the working substance is forced out of the space of one gear by the tooth of another one into the exhaust chamber. When the tooth space gets in the contact with the inlet chamber, the teeth disengage, and the fluid rushes into the increasing teeth space again. The cycle repeats.

2.2 The gear pump design

Depending on section number, the pump can be single-section or multi-section. The dimensions and weight of the multi-section pump are less and the drive is simpler at the same capacity.

Depending on stage number, the pump can be single-stage or multi-stage. Each stage of the multistage pump is designed to have the greater capacity than the next one to ensure required head at the inlet of the next stage. The surplus flow at the stage outlet is guided to its inlet through the check valve adjusted to the definite pressure.

The multistage pump is able to increase pressure a lot but the disadvantage is a low total volumetric efficiency.

Depending on a number of gears in a single pumping unit, there are dual-gear (Fig. 2.1) and multiple gear (more often three-gear, Fig. 2.2) pumps. The bearings of a drive gear in such pump are unloaded from the forces of a fluid pressure. The pump is more compact in this case.

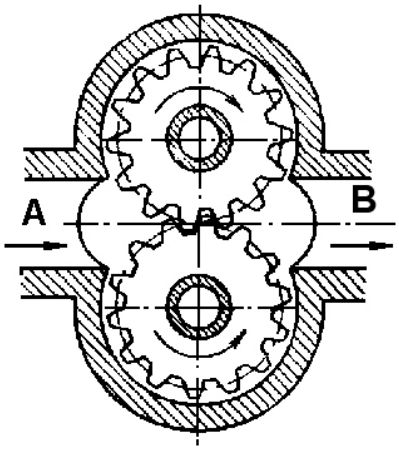

Fig. 2.1 – Dual-gear pump diagram

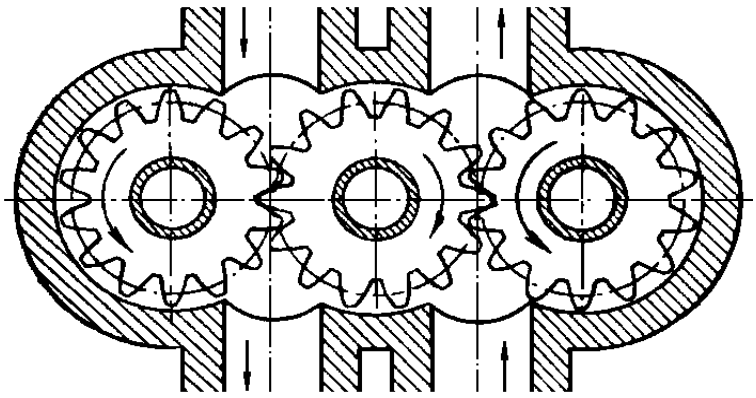

Fig. 2.2 – Three-gear pump diagram

Depending on the tooth shape, there are pumps with spur, helical and herringbone gears.

The problems of pump with the spur gears are related to their production accuracy. If the accuracy is not enough, then the pump makes a lot of noise during operation, the driven gear jerks and wears out intensively, capacity pulsates.

Intermesh and disengagement are two gradual processes in the pumps with helical and herringbone gears. Hence, these pumps operate making much lower noise. They are also not susceptible to pressure fluctuations and choking in the cavities.

The axial force in the helical gearing presses the gears to the casing. This lack is eliminated in herringbone gears, however the latest ones have much complex manufacturing process.

Depending on a gearing, there are the pumps with external gearing which are the most widespread and the pumps with internal gearing (ge-rotor pumps, Fig. 2.3). Internal gear pumps are more compact and more immune to cavitation. The internal gear has 2…3 teeth less than the external gear (see figure 2.3, a). The discharge chamber is separated from the suction chamber by a crescent seal. Besides there are pumps with a special tooth structure which do not have the crescent seal: the internal gear of these pumps has one tooth less than the external one (see figure 2.3, b). The disadvantage of pump with the internal gearing is a high production cost.

Depending on the operational pressure, pump can be:

1) low-pressure pump - up to 2 MPa;
2) mean-pressure pump - from 2 to 10 MPa;
3) high-pressure pump - more than 10 MPa.

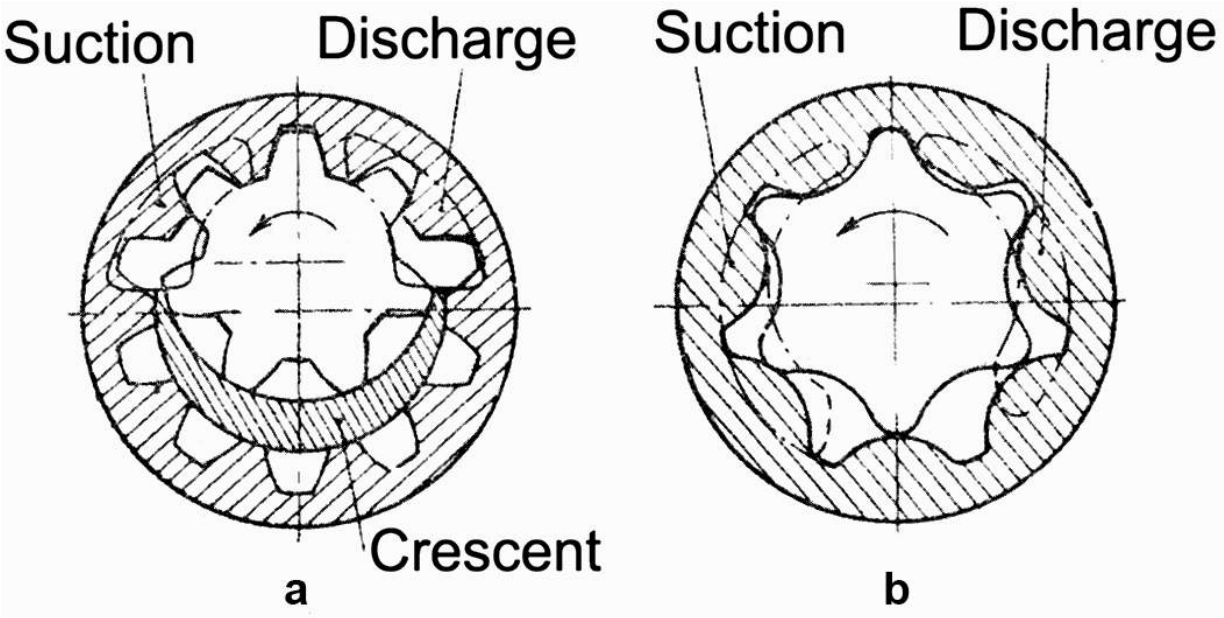

Fig. 2.3 – Internal gear pump

2.3 Pressure head

The main functions of the pump is to provide the required pressure head and the capacity.

The requirement to the head determines a construction and manufacturing method of pump components that have an effect on the leakages. The requirement to the capacity determines the sizes and the rotational speed.

Ceteris paribus, the quality of sealing, durability and rigidity of parts ensure the head.

The fluid leaks from the high pressure chamber to the low pressure chamber over the tip and face clearances between the gears and the casing (Fig. 2.4). If the accuracy of gear manufacturing is high, then the leakage through the profile of meshed teeth can be completely eliminated because the torsion torque provides a tight contact.

It is allowable to consider that the pressure along the tip clearance between inlet and outlet cavities varies approximately linearly (Fig. 2.5). The leakage from outlet to inlet cavity happens under the influence of pressure drop.

The gears rotating opposite to a leakage flow side, prevent fluid flow through a tip clearance. Besides, when the fluid passes through the tip clearance it experiences a set of compressions and expansions in the clearance. As you already know, this reduces the leakage head.

The role of the tip clearance is rather insignificant. Virtually, the tip clearance varies in the range 0.02 to 0.2 mm. The clearance of pumps, which operate under more than 10 MPa pressure drop must be minimal.

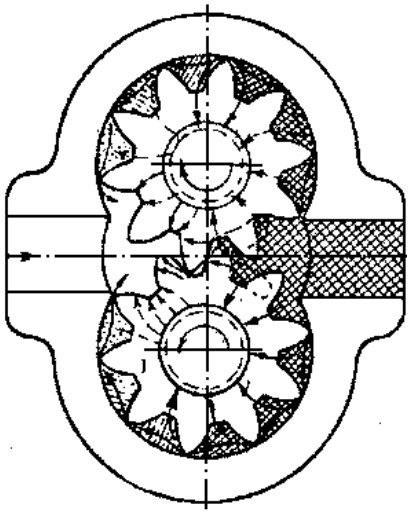

Fig. 2.4 – Leakage direction in the clearances of the gear pump

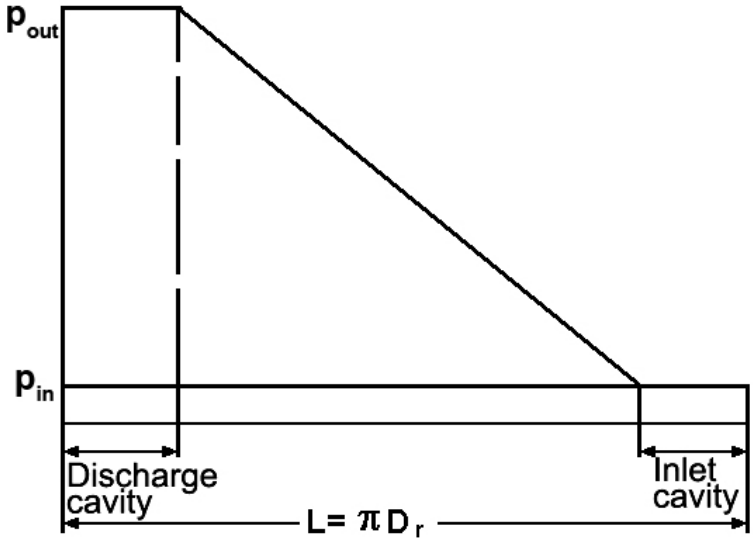

Fig. 2.5 – Pressure variation in a radial clearance in case of concentric gears

The fluid leaks over the face clearance radially from the gear cavity through the bearing to the inlet. The portion of the leakage flows across the

teeth near a gearing pole. In both cases the fluid overcomes only a narrow fillet. The gear rotation does not hinder from the leakages in this case.

The face clearances make more effect on leakages than the tip clearances. Therefore, they are smaller (0.01 - 0.1 mm) and depends on pressure and fluid viscosity.

The leakage through the face clearance is 75 - 95 % of total internal leakage.

The elements of the pump must be manufactured at high accuracy for a stable jamming less pump operation.

Non-parallelism of gear wheel finished faces and the casing planes and their non-perpendicularity rotation axes is not more than 0.01 mm on radius of 50 mm.

To prevent the winding of the case material on gear faces, the case is covered with an antifriction material.

The gear contacts with the shaft through three balls. This design provides a self-adjusting of the gears during operation. It is necessary to compensate the non-perpendicularity between the gear rotational axes and the casing face (Fig. 2.18).

It is obvious that the leakages become less when the pump parts become more rigid. With this purpose the casing is sometimes ribbed, and the covers are made thicker and have the spherical shape. A close fit of the joints is provided with a plenty of coupling bolts. In order to prevent the disjunction because of the high pressure fluid in the clearances, this fluid is drained over the channeling to a suction chamber.

If the output pressure is very high or the pressure is moderate at the low fluid viscosity, then the special face sealing is used. This sealing is a bronze bushing pressed to gear faces by the operational pressure of a pumped fluid. To prevent the bushing warp, it is non-uniformly tighten to the gear. The non-uniformity of tight corresponds to pressure distribution in a face clearance and in operating cavities.

2.4 The pump capacity

A tooth cavity volume, a number of cavities, the rotational speed and the volumetric efficiency determine the capacity of a gear pump.

Each revolution gear pump supplies a fluid volume equal to the volume of all cavities of two gears minus gearing radial clearance volumes, i.e.

$$Q_{id} = 2 \cdot F \cdot b \cdot z \cdot n,$$

where F - cross sectional area of the cavity volume;
z - driving gear teeth number;
b - gear width (a tooth length);
n - driving gear rotational speed, rps.

Generally it is difficult to evaluate F, especially for corrected gears. It's much simpler to express F using an approximate formula, considering that volume of the cavities is equal to the volume of teeth and taking into account that the bottom of the cavity with height $h_{foot} - h_{head}$ is dead space

$$F \cdot z = \pi \cdot D_{in} \cdot \frac{h}{2} = \pi \cdot D_{in} \cdot m,$$

where m - module;

h - height of a tooth operating segment (cavity effective depth);

D_{in} - pitch circle diameter of driving gear.

Thus,

$$Q_{id} = 2 \cdot \pi \cdot D_{in} \cdot m \cdot b \cdot n.$$

In fact cavities are greater than the teeth, therefore the formula above gives a little bit underestimated Q_{id} values $(0.97 - 0.98)Q_{id}$.

If the number of teeth is z = 8…16, then the capacity of such pump can be evaluated by the empirical formula that gives more precise result:

$$Q_{id} = 6{,}5 \cdot D_{in} \cdot m \cdot b \cdot n.$$

The real capacity in the general case is

$$Q_p = K \cdot 2 \cdot \pi \cdot D_{in} \cdot m \cdot b \cdot n \cdot \eta_v,$$

where K is a correction factor which depends on the teeth number, a gearing angle and a tooth formation method. This factor can be considered 1.15 for the approximate analysis.

Let us investigate the way how each parameter influences the capacity. For this, we transform the previous formula considering that $D_{in} = m \cdot z$:

$$Q_p = 2 \cdot \pi \cdot K \cdot \frac{D_{in}^2}{z} \cdot b \cdot n \cdot \eta_v = 2 \cdot \pi \cdot K \cdot m^2 \cdot z \cdot b \cdot n \cdot \eta_v.$$

1. *Influence of* z *on* Q_p.

The greater number of teeth z at constant D_{in}, the lower the Q_p.

The greater number of teeth z at constant Q_p, the more D_{in} proportional to $\sqrt{z}$.

So, the extreme condition, when the pump has the maximum capacity at minimum sizes is reached when the pump has the minimum number of teeth.

The gears with 8 - 16 teeth and m = 2 - 4 mm module are the most widespread.

The gear correction eliminates a tooth root undercut. But it results in tooth tip sharpening that reduces tooth durability and increases the leakages over the radial clearance. To eliminate these undesirable phenomena z is set to provide the width of a tooth cylindrical segment at an outer diameter being more than (0.1 - 0.2) m.

2. *Influence* of b *on* η_V. Other conditions being equal, the gear pump with greater tooth width has the higher Q_{id}, the lower relative leakages and the higher η_V (Fig. 2.6).

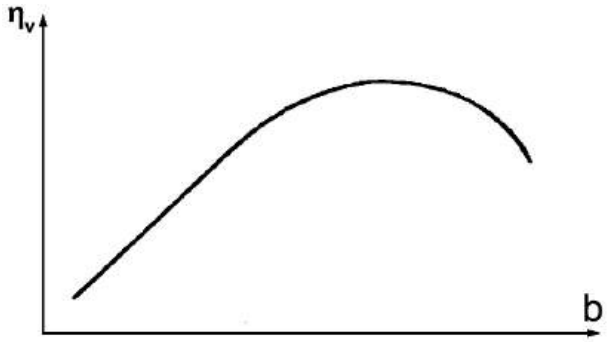

Fig. 2.6 – η_V vs b

Really, if the face clearance is constant then the leakages over it are width independent and the radial leakages grow proportionally to the width. As the absolute radial leakage is much less than the face one, so the total leakage grows much slower than the gear width. Hence, Q_p grows proportionally to the width making η_V grow.

In fact, b is limited by the production considerations. It is hard to manufacture a wide tooth making contact along the entire length. Therefore most of the developed high-pressure pumps have the $\frac{b}{D_{in}}$ ratio being within the range 0.4 - 0.6. The condition of proportionality relating the width of the gear with its module is in use more often for pump development:

$$b = c \cdot m,$$

where c = 4 - 10 is a proportionality factor, which is limited by manufacturing considerations.

3. *Influence of* n *on* Q_p reveals itself in η_v change. Q_{id} grows proportionally to n.

The η_v of any positive displacement pump (including gear pump) grows when the rotational speed goes up. This phenomenon is caused by lower relative leakages ΔQ_{leak} at high speeds. (see Fig. 1.6). But this remains true only up to definite rotational speed.

When the rotational speed breaks some critical value the η_v drastically falls because of the intense suction losses. When the slot passes the inlet chamber at too high speed, and the pressure in the cavity is insufficient, then the slot cannot be filled entirely with the viscous fluid. Besides, it is obvious that rotational speed affects the centrifugal force acting the fluid. At high rotational speeds the centrifugal force forces the fluid out of the tooth slots.

To estimate an influence of the centrifugal force let us consider a balance of an elementary volume of the fluid in a rotating cavity.

The volume is limited by two cylindrical surfaces with radiuses r, $r + dr$ and by two meridional planes. An angle between the planes is $d\varphi$. An element width is equal to unity (Fig. 2.7).

The element is affected by:

– centrifugal force applied to the center of gravity

$$r \cdot \omega^2 \cdot dm = r \cdot \rho \cdot \omega^2 \cdot dr \cdot r \cdot d\varphi;$$

– pressure forces of the fluid acting the element boundaries:

a) on inner face $p \cdot r \cdot d\varphi$;

b) on external face $\left(p + dp\right) \cdot \left(r + dr\right) \cdot d\varphi$;

c) on side face $\left(p + \frac{dp}{2}\right) \cdot dr$.

Summing up the projections of all considered forces on an element symmetry axis and truncating the values of second-order smallness, we get:

$$dp = \rho \cdot r \cdot \omega^2 \cdot dr,$$

whence after the integration (Fig. 2.8)

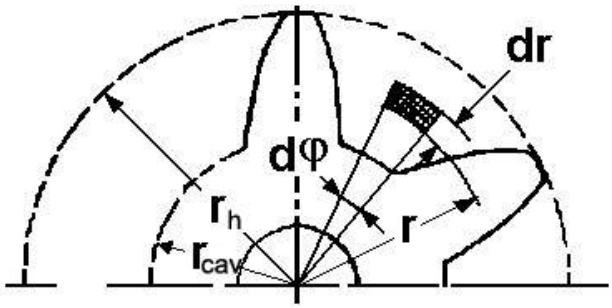

Fig. 2.7 – The design scheme for fluid centrifugal forces determination

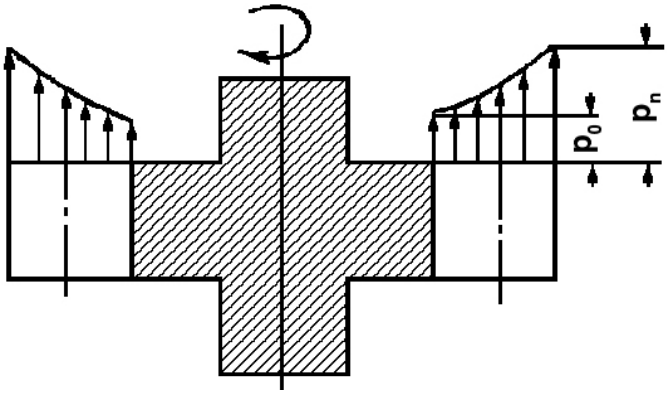

Fig. 2.8 – Pressure generated by the centrifugal forces vs radius

$$p = p_0 + \frac{\rho}{2} \cdot \left(r^2 - r_{cav}^2 \right) \cdot \omega^2,$$

where p - current pressure along a cavity height;

p_0 - pressure at the root of the slot;

r - current radius;

r_{cav} - circle radius of cavity bedplate (bottom);

ρ - density;

ω - angular velocity.

Pressure at a pump inlet:

$$p_{in} \geq p_{0_{min}} + \frac{\rho}{2} \cdot \left(r_h^2 - r_{cav}^2 \right) \cdot \omega^2,$$

where $p_{0_{min}}$ is the minimum pressure in the inlet cavity that provides cavitation free operation;

r_h - circle radius of teeth tips (heads).

In general, the minimal cavitation-free pressure is a vapor pressure at the constant temperature plus some pressure reserve

$$p_{0_{min}} = p_t(t) + \Delta p_{cav.min}.$$

The minimal cavitation-free pressure of the aviation oils is $p_{0_{min}} = 0.04$ MPa.

If we know $p_{0_{min}}$ and p_{in} we can find the maximum rotational speed from $p_{in} = p_h$ condition:

$$\omega_{max} \le \sqrt{\frac{2}{\rho} \cdot \frac{p_{in} - p_{0\,min}}{r_h^2 - r_{cav}^2}}.$$

The angular speed of rotors in modern gear pumps is set to limit the circumferential velocity of the gear tip u_h (less than 10 m/s). The typical values are 6…8 m/s (for pumps without pressure head at the inlet).

The circumferential velocity of the gear tip can be assumed equal to the circumferential velocity on the gear pitch circle u_{in}.

If n breaks the limit, then some part of a tooth slot is filled with the fluid vapor. Hence, Q_p diminishes causing an emulsification and enlarged wear out of the pump parts.

Pump drives are designed with the great gear ratio to ensure the n variation within the allowable range. Usually $n_{max} = 2000 - 4000$ rpm. The reliability of filling the tooth slot also depends on other factors:

– an inlet chamber size;
– the shape and size of channels feeding the slots;
– presence of dissolved air and gases in the fluid;
– dead space in a tooth slot.

To eliminate the losses at the inlet more than the quarter of the gear circumference must be drowned to the inlet cavity. The fluid is fed to slots along the full gear width and also from the face of teeth root.

The gear chamber from the exhaust side is slotted with 0.5 - 0.6 mm width, 10 - 12 mm length grooves to reduce the hydraulic shock that is a result of incomplete cavity filling.

The most effective method to prevent the cavitation in the cavities is to pressurize the inlet. It is perspective to use centrifugal-gear pumps where fluid gets to the cavities being forced by the centrifugal forces. Such pumps can operate at high rotational speed without any booster pump.

2.5 Fundamentals of gear pump analysis

The initial equation for gear pump construction analysis is an equation of the ideal capacity:

$$Q_{id} = 2 \cdot \pi \cdot K \cdot D_{in} \cdot m \cdot b \cdot n = 2 \cdot \pi \cdot K \cdot m^2 \cdot z \cdot b \cdot n.$$

If we express gear rotational speed in terms of given velocity $u_{in} = \pi \cdot D_{in} \cdot n$ and target value of a pitch diameter $D_{in} = m \cdot z$, and also use the proportionality equation $b = c \cdot m$, then we deduce an expression for the gearing module:

$$m = \sqrt{\frac{Q_{id}}{2 \cdot K \cdot c \cdot u_{in}}}.$$

The obtained fractional module must be rounded to the closest standard module. Afterwards we set the teeth number and find the rotational speed and the gear width .

To check the ideal capacity we put the obtained and chosen values K, m, z, b and n to the considered above equation. The values must be corrected until the desired Q_{id} is obtained.

2.6 Forces acting on the gear pump supports

Forces that act on the pump bearings are (Fig. 2.9):

– side force acting on a gear P_s (the force appears due to the pressure drop between the outlet and inlet pressure);

– reaction P_M (the reaction appears because of a torsion torque applied to the gear);

– pressure forces between the meshed gears (the force appears due to the fluid compression) etc.

If we assume that the pressure in a radial clearance changes linearly (Fig. 2.10) (that is fair only when $z \to \infty$) and the length of the inlet and the exhaust cavities is the same, then

$$P_s = a \cdot \Delta p \cdot D_{in} \cdot b,$$

where a is a proportionality factor, which depends on the length of the inlet and the exhaust cavities. So, the extreme case is when each cavity occupies 1/2 of circle. The value of a in the extreme case is equal to unity (if 1/4 then a = 0.818; if 1/6 then a = 0.71; if 1/8 then a = 0.65).

The force P_s is perpendicular to the line that connects the centers of gears.

If we know the power consumed by the pump and its sizes we can find the reaction P_M. The reaction P_M depends on the torque, gear diameter, position of a meshing point (or gear rotation angle). The gear angle and friction of sliding teeth determine the direction of the reaction. The nominal reaction is accepted for the analysis.

After summing up P_s and P_M, we can conclude that P_Σ is less for the driving gear than for the driven one, hence the driving gear bearing is less loaded than driven gear bearing.

The total force acting on the bearing of the normal size is usually 0.9 P_s – for driving gear and 1.1 P_s – for driven gear, i.e. approximately 20% more.

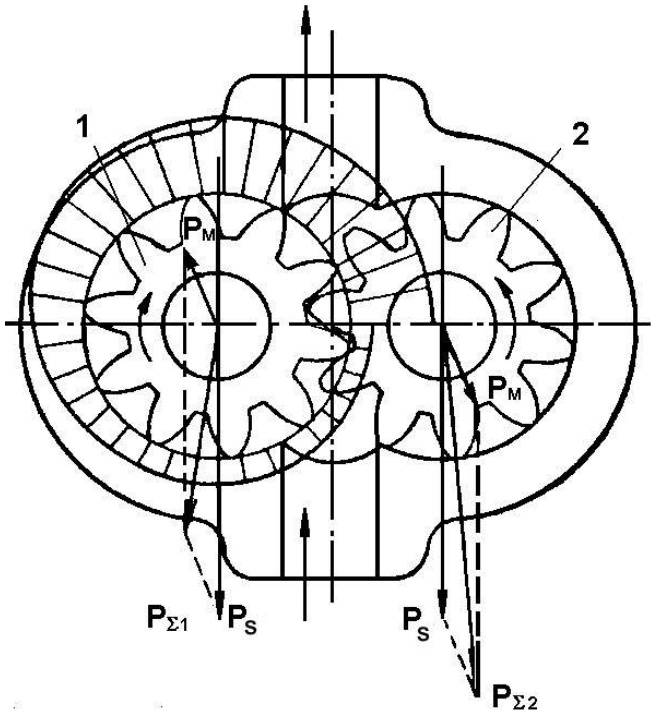

Fig. 2.9 – Forces acting on the bearings:
1 – driving gear; 2 – driven gear

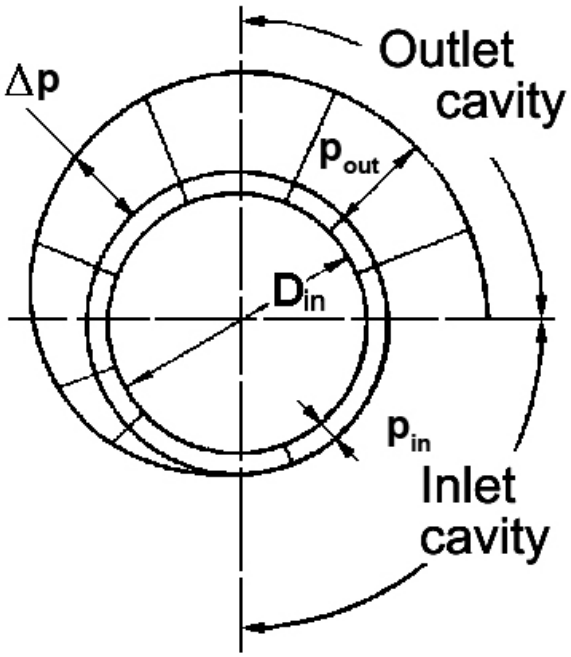

Fig. 2.10 – Pressure distribution in the radial clearance (the inlet and discharge cavities angular length is 45°)

It is obvious that the bearing of the driven gear must be more powerful to keep the bearings equally loaded. In case of sliding bearings, to keep the bearings equally loaded, the bearing of the driven gear must be of greater length or diameter. Both gear bearings are often similar for the sake of manufacturability.

As the gear side pressure basically determines forces acting on the bearing, so it is necessary to reduce the length of the exhaust chamber, the gear diameter and the width when designing a high-pressure pump. However, you must always keep in mind the gearbox with short gears has an extremely low volumetric efficiency.

Taking into account the pressure forces between the meshed gears and the pressure pulsations, the evaluated value of force for the driving gear in predesign:

$$P_{d_1} = P_s .$$

For the driven gear

$$P_{d_2} = P_s + P_M \text{ or } P_{d_2} = 1.2 P_s.$$

The sliding bearings of low-pressure pumps are designed using the specific load acting on the bearings:

$$K = \frac{P_d}{d_b \, L_b},$$

where d_b is the diameter of a bearing journal;

L_b is the length of a bearing support surface.

The acceptable specific load for tin-and-leaden bronze bearings for oil pumps must be less than 8 - 10 MPa, for fuel pumps – less than 2 - 2.5 MPa. At the same time the circumferential velocity of the journal must not exceed 5 m/s. If the specific load is out of the specified range then the designer must increase the bearing size or apply hydraulic unloading of the supports, or to use the rolling bearings.

The hydraulic unloading is a process when the pressure is delivered to the chamber located diametrically opposite to the outlet cavity. Choosing dimensions of the channel and the chamber it is possible to unload bearings up to the acceptable limits (Fig. 2.11). But in this case volumetric efficiency is less.

The rolling bearings and especially needle bearings are widespread in aircraft pumps. It is a very hard task to produce many needles of the similar size. That is why the needles must be selectively assembled to meet the following requirements:

– the difference of the diametrical size must not exceed 0.002 mm;

– the total circumferential clearance between needles in the assembled bearing must be within the range 0.2 to 0.4 mm;

– the total axial clearance between needles in the assembled bearing must be within the range 0.2 to 0.4 mm.

The shafts must have the rigidity enough to provide the sag less than the radial clearance between gears and the gear chamber. If the rigidity is not enough then the normal gearing condition is violated resulting in the case scores.

When calculating a driving shaft for torsion it is necessary to remember that the pressure fluctuations result in a significant bursts of the acting load.

Therefore, drives of gears should be 20 - 25% more durable than the analytically determined average torsion torque.

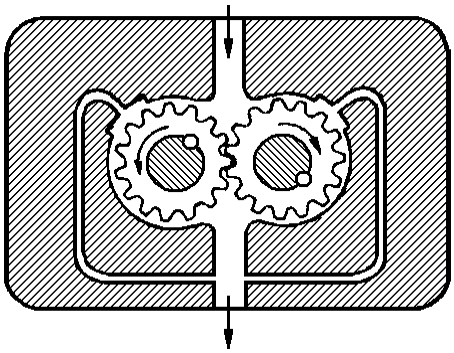

Fig. 2.11 – Hydraulic unloading by the fluid pressure

2.7 Design of gear pumps and materials

As the gear ratio exceeds unity, some fluid can be blocked in the cavities between the meshed teeth causing the high fluid pressure. This causes the additional force acting on the bearings and fluid heating.

Fluid compression in tooth slots appears due to the clearanceless closure of one or several slots. Especially, when the tooth enters the cavity during rotation, it closely contacts with the opposite gear in two points c and d (Fig. 2.12, a), some fluid is blocked in the considered volume. Gear turning makes the cavity diminish, thereby compressing the fluid inside.

Fig. 2.12, a shows that the least closed volume corresponds to a position when the tooth is relatively symmetric to a center line.

The smaller tooth thickness eliminates the contact in point c and prevents fluid from being blocked in the meshed teeth cavity. Thinner teeth provide the clearance s everywhere along the normal line to a profile (Fig. 2.12, b).

However, when the contact ratio exceeds unity, close contact of the second pair of gearing teeth generates the cavity with the blocked fluid. The cavity is greater, so the problem is not as urgent as in the previous case. The locked cavity is formed by the closed contact of two geared teeth pairs in points e and f (Fig. 2.12, c).

It consists of two slots formed by the geared teeth of driving and driven gears and connected by the gap s. When the gear rotates as it is shown in the figure, the bottom part of this cavity decreases and the top one – increases. It is obvious, that if total volume of closed cavity does not change then the fluid stays uncompressed. Actually the closed cavity varies achieving the minimal volume when the mechanical center of the closed area coincides with a centerline (Fig. 2.12, d).

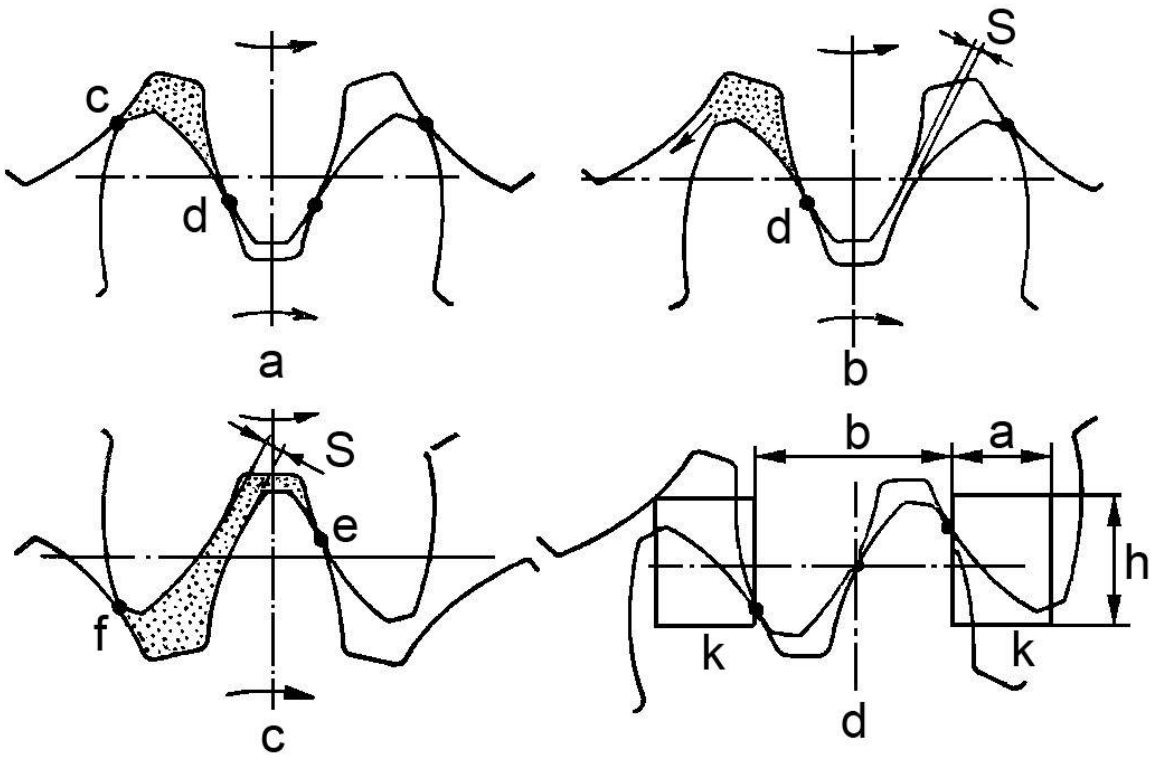

Fig. 2.12 – The fluid blockage in the gear cavities

Special sewer grooves *k* are milled in face covers. They serve to escape the blocked fluid from the cavities.

The positions of the sewer grooves must be chosen to meet the following requirements:

– when the cavity diminishes, it must be interconnected to the outlet zone;

– when the cavity grows, it must be interconnected to the suction zone (this prevents the cavitation);

– the grooves must be distant enough to prevent the contact between the sewer grooves through the tooth cavity.

All mentioned requirements are met when the partition value b between the grooves k is equal or close to the circular pitch, i. e.

$$b = \frac{\pi \cdot D_{in}}{z} = \pi \cdot m .$$

The examples of the unloading grooves in gear cavities are in Fig. 2.13.

The grooves for the fluid blockage prevention are arranged at the exhaust part of the pump. The similar grooves are on the inlet side to prevent the discharge from a cavity volume.

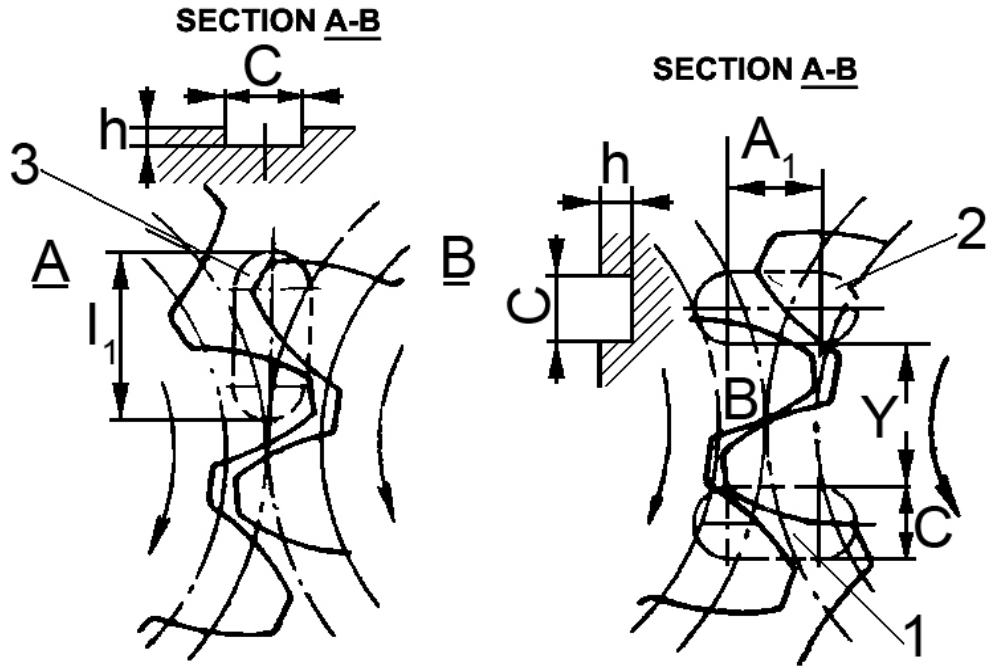

Fig. 2.13 – The drainage of the blocked fluid through the sewer grooves :
1 - inlet chamber; 2 and 3 - exhaust chamber,
s is the distance between gear axes

In case of identical gears, the distance between gear axes is equal to a pitch diameter. The characteristic dimensions from the Fig. 2.13 are determined by the semi-empirical relations.

$$h \approx 0.5m; \quad c \approx (1-1.2)m; \quad l_1 = (1.5-2)m;$$

$$l = 2.95m\sqrt{1-0.88\frac{m^2z^2}{s^2}}; \quad y = 2.78\frac{m^2z}{s}.$$

Fig. 2.14 shows less effective and rarely used draining ways of gear cavities.

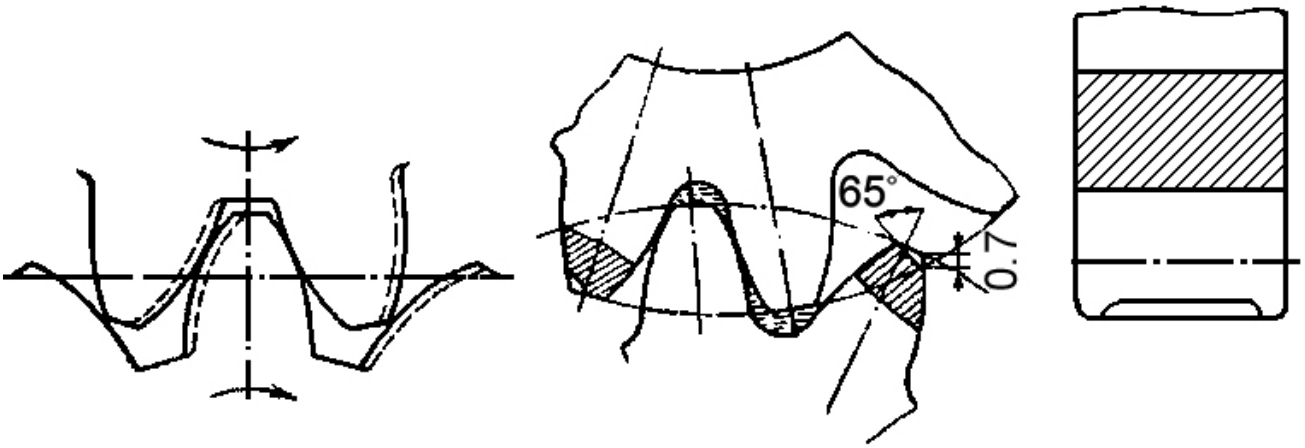

Fig. 2.14 – The closed cavity is drained through grooves at the tip of the teeth (to the right) and grooves along the teeth (to the left) on the dwell track of teeth

Gear and shaft can be manufactured separately or as a single piece. In the first case the design and manufacturing becomes simpler. In the second case the treatment of the mounting surfaces and gear faces (both gears for one pass) becomes simpler.

The gear mounting on the shafts can be carried out using key (Fig. 2.15, 2.16), pins (Fig. 2.17) and balls (Fig. 2.18). Key transfers the large torque. The pins fit the narrow gears the best, and the balls provide a gear self-adjustment.

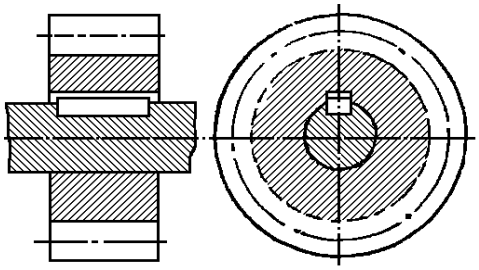

Fig. 2.15 – Key joint of the gear with the shaft

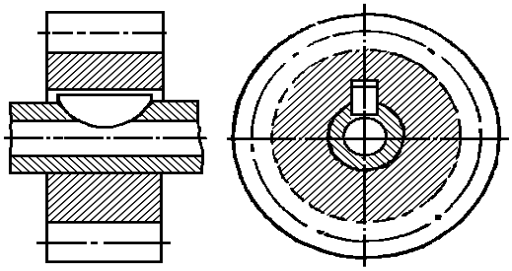

Fig. 2.16 – The semicircular key joint of the gear with the shaft

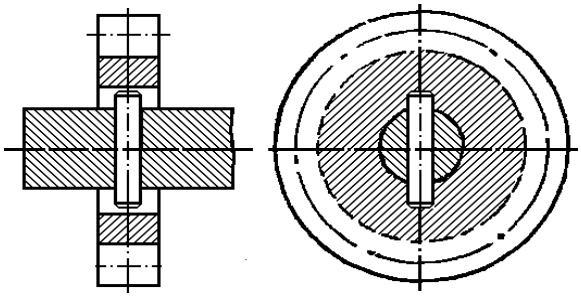

Fig. 2.17 – Pin joint of the gear with the shaft

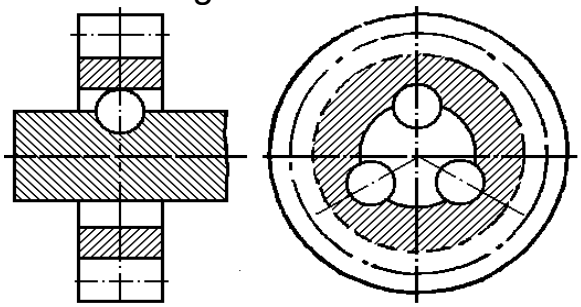

Fig. 2.18 – Ball joint of the gear with the shaft

Gear are manufactured of the alloyed steel (12ХН3А, 18ХНВА, 38ХМШ).

The teeth and faces are polished. Faces are sometimes grounded in. Sometimes gears are made of bronze and austenitic steels (i.e. from materials with increased linear expansion factor) in order to prevent the large variation of clearances generally in case of manufacturing gear chamber from light-metal alloys. The shafts are made of the alloyed cemented and nitrated steels. The axles are made of alloyed steels and also of a cast-iron, a bronze or a duralumin.

Gear chambers are usually made of light-metal alloys - aluminium or magnesium (Мл-2, Мл-5, Ал-5, Ал-9). Sometimes the cast iron is used to reduce the clearances between the heated parts.

Sliding bearings are used in low-pressure pumps. Bushings of the bearings are made of bronze. The steel shafts are able to operate right in the bored surfaces of gear chambers made of aluminum alloys.

Rolling bearings (needle, roller and ball) are used in the high-pressure pumps.

3 PISTON PUMP

3.1 Structure and operation

The piston pumps are applied in high-pressure systems, for example, a fuel system of an engine or a hydraulic system of an airplane.

The specific features of the piston pump are the high leak tightness of a pumping unit and the high stiffness of its components. Hence, piston pump is capable of building up the high pressure.

The piston pump is of a simple structure. Nevertheless, its construction makes the capacity control at the steady drive shaft speed possible.

But, it has its own weak points along with the mentioned advantages, which are

- more complex structure over against the other positive displacement pumps;
- great overall dimensions and mass;
- high production cost;
- plentiful positive suction head (0.15 - 0.35 MPa);
- fine working substance filtration.

The pumping unit consists of a cylinder barrel with pistons reciprocating in cylinders. The cylinders have ports at the ends, which are in a permanent contact with the port plate, which alternately interconnects the cylinders with an inlet manifold and an outlet manifold.

When the piston travels from a top dead center (TDC) to a bottom dead center, the working substance rushes into the cylinder from the inlet port. During the return travel, the piston pushes the working substance out of the cylinder to the outlet manifold.

Depending on a piston arrangement, the piston pumps can be distinguished into an axial-piston pump, an inline piston pump, a radial piston pump, a bent-axis pump.

The pistons in an ***axial piston pump*** (Fig. 3.1, a) reciprocate parallel to the centerline of the drive shaft of the cylinder barrel. That is, rotary shaft motion is converted into axial reciprocating motion. Most axial piston pumps are multi-piston and use check valves or port plates to direct liquid flow from inlet to discharge. The axial piston pumps became abundant in an aircraft star-shape direct injection reciprocating engine field, a gas turbine engine pump-governors field and an aircraft hydraulic system field.

The simplest type of the axial piston pump is the swashplate design (***the inline piston pump***) in which a cylinder barrel is turned by the drive shaft. The pistons fitted to the cylinders in the cylinder barrel are connected through piston shoes and a retracting ring, so that the shoes bear against an angled swashplate. As the barrel turns, the piston shoes follow the swashplate, causing the pistons to reciprocate.

The inline piston pumps found their wide use in the reciprocating engine field.

The ***bent-axis pump*** (Fig. 3.1, b) consists of a drive shaft which rotates the pistons, a cylinder block, and a stationary valving surface facing the cylinder barrel, which ports the inlet and outlet flow. The drive shaft axis is angular in relation to the cylinder block axis. Rotation of the drive shaft causes rotation of the pistons and the cylinder barrel.

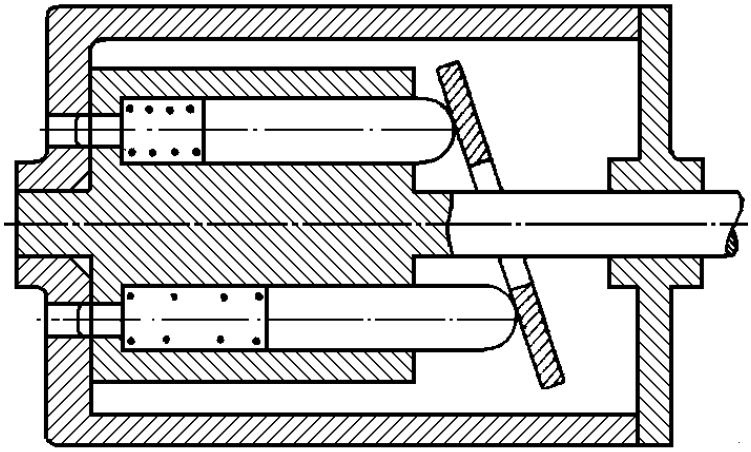

a

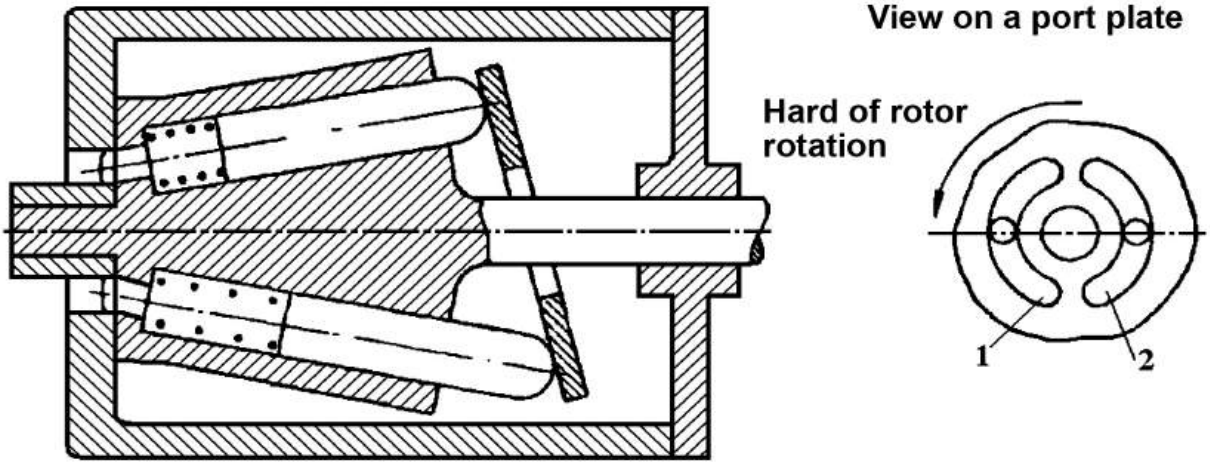

b

Fig. 3.1 – Piston pump

Because the plane of rotation of the pistons is at an angle to the valving surface plane, the distance between any one of the pistons and the valving surface continually changes during rotation. Each individual piston moves away from the valving surface during one-half of the shaft revolution and toward the valving surface during the other half.

In ***radial-piston pumps***, the pistons are arranged radially in a cylinder barrel; they move perpendicularly to the shaft centerline. Two basic types are available: one uses cylindrically shaped pistons, the other ball pistons. They may also be classified according to the porting arrangement: check valve or pintle valve. They are available in fixed and variable displacement, and variable

reversible (over-center) displacement. The radial-piston pumps are used in an aircraft hydraulic system field.

The permanent contact between the piston and the control element at suction stroke is provided by a spring.

The piston pumps may come in ***fixed*** and ***variable displacement*** configurations.

The piston pump capacity can be controlled by

– turning the piston with skewed ends in the axial piston pump and in radial-piston pumps with a cam plate;

– varying the displacement (the radial piston pump has the special reaction ring to increase or decrease piston travel, varying eccentricity);

– varying a swash plate angle (this control method is typical for the axial piston pump).

In the first case the piston travel changes at constant piston stroke, in latest two cases the stroke changes.

The pistons of the axial or inline piston pump have the shorter, but more uniform by phase angle, stroke. The centrifugal forces of the piston mass do not press the cylinder barrel to the port plate in this case. Hence, the spring or the springs must be much stiffer. The mass and the overall sizes of the piston pump increase.

The pistons of the piston pump, which travel trajectory is not parallel to the cylinder barrel axis, has greater, but less uniform by phase angle, stroke. The centrifugal forces of the piston mass press the cylinder barrel to the port plate in this case. Hence, the spring or the springs can be less stiff. The overall sizes of the barrel from the port plate side decrease leading to mass reduction. The production becomes much complex and more expensive.

The latest described pump is widely used in aircraft gas turbine power plants.

Depending on the drive method, the piston pumps divide themselves into the piston pumps with the rotating or immovable cylinder barrel.

The piston pump with the immovable cylinder barrel contain the rotating port valve, which complicates the capacity control. The pump itself becomes more complex (Fig. 3.2).

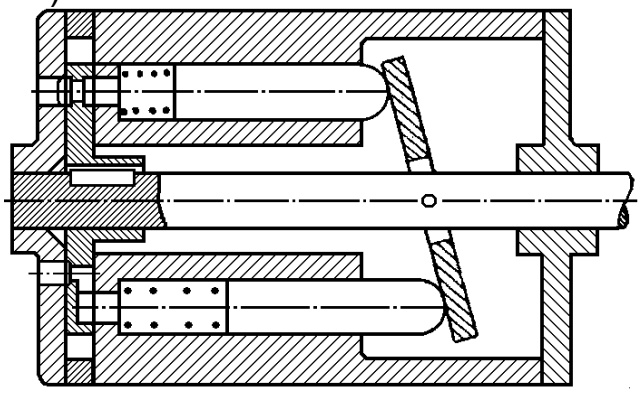

Fig. 3.2 – The scheme of the axial piston pump with the rotating swash plate and port plate

The control of the swash plate angle is much easier in the pump with the rotating cylinder barrel and the fixed port plate. However, the operation of the cylinder barrel and the pistons is much hampered because of inertia.

That is why, the pumps of the first group are usually constant capacity pumps. The pumps of the second group are controlled capacity.

Depending of the working substance distribution, the pumps divide themselves into pumps with the port plate (mean pressure pumps) or the valve plate (high pressure pumps). The latest piston pumps are more leakproof.

Let us consider some aspects of the piston pump operation. We will mostly address the pumps with the swash plate the rotating cylinder barrel, because they are widely used in the gas turbine power plants.

3.2 Output pressure

The piston pump generates the highest pressure among all positive displacement pumps. The high pressure is provided because the pumping unit is well sealed, and the parts are strong and stiff enough.

The fluid leaks from the cylinder cavity to the low pressure cavities over the side clearance between the cylinder wall and the side surface of the cylinder and through the clearance between the cylinder barrel and the port plate.

On one hand, the engineers design the piston pump to provide the minimum clearances in the pumping unit, one the other hand, the clearances must be great enough to avoid jamming and intense wear out of the friction pairs.

For the above considered reasons the piston pump must meet the stringent requirements to the production accuracy (geometrical sizes), quality of the working surfaces and appropriate materials for the friction pairs.

The main requirements are ovality and circular parallelism. They must not exceed 0.001…0.003 mm.

The piston is loosely fitted in the cylinder (the clearance is 0.005 - 0.020 mm). The clearance is very small, so to meet this requirement each piston is individually selected for the cylinder (selective assembling).

Obviously, the parts in the pair are not interchangeable.

The roughness of the cylinder and piston side surfaces must be Ra 0.32 - Ra 0.04, i. e. the arithmetic average distance between the peaks and the valleys must not exceed 0.5 - 1 μm. Sometimes, inner walls of the cylinders have the ring grooves (Fig. 3.3). They improve the operational conditions of the piston pair. The grove spreads the leaking fluid round the piston and averages the pressure acting the piston from each side. The piston eccentricity decreases, the friction losses and the leakages over the side clearance become lower. The eccentric position of the piston in the cylinder two and a half times enlarges the

leakages. Besides, the solid particles are accumulated in the grooves reducing the friction and piston (cylinder) wear out.

To make the leakages in the clearance between the cylinder barrel and the port plate lower, the wedging of the face surfaces and their misalignment to axis of rotation must not exceed the 0.005 - 0.010 mm. The nonflatness must not exceed 0.005 mm.

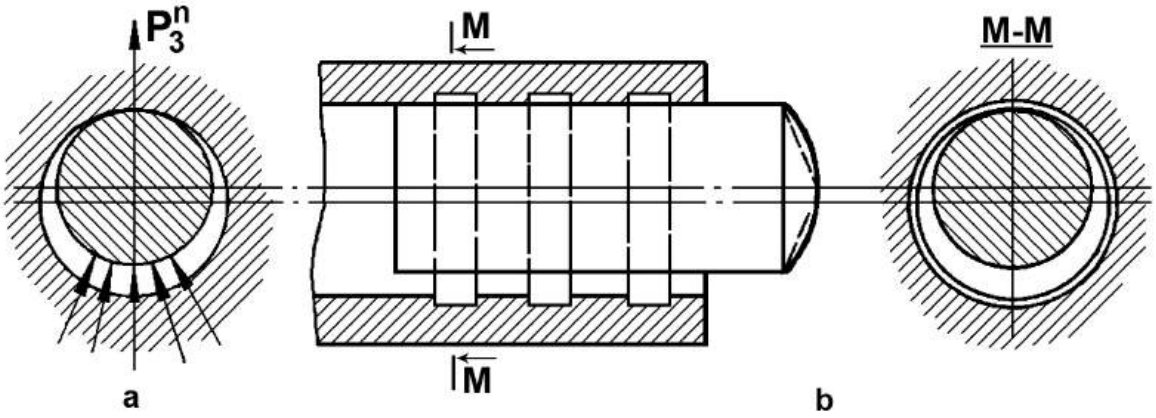

Fig. 3.3 – The unbalanced fluid pressure in the eccentric clearance between the piston and the cylinder

The amount of the working substance leaking through the face clearance depends on the force pressing the cylinder barrel to the port plate. The cylinder barrel is pressed (P_{pr} pressing force) jointly by the spring force and the pressure in the cylinder. The pressure acts the shoulder, which is an area formed by the difference between the cylinder diameter and the orifice diameter.

The barrel is not in a direct contact with the port plate. There is a thin film of the working substance there. The pressure of the film and the output pressure act the face of the cylinder barrel to force back the barrel from the port plate. The force-back force P_{fb} acts only on the part limited by the port in the port plate and orifices in the barrel.

The force-back force increases when the output pressure increases or the rotational speed goes up.

The piston pump, which pistons are not parallel to the cylinder barrel axis has the less stiff springs. So it need the higher pressure in the swashplate cavity to provide the reliable contact between the port plate and the barrel. The working substance is supplied to the cavity through the small channels between the cylinders of the barrel.

The balance of the pressing force and the force-back force is characterized with a tightness ratio:

$$K_T = \frac{P_{pr}}{P_{fb}}.$$

3.3 Kinematics of the axial piston pump with a flat swash plate

Let`s suppose that the contact point between the piston and the swash plate belongs to the piston axis at any swash plate angle and any angular position of the rotor (as if piston ends with a spike, see Fig. 3.4). These assumptions are made to calculate a stroke, a velocity and an acceleration.

The piston upstroke (when piston travels from the bottom dead center) is calculated as

$$s = R\left(1 - cos\,\alpha\right)\ tg\gamma,$$

where α is the angular position of the rotor.

The maximum piston stroke corresponds to 180° position of the rotor. It can be calculated as

$$s_{max} = 2Rtg\gamma.$$

The maximum piston stroke determines the capacity.

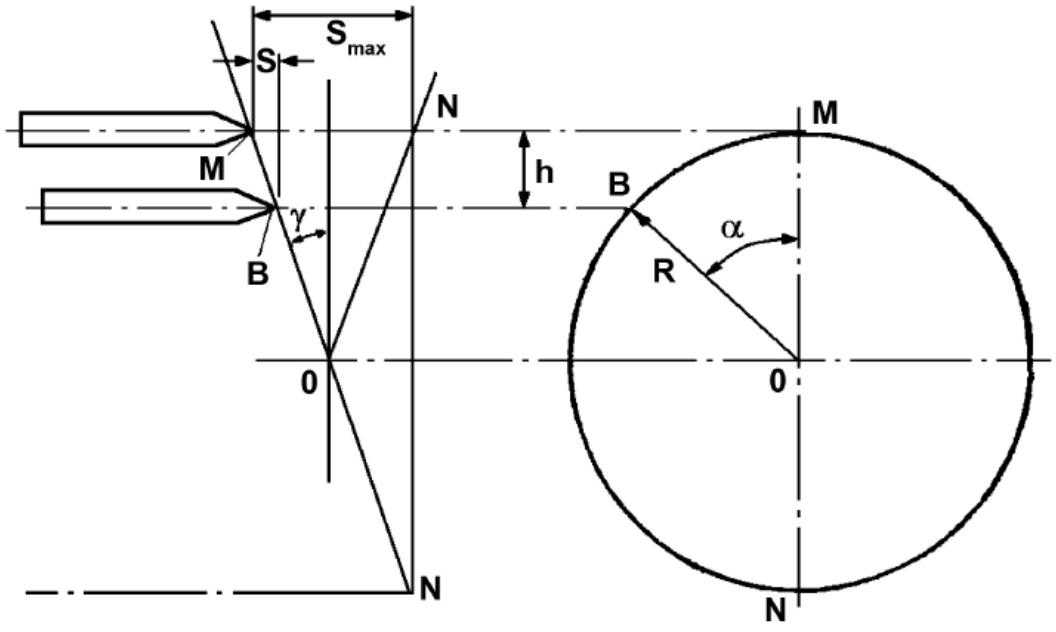

Fig. 3.4 – The design scheme for a kinematic analysis of the axial piston pump with the flat swash plate

A relative piston velocity is a time derivative of the piston stroke. It is calculated as

$$v_r = R\,\omega\, tg\gamma\, sin\,\alpha,$$

where $\omega = \dfrac{d\alpha}{dt}$ is an angular speed of the drive shaft.

The relative piston velocity becomes maximum at $\alpha = 90°$ and $\alpha = 270°$ positions. The maximum relative piston velocity is calculated as

$$v_{r\ max} = R\omega tg\gamma\,.$$

A relative piston acceleration is a time derivative of the relative piston velocity.

$$j_r = R\omega^2 tg\gamma\ cos\alpha\,.$$

The relative piston acceleration becomes maximum at $\alpha = 0°$ and $\alpha = 180°$ positions.

Piston also accelerates in a translational motion. The acceleration vector is directed to the cylinder barrel axis:

$$j_e = R\omega^2\,.$$

It is perpendicular to the cylinder barrel axis.

Except the considered above accelerations, the piston of the bent-axis pump experiences Coriolis acceleration. It is calculated as

$$j_c = 2\ \bar{v}_r\,\bar{\omega} = 2\ v_r\omega\, sin\,\psi\,,$$

where ψ is a swivel angle.

The Fig. 3.5 contains the graphs of the displacement (s), the velocity (v_r)

and the acceleration $\left(j_c\right)$ on the angular position of the rotor.

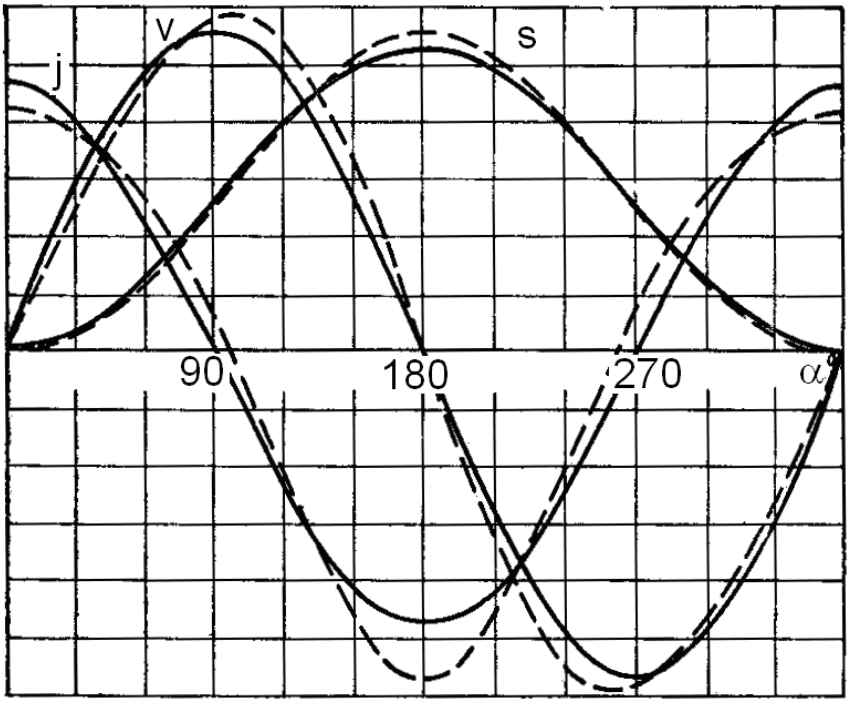

Fig. 3.5 – The kinematics of the piston pump with the flat swash plate (solid line – axial piston pump, dash line – bent-axis piston pump)

3.4 Pump capacity

The capacity is determined as

$$Q_p = Fbzn\eta_v ,$$

where $F = \dfrac{\pi d^2}{4}$ is a piston sectional area;

$b = s_{max}$ is the piston stroke;

z is the amount of pistons;

n is a secondary rotational speed, rps.

Thus,

$$Q_p = \frac{\pi d^2}{4}\, s_{max} zn\eta_v .$$

The capacity of the axial piston pump (see Fig. 3.1).

$$Q_p = \frac{\pi d^2}{4} 2Rzn\eta_v tg\gamma = \frac{1}{2}\pi d^2 Rzn\eta_v tg\gamma,$$

where R is a pitch radius; γ is the swash plate angle.

The parameters of the piston pump are similar to the parameters of the other volumetric pumps. However its maximum volumetric efficiency is considerably greater. It may make up 0.97 - 0.98, and even 0.99.

The minimum rotational speed (the speed when the capacity exceeds the leaks) is 5 - 10 rpm. The corresponding rotational speed of the gear pump is 80…100 rpm.

3.5 The problems of the uniform delivery and the cylinder filling

An instantaneous capacity of the every piston is proportional to the relative piston velocity at the moment

$$q = \frac{dQ}{dt}, \text{ or } q = Fv_r.$$

As the relative piston velocity varies, so the instantaneous capacity varies too.

The instantaneous capacity of the pump is equal to the sum of instantaneous capacities of all pistons:

$$q_\Sigma = \sum q_i.$$

The piston pumps with the great number of pistons provide more uniform delivery. The fluctuation amplitude decreases, but the frequency grows up. The fluctuations are determined as

$$\sigma = \frac{q_{max} - q_{min}}{q_{mean}} \cdot 100, \text{ (\%)}.$$

The piston pump with the *odd* number of the pistons deliver more uniform working substance than that with the *even* number of the pistons. This can be directly attributed to the fact that every piston has its twin piston at the opposite side of the cylinder barrel. The top dead center position of the piston is

simultaneous with the bottom dead center of the twin piston which in its turn leads to a sudden capacity drop (Table 3.1).

Table 3.1

z	4	5	6	7	8	9	10
σ,%	45	7	20	4	8	2	6

The following equations can be used for the approximate pulsation analysis:

– odd piston number

$$\sigma = \frac{1{,}25}{z^2} \cdot 100;$$

– even piston number

$$\sigma = \frac{5}{z^2} \cdot 100.$$

The capacity fluctuations of the pumps with the various number of the pistons are presented in Fig. 3.6.

The pressure fluctuations may exceed the capacity (the pressure is proportional to the squared capacity of the incompressible fluid at a constant flow section of an absolutely rigid system). When some pumps with nonuniform capacity feed the engine through the common pipeline, then their operation must be phase coordinated to reduce the fluctuation amplitude.

The piston travels in the cylinder at the variable velocity. Hence, the filling and expulsion rates are also variable. The diameter of the orifice at the bottom of the cylinder is less than the piston diameter. So the orifice area progressively increases during the filling stroke from zero to the full area. If the pressure in the orifice at the bottom of the cylinder is not sufficient then the cavitation may originate in this orifice. Then it propagates to the cylinder. To prevent this phenomenon, the piston pump is supercharged.

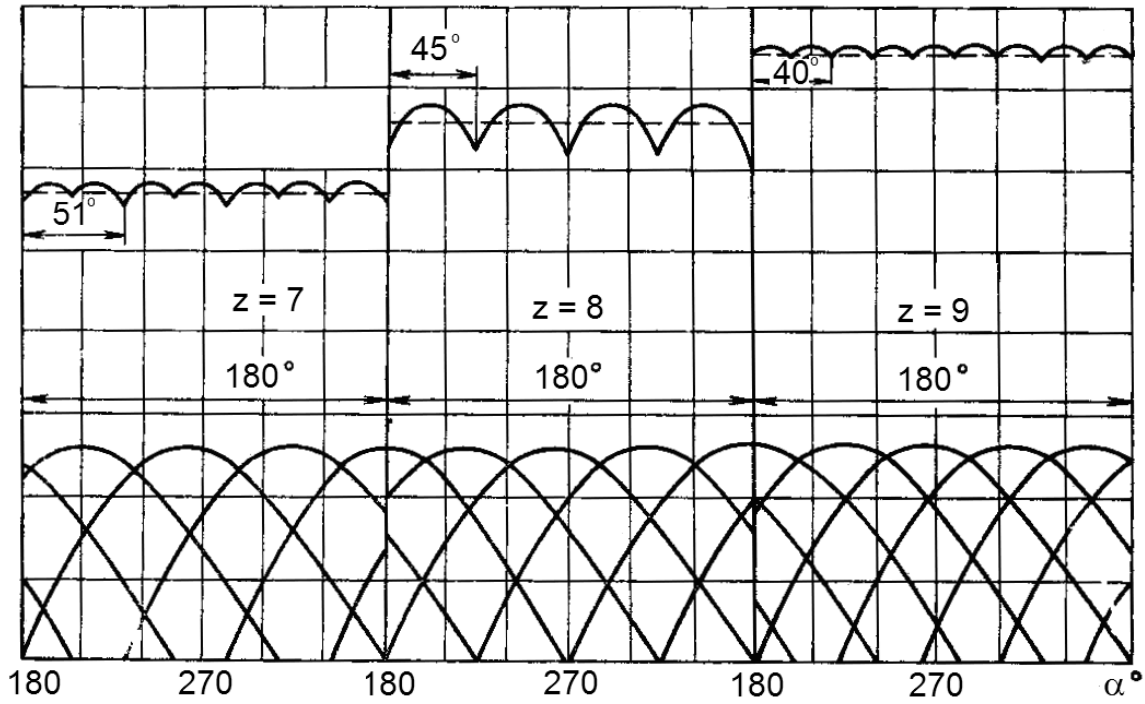

Fig. 3.6 – Fluctuations in the fuel supply manifold generated by the piston pumps with the different number of the pistons

As the diameter of the orifice at the bottom of the cylinder d_1 (the orifice joining the cylinder with the port plate) is less than the cylinder diameter d, so the fluid velocity in the orifice v_1 at the filling and the expulsion are higher than the piston speed at the same moment of time.

Besides, when the cylinder starts getting in and out of the contact with the inlet or outlet port of the port plate, the orifice at the bottom of the cylinder (d_1) is not used completely. When the cylinder progressively gets in contact with the port, then the active orifice area F_1 permanently increases from zero to the full area. And inversely, when the cylinder progressively gets out of contact with the port, the active orifice area F_1 permanently decreases from the full area to zero. Then

$$v_1 = v_{rel} \cdot \frac{F_{pl}}{F},$$

where v_1 is the fluid velocity in the orifice channel;

v_{rel} is the relative piston speed in the cylinder;

F_{pl} is the cross-sectional area of a piston (cylinder);

F is the active orifice area.

The maximum area of the orifice at the bottom of the cylinder is $F_1 = \frac{\pi d_1^2}{4}$.

Thus, the velocity v_1 changes in a very complex manner because it depends on the piston speed v_{rel} and the active orifice area F. The piston speed depends on the cylinder barrel position. As it has been mentioned, the active orifice area becomes smaller at the beginning and the end of the filling and the expulsion.

The change of v_1 velocity at the filling $(\alpha = 0 - 180°)$ is shown in Fig. 3.7.

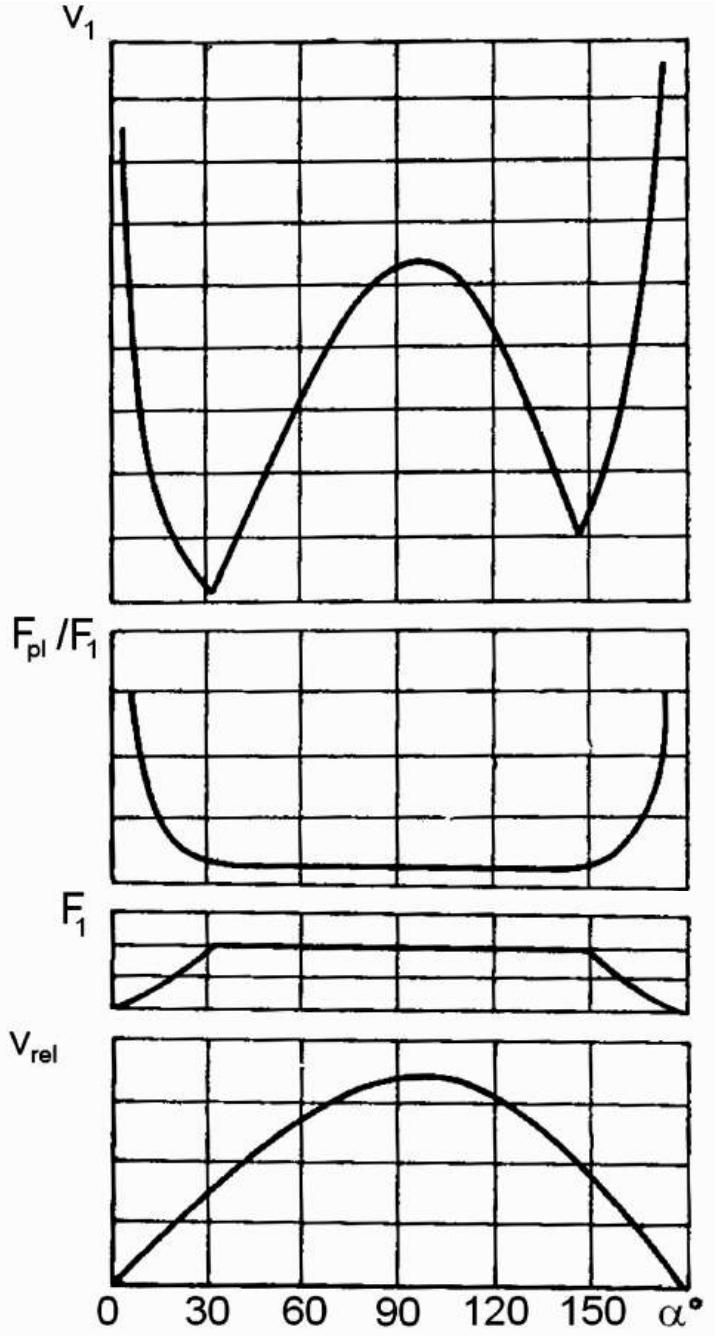

Fig. 3.7 – Piston velocity v_{rel}, active orifice area F_1 and fluid velocity in the orifice channel v_1 vs cylinder barrel angular position

If the pressure in the inlet manifold is not enough for the required fluid velocities in the orifice, then a cavitation may originate in the orifice, followed by the cavitation in the cylinder. The cavitation reduces the capacity and, in the worst case, may damage the pump. So, it is essentially important to provide enough pressure in the inlet cavity to avoid the cavitation.

The fluid speed v_1 in the orifice at the expulsion (α = 180 - 360°) varies in the opposite manner to the presented one in Fig. 3.7. The graph will be mirrored from that presented one in Fig. 3.7 (in case fluid is incompressible and there are no leakages over the clearances in the pumping unit, which is especially important for high pressures). Considering the fluid leakages through the clearances, the speed growth of the compressible fluid (compressibility is mostly perceptible at the filling start, i.e. when the fluid volume in the cylinder is great comparing to a momentary capacity) at the beginning and the end of a supercharging is not so big. The fluid speed may not exceed the operational domain at some size combinations.

3.6 Dynamics of the piston pump

The piston, which is not parallel to the barrel axis is balanced by the following forces and moments acting on it (Fig. 3.8):

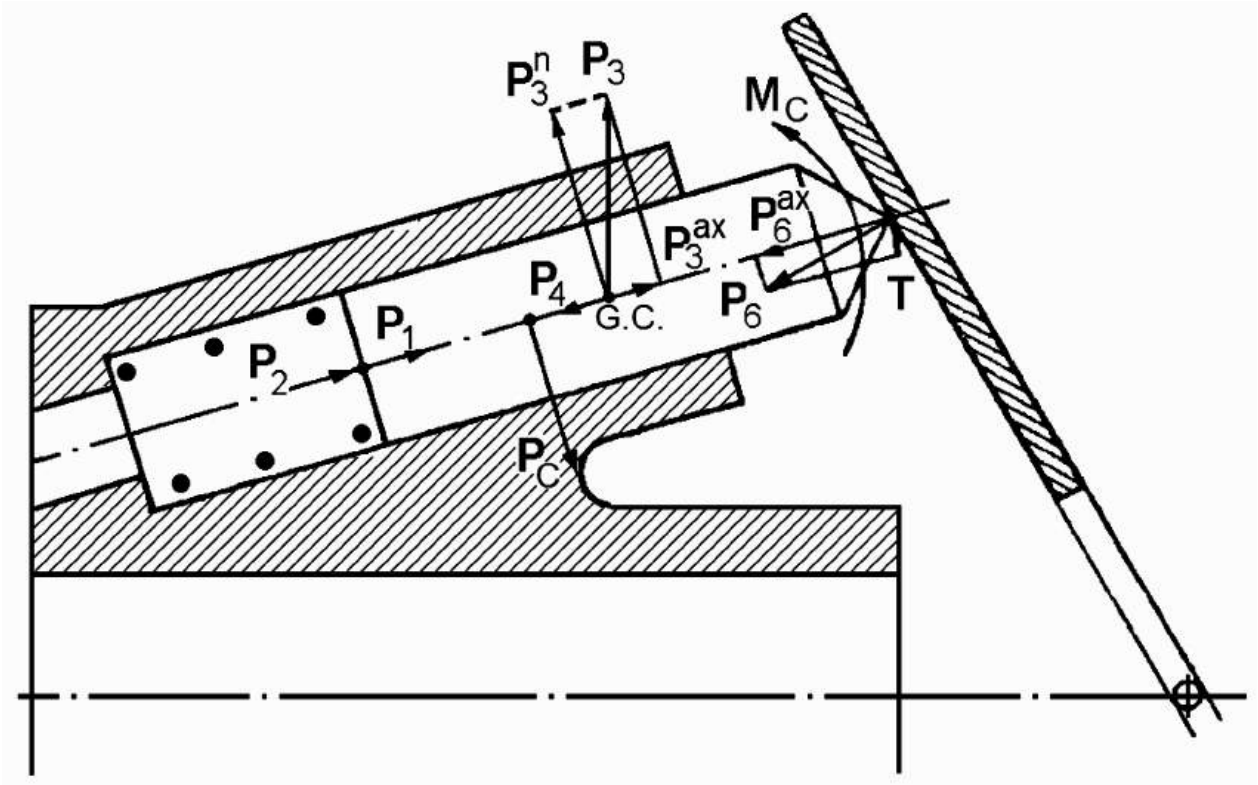

Fig. 3.8 – Forces and moments acting on piston

1. Spring force

$$P_1 = P_{pt} + k_s s,$$

where P_{pt} is a spring pretension at the bottom extreme position (bottom dead center), when the phase angle is 180°;

k_s is a spring rate (spring constant);

s is a current piston distance from the bottom dead center.

2. Hydraulic force

$$P_2 = \left(p_c - p_{sp}\right) F,$$

where p_c is the pressure inside the cylinder;

p_{sp} is the pressure in the swash plate cavity;

F is the piston cross-sectional area.

The hydraulic force presses the piston to the swash plate at the expulsion stroke and forces it back of the swash plate at the filling stroke.

3. The centrifugal force of masses in a relative motion

$$P_3 = m_p R\omega^2,$$

where m_p is the mass of the piston; R is the distance from the cylinder bore axis to the gravity center of the piston.

The centrifugal force is perpendicular to the cylinder barrel axis and directed radially. When the cylinders are not parallel to the barrel axis, then the force P_3 can be decomposed into the component coaxial to piston axis and perpendicular to it:

$$P_3^{ax} = P_3 \sin\psi \text{ and } P_3^n = P_3 \cos\psi.$$

4. Inertia in the relative motion

$$P_4 = -m_p \; j_r \, .$$

Inertia acts along the cylinder axis. As you can see from the equation, it depends on the relative acceleration and its direction

5. The Coriolis force acting the piston, which is not parallel to cylinder barrel axis is

$$P_5 = -m_p \cdot j_C \, ,$$

where j_C is a Coriolis acceleration $\left(j_C = 2 \cdot \vec{v}_r \cdot \vec{\omega} \right)$.

The force P_5 is constantly directed normally to the piston plane. It is directed opposite to the rotation at $\alpha = 0° - 180°$, and to the hand of rotation at $\alpha = 180° - 360°$.

6. Swash plate reaction P_6 . The force is applied to the contact point, i.e. the point at which piston touches the swashplate. It is normal to the swashplate. The swash plate reaction has two components: axial component P_6^{ax} (directed along the cylinder axis) and normal component T .

$$P_6 = \sqrt{\left(P_6^{ax} \right)^2 + T^2} \, , \; T = P_6^{ax} tg\gamma \text{ and } \; P_6^{ax} = P_6 \cos\gamma \, .$$

7. Cylinder reaction P_c .

8. Reactive moment of the cylinder M_c .

The friction forces are negligibly small and can be neglected.

The unknown swash plate reaction $\left(P_6 \right)$, cylinder reaction $\left(P_c \right)$ and reactive moment of the cylinder are obtained from the balance of forces and moments acting on the piston.

So, the sum of all forces projected on the piston axis is

$$P_6^{ax} = P_1 + P_2 + P_3^{ax} + P_4 \, .$$

Then the sum of all forces projected in the axis perpendicular to the piston axis is

$$P_c = P_3^n + T\,.$$

Let us write the balance of the moments generated by the forces by the reference to the gravity center of the piston. Then, the moments of forces P_1, P_2, P_3, P_4, P_5 and P_6^{ax} are zeros. The rest forces cause the moment

$$M_c = Th_6 + P_c h_c\,,$$

where h_6 is a distance between the contact point to the center of gravity;

h_c is a distance between the origin of the cylinder reaction (the middle of the piston bearing surface) and the gravity center.

3.7 The strength analysis of the piston pump parts

The bearing stress generated by the contact stress is the most crucial for the spherical head of the piston (Fig. 3.9).

If the swash plate is flat or conical, then

$$\sigma_{max} = 0.616 \sqrt[3]{\frac{P_6 E^2}{D^2}}\,,$$

where E is the elasticity modulus;

D is a diameter of the spherical head.

The maximum bearing stress $\left(\sigma_{max}\right)$ of the contacting steel piston and steel swash plate may reach 2000 MPa. If the swash plate is spherical then

$$\sigma_{max} = 0.616 \sqrt[3]{\frac{P_6 \cdot E^2}{D^2}\left(1 - \frac{D}{D_1}\right)^2}\,,$$

where D_1 is a diameter of the spherical swash plate.

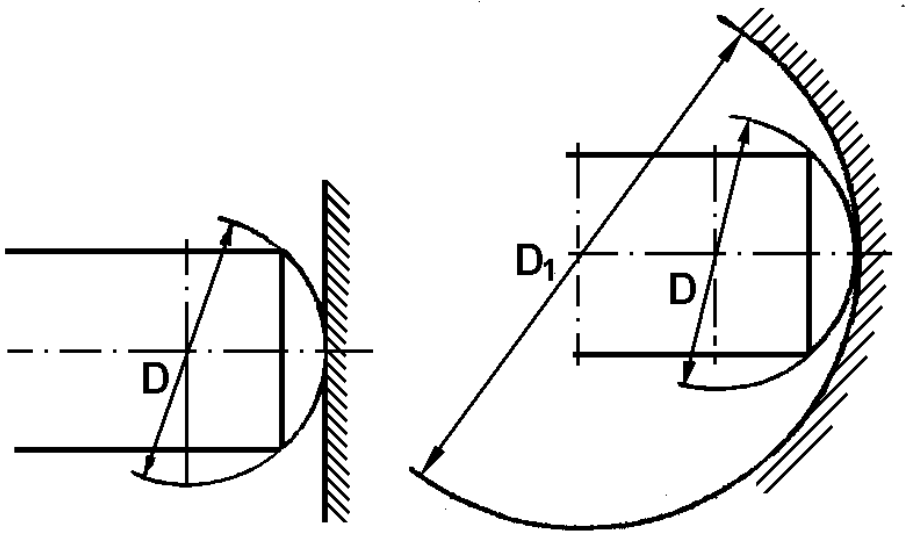

Fig. 3.9 – The design scheme of the piston head strength analysis

The piston head and the swash plate are designed to keep their spherical surfaces in the permanent sphere-to-sphere contact. That is why, their radiuses can not be independent. For the axial piston pump, they are obtained from the following condition:

$$D_1 \le \frac{D}{\sin \gamma_{max}}.$$

Usually the maximum swash plate angle is $\gamma = 15^o$, therefore $D_1 \le 2D$.

To reduce the contact stress in a "swashplate-piston" pair, the piston may have a hinge pivot. This design solution let the piston have the greater D_1, hence the point contact is changed to the surface contact (Fig. 3.10).

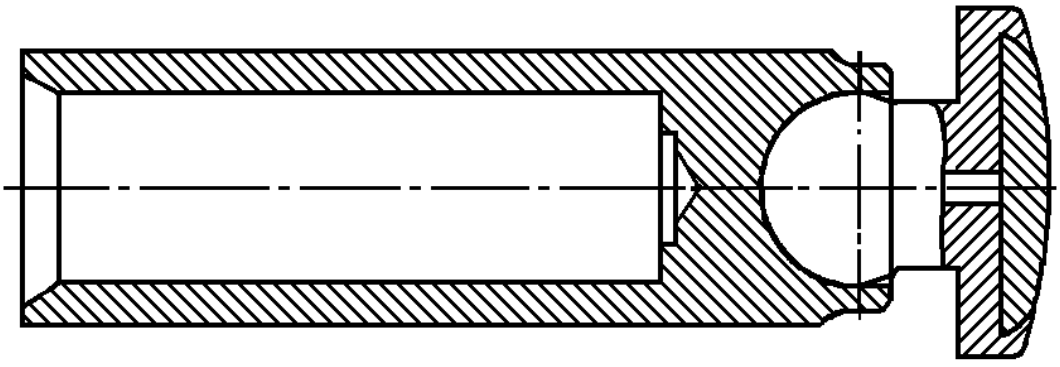

Fig. 3.10 – Hinge pivot piston

However the design of the hinge pivot piston turns out more complex. The pump must have the retracting ring, which constrains the pivots from the harmful displacements caused by the gravity and the inertia.

To make the piston operation even more efficient, the hydrostatic slipper pad is used (Fig. 3.11). The pad reduces the contact stress and hence the wear out. The lifetime of the slipper pad and the piston as a whole becomes greater.

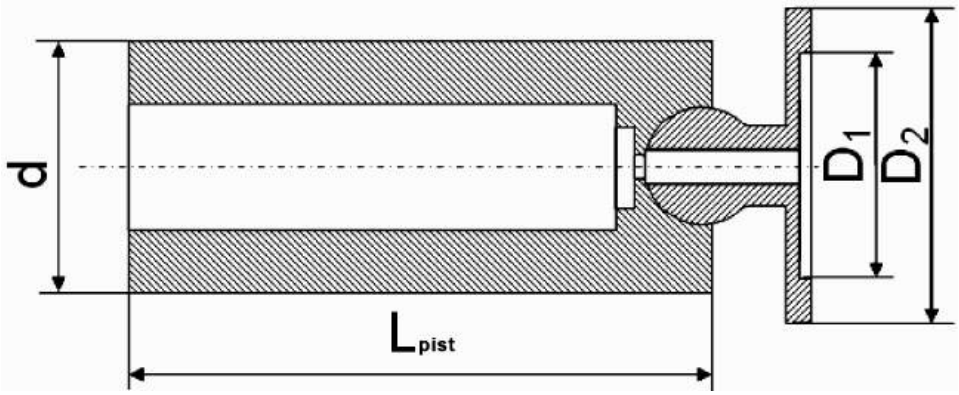

Fig. 3.11 – Slipper pad piston

The working substance from the cylinder is supplied to the clearance between the slipper pad and the swash plate. The pressure in the clearance balances the swash plate reaction making the piston “surface” upon the swash plate. The slipper pad piston must always have the retracting ring, which makes it heavier. Besides, piston pumps with the slipper pad pistons are less efficient.

The port plate has the design that intends to minimize the leakages and reduce the wear out of the contacting surfaces. The pressure acting on the sliding side of the swash plate must not exceed 15 - 20 % of the output pressure.

The lateral surface. The lateral surface mostly experiences the forces perpendicular to the piston axis, which are the Coriolis force $\left(P_5\right)$, normal component of the centrifugal force $\left(P_3^n\right)$, normal component of the swash plate reaction $\left(T\right)$ (Fig. 3.12). These forces cause the bending and the shift of the piston and the bearing of its side surface. They also cause the bearing of the cylinder wall. The maximum Coriolis force appears at 90° phase angle $\left(\alpha\right)$. The forces P_3^n and T are extreme at 180° phase angle, when the Coriolis force is zero. For this reason, the force P_5 is neglected in the calculations.

The profile of the pressure acting the side surface of the piston is derived upon the following assumptions:

– the strains are elastic;

– the cylinder is compliant;

– the piston is absolutely rigid;

– the clearance between the piston and the cylinder wall is very small.

If the clearance is small then

1. the forces acting on the piston can be simulated by the force q_1 evenly distributed along the piston length;

2. the moment of the forces acting on the piston can be simulated by the linearly decreasing force q_2.

Then

$$q_1 \cdot l_{bear} = P_c \text{ and } q_1 = \frac{P_c}{l_{bear}},$$

where l_{bear} is the length of the bearing surface.

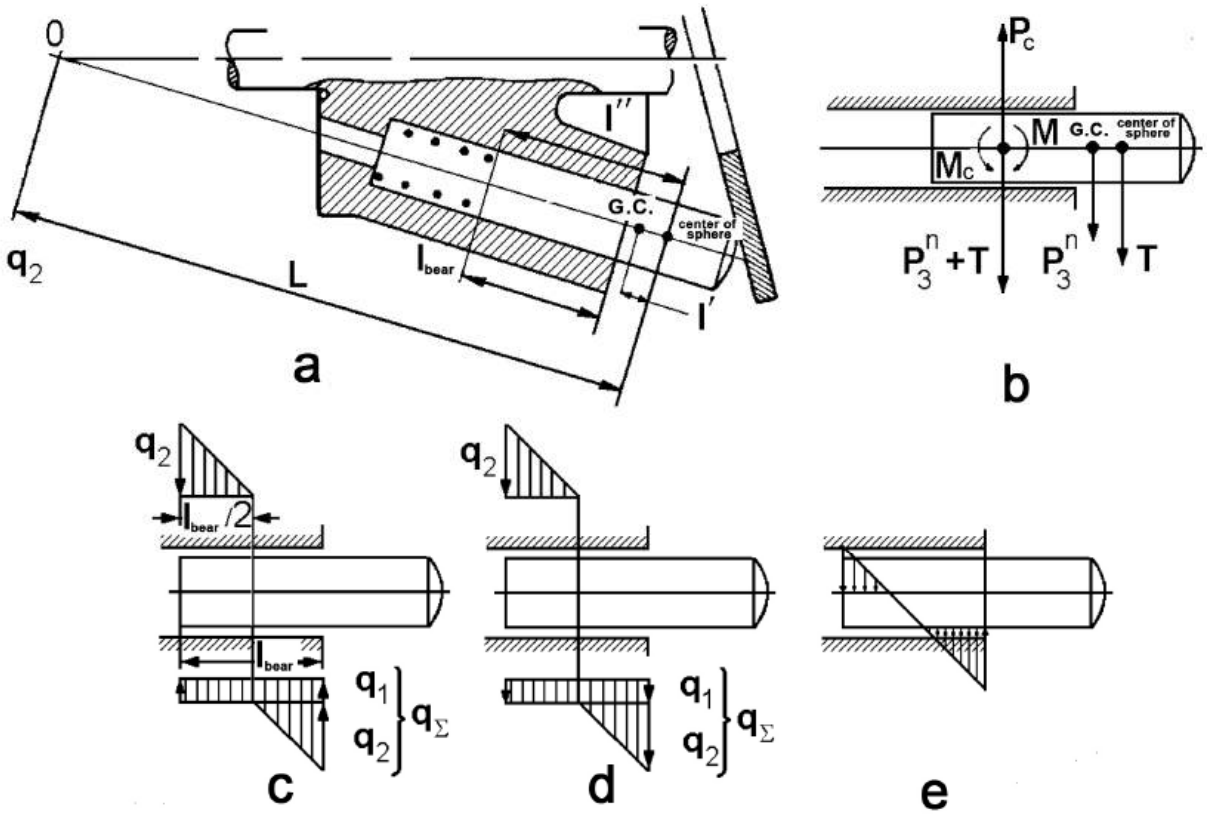

Fig. 3.12 – The design scheme for the lateral surface strength analysis:
a - the design scheme to calculate the length of the bearing surface;
b - the loading scheme; c - piston load; d - cylinder load;
e - resultant load acting the piston

The maximum value q_2 can be obtained from the expression

$$\frac{1}{2} q_{2\ max} \frac{l_{bear}}{2} \cdot \frac{2l_{bear}}{3} = M_c,$$

whence

$$q_{2max} = \frac{6 \cdot M_c}{l_{bear}^2}.$$

The maximum linear load generated by the forces and the moment at the cylinder inlet edge is calculated as

$$q_{\Sigma_{max}} = \frac{P_c}{l_{bear}} + \frac{6M_c}{l_{bear}^2} = \frac{1}{l_{bear}} \left(P_c + \frac{6M_c}{l_{bear}} \right).$$

The bearing stress acting on the piston surface or the cylinder surface are calculated as $K_{max} = \frac{q_{\Sigma max}}{d}$.

Typically, bearing stress is within the range $K_{max} = 10 - 15\ MPa$ (the pistons are made of the alloyed steel and the cylinders – of the bronze).

The pistons do not need to be checked for a bending, because they are usually negligibly small.

The sliding side of the port plate

The cylinders are filled via the ports in the port plate (Fig. 3.13).

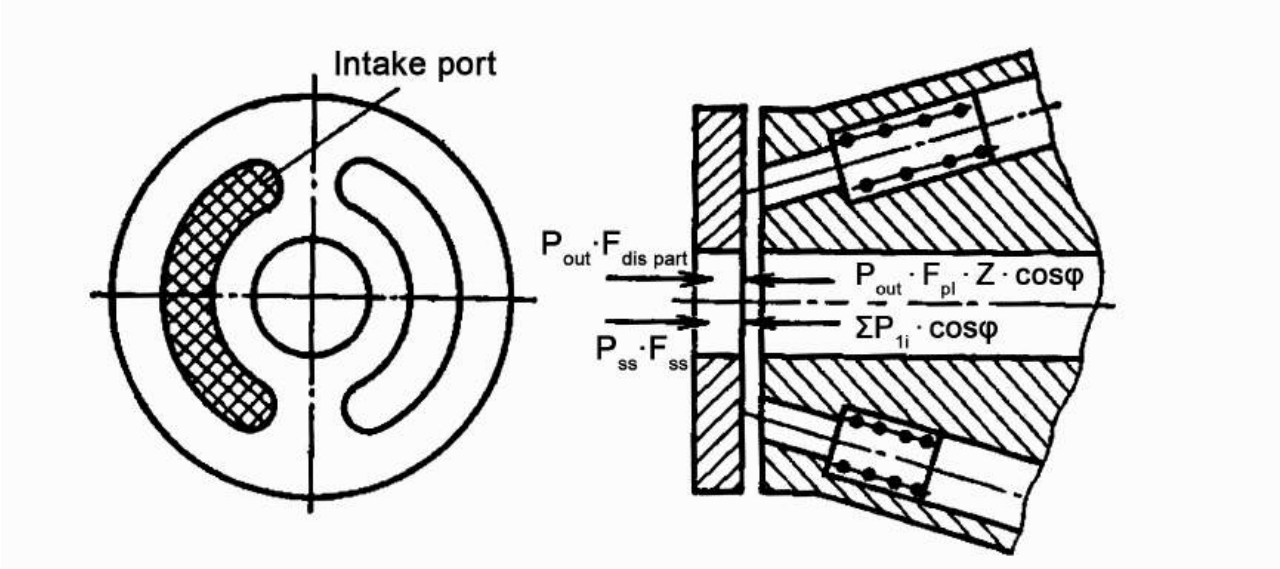

Fig. 3.13 – The design scheme of the sliding side

The cylinder barrel must remain in the permanent strong contact with the port plate for the stable operation. The pressure in the cylinder (especially when the cylinder is in the filling phase) and the springs inside the pistons press the cylinder barrel to the port plate. The pressing force can be calculated as

$$P_{pr} = \left(p_{out} \cdot F \cdot z' + \sum_{i=1}^{z} P_{1i} \right) \cdot \cos\psi ,$$

where p_{out} is the output pressure;

F is the cross-sectional area of the piston;

z' is a minimum number of the cylinders that are in a simultaneous contact with the discharge port.

The cylinder barrel is forced back from the port plate by the pressure in the discharge port and the fluid pressure in the clearance between the sliding side (p_{ss}) and the cylinder barrel.

The force-back force can be calculated as

$$P_{fb} = p_{out} \cdot F_{dis\ port} + 0.5 \cdot p_{ss} \cdot F_{ss} ,$$

where $F_{dis\ port}$ is the discharge port area;

F_{ss} is the contact area between the cylinder barrel and the valve plate (except areas of the intake and discharge ports and areas of other holes).

The following condition must be met for the reliable permanent contact between the cylinder barrel and the port plate

$$P_{pr} = P_{fb} .$$

The pressure acting the sliding side $\left(p_{ss}\right)$ must not be too high not to squeeze oil completely form the clearance. In this case the dry friction will cause the considerable wear out of the contacting parts and the cracks in the contacting surfaces.

To meet the requirement presented before $\left(P_{pr} = P_{fb}\right)$ designers can vary the spring force $\left(P_1\right)$ and the area of the contact area $\left(F_{ss}\right)$.

The typical for modern piston pump pressure acting on the sliding side is $p_{ss} = 1.3 - 2$ MPa at the output pressure $p_{out} = 9 - 10$ MPa.

Hence, it is obvious that rotor must not have any axial fixation, except the port plate.

Size and position of ports in the port plate

The port width is equal to the diameter of the orifice at the bottom of the cylinder interconnecting the cylinder with the intake and discharge ports. The bridge must be long enough to prevent the fluid from the discharge port leaking to the input port. In the other words, the bridge length (δ) must be greater than the diameter of the orifice interconnecting the cylinder with the port (d_1) (Fig. 3.14).

$$\delta \geq d_1.$$

When the cylinder passes the bridge, the pressure starts increasing before it gets in contact with the discharge port. This causes the drastic increase of the pressure in the cylinder. The peak pressure may become even greater than the output pressure.

To prevent the pressure shock, the intake port is designed shorter than the discharge one. The piston then starts the upstroke only when the cylinder gets in contact with the discharge port and ends it – when the contact terminates.

The other method to prevent the shock is to drill a small hole, which interconnects the cylinder with the additional cavity. The channel is blocked by the check valve, which is acted by the pressure in the cylinder on one side, and by the pressure in the discharge port – on the other side.

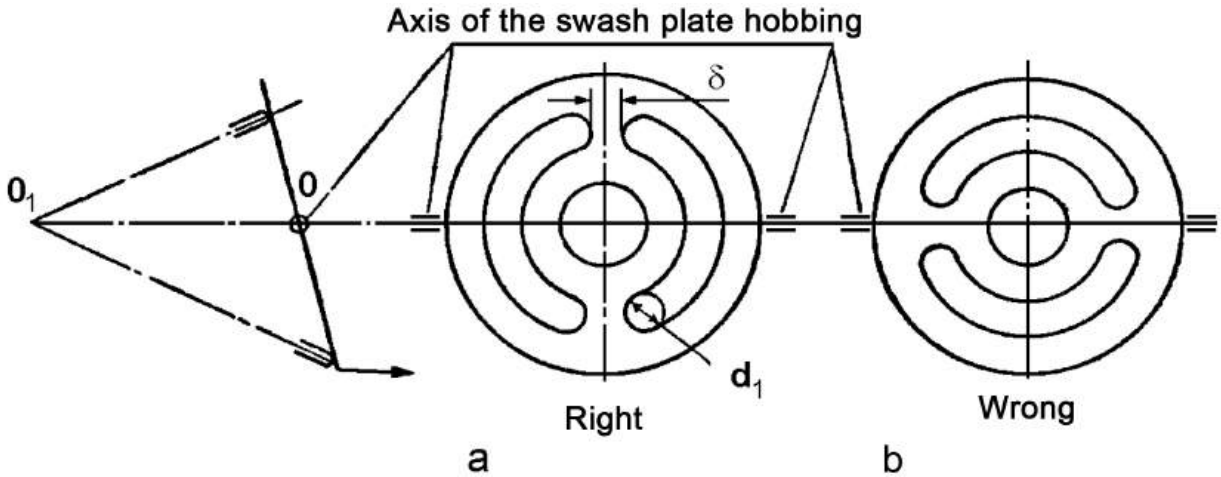

Fig. 3.14 – The position of ports in relation to the swash plate turning axis

Fluid distribution

The modern piston pumps implement the port fluid distribution (Fig. 3.15). The fluid is distributed through sickle-shape ports *a* and *b* in the port plate. The cylinders progressively encounter the ports during their travel.

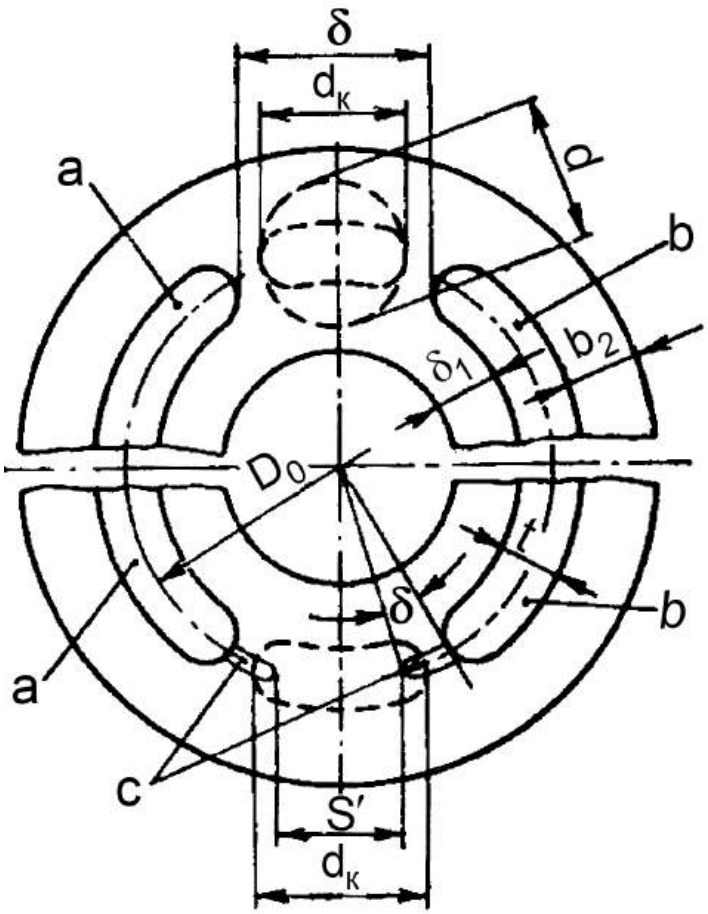

Fig. 3.15 – Port plate

The orifice at the bottom of the cylinder is circular or elongated. In the latest case the orifice diameter is equal to the port width (ports *a* and *b*), and the orifice length (d_C) is equal to the cylinder diameter (d). The diameter of the circular drillings (d_1) is equal to the port width.

The port width is typically set equal to

$$t = 0.5\,d$$

thereby determining the orifice width (or its diameter, in case it is circular).

Finally, diameter d_1 is equal to t for the axial pump (see Fig. 3.1, a and 3.2) or to $d_1 = t/\cos\psi$ for the bent-axis pump (see Fig. 3.1, b).

In the top and bottom dead centers, the orifice at the bottom of the cylinder is overlapped by the top and bottom bridges. The bridges are between the ports *a* and *b*. The bridge length δ is few times greater than the orifice diameter. Practically, the bridge length is determined as

$$\delta = (1.1 - 1.2) \cdot d,$$

where d is a bigger axis of the orifice channel joining the cylinder with the port plate (if the orifice is circular, then the d is equal to d_1).

Total width of seal shoulders is equal to

$$b_1 + b_2 = 0.25\,d$$

For the approximate analysis, the shoulder widths are considered equal. Nevertheless, the wear out of each shoulder is different because they rotate at the different circumferential speeds. Hence, it is reasonable to choose the shoulder widths from the relation

$$\frac{b_1}{b_2} = 0.8.$$

Narrow grooves are usually milled at the ends of ports *a* and *b* to prevent the pressure shock from the reverse fluid flow. The shock appears when the cylinder gets in contact with the discharge port. The grooves interconnect the cylinder with the discharge port before the cylinder gets in contact with the ports *a* and *b*. The groove is 1-2 mm wide. It is narrowed both in the depth and in the width.

The distance between the grooves is usually selected to meet the $s' > d$ condition. But, to reduce the noise and make operation much smoother, some pumps are designed to meet the opposite condition $(s' < d)$. The leakage rate of such pumps is higher.

3.8 Forces in the fluid distribution assembly

The fluid pressure acts on the cylinder barrel (Fig. 3.16). The pressure generates force pressing the rotor to the port plate P_{pr} and to force it back

from the port plate P_{fb}. The stable pump operation is possible only when the cylinder barrel and the port plate are in the permanent thorough contact.

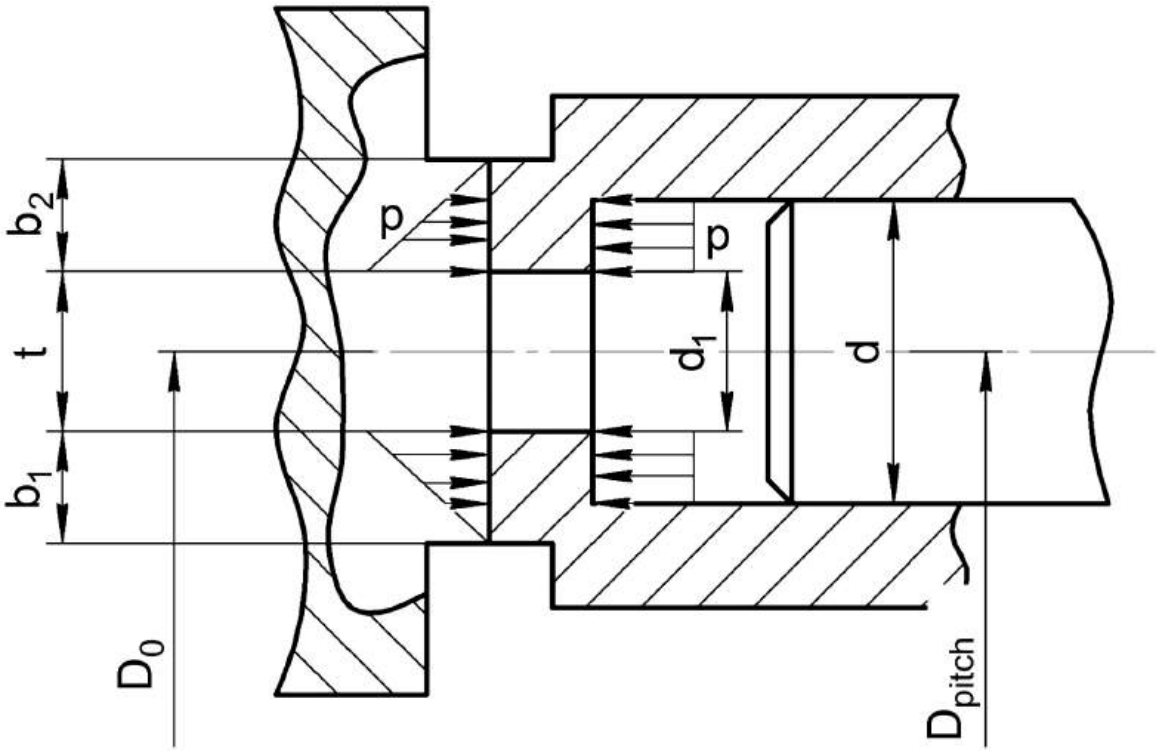

Fig. 3.16 – The design scheme of the pumping unit of the axial pump

The pressing force $\left(P_{pr}\right)$ acts on the cylinder end, which is interconnected to the discharge port. They press the rotor to the port plate. The force-back force $\left(P_{fb}\right)$ counteracts the pressing force. The force-back force depends on the fluid pressure inside the port and the clearance between the port plate sliding side and the cylinder barrel face.

The pressing force area is evaluated as

$$S_{pr} = S_1 = \frac{\pi \cdot \left(d^2 - d_1^2\right)}{4}.$$

Besides, the cylinder barrel is pressed to the port plate by the spring. But the spring pretension generates the relatively low force. That is why this force is usually neglected in calculations.

The force acting the cylinder barrel from the piston side P_{pr} is obviously not symmetrical, because only part of the cylinders is interconnected with the discharge port. Besides, permanent alternate interaction with intake and

discharge ports tends to the pressure center oscillations around the swash plate turning axis. At the same time, P_{fb} is also asymmetric. The port plate also has the ports *a* and *b* (see Fig. 3.15) with the fluid pressures corresponding to the pressures in the input and discharge manifolds. The contact part of the sliding surface (a part of the sliding surface without the ports) is acted by the averaged pressure of the fluid in the clearance between the port plate and the cylinder barrel. The fluid gets to the clearance from the ports *a* and *b*. From the above presented considerations it is obvious that shoulder areas (the b_1-wide shoulder and the b_2-wide shoulder) must balance P_{pr} (see Fig. 3.15).

Designer must chose the parts` sizes to ensure the reliable contact between the cylinder barrel and the port plate (see Fig. 3.16). It goes without any explanation that the reliable contact is provided only when

$$P_{pr} > P_{fb}.$$

The excess $\left(\Delta = P_{pr} - P_{fb}\right)$ must not result in the increased wear out of the friction pair. The excess is characterized by a press ratio.

$$k_{pr} = \frac{P_{pr}}{P_{fb}}.$$

The implemented designs have the press ratio within the range 1.06 -1.1 for pumps with good controlled manufacturing quality of their parts, and from the range 1.15 - 1.2 – in the rest cases.

The main issue in P_{fb} evaluation is the determination of the average pressure $\left(p_{av}\right)$ in the clearance between the cylinder barrel and the port plate. The clearance depends on the manufacturing accuracy of the friction pair, the materials, the used fluid and some other various aspects.

In a routine practice the pressure distribution in the clearance is considered linear (see Fig. 3.16):

$$p_{av} = 0.5 \cdot p_{out},$$

where p_{out} is the out pressure.

Let us get the formula to determine the force-back force. First, one must introduce the taken assumptions. The first assumption addresses the pressure in the clearance. It is assumed to act only from the high pressure portion of the contact surface. (i.e. high pressure acts only half of the contact surface). The second assumption addresses the pressure from the intake portion of the contact surface. It is neglected. So, finally

$$P_{fb} = p_{out} \cdot S_{port} + 0.5 \cdot p_{out} \cdot S_{slide},$$

where $S_{port} = \frac{\pi}{2} \cdot d_1 \cdot t$ is a port area;

$S_{slide} = \frac{\pi}{2} \cdot D \cdot (b_1 + b_2)$ is the sliding area (i.e. the area of the sliding surface between the cylinder barrel and the port plate.

The pressing force is evaluated as

$$P_{pr} = c \cdot p_{out} \cdot F,$$

where F is the piston sectional area;

c is the minimum number of cylinders that can simultaneously be in contact with the discharge port (for the simplified calculations $c = 0.5 \cdot z$).

Thus, the correctness of the design can be estimated by the press ratio:

$$k_{pr} = \frac{F \cdot z}{2 \cdot (S_{port} + 0.5 \cdot S_{slide})}.$$

Unloading the sliding surface

The simplest method to affect the press ratio is to vary the sliding side area (which is the contact area between the cylinder barrel and the port plate). Strength is the main factor limiting the minimization of the sealing shoulder area. The shoulder can be crumpled by the forces acting it. So, special valve plates are implemented to prevent the shoulder crumpling. These shoulders let the diminution of the shoulder area, keeping the required contact area unchanged.

The blind groove *e* is milled in the outer contact shoulder (see Fig. 3.15, b). It splits the outer shoulder area into two parts. The outer one part m is unloaded from the pressure (pressure in the groove *e* is equal to drain pressure) by the draining grooves k. Then, there is the drain pressure in the clearance between the outer shoulder m and the cylinder barrel face. This shoulder serves only as a support. The area of the shoulder makes no effect on the balance of forces in the clearance. The considered support shoulder provides the contact pressure decreasing in the fluid distribution assembly up to the required magnitude.

But, when this kind of pump flushes the contaminated fluid, then the contacting surfaces are worn out non-uniformly. The shoulders that experience the pressure drop are worn out the most. At the same time, the outer shoulder m remains almost unworn. In this case, the leak proofness of the fluid distribution assembly is disturbed (the cylinder barrel drops on the outer shoulder forming the clearance between the sealing shoulder *n* and the cylinder barrel).

Opposite to the considered construction, the contacting surfaces of the pump without the shoulders (see Fig. 3.15, a) have more uniform wear out. In this case, the leak tightness is disturbed less intensively.

Piston shoe strength analysis

The pistons of the axial piston pump rest on hydrostatic balanced shoes. The oil is delivered from inside of the cylinder. The shoe is placed next to the piston head and the swash plate. They are pressed to the swash plate by a retracting ring and springs (see Fig. 3.11).

The hydrostatic balancing of the piston shoe

The equilibrium condition is

$$p_{out} \cdot F = p_{react} \cdot S_{back},$$

where p_{out} is the output pressure;

p_{react} is the pressure acting the piston shoe face;

S_{back} is a force-back area (the pressure $p_{reaction}$ acts on this surface).

The area of the force-back surface is

$$S_{back} = \frac{\pi \cdot \left(D_{shoe\ 2}^2 - D_{shoe\ 1}^2 \right)}{8 \cdot ln\left(\frac{D_{shoe\ 2}}{D_{shoe\ 1}} \right)},$$

where $D_{shoe\ 2}$ is the external surface of the shoe sealing shoulder;

$D_{shoe\ 1}$ is the internal surface of the shoe sealing shoulder.

The diameters of the sealing shoulder must meet the conditions

$$D_{shoe\ 2} > d\ ,\ D_{shoe\ 1} < d\ .$$

Equating the fluid flow rate through the clearance between the shoe and the swash plate with the fluid flow rate through the axial drilling in the piston, one can deduce the equation for the drilling diameter.

The pressure drop $p_{out} - p_{react}$ must be minimal, so the drilling diameter must be great. Then the assumption $p_{out} = p_{react}$ is acceptable. The press ratio is equal to:

– at zero swash plate angle

$$k_{pr\ 0} = \frac{F}{S_{back}};$$

– at maximum swash plate angle

$$k_{pr\ max} = \frac{F}{S_{back} \cdot cos(\gamma)}\ .$$

Materials

The contacting pairs are usually manufactured from steel and bronze. Thus if one part is made of steel, then the other one is made of bronze, and vice versa.

So, if the port plate is made of steel (Х12Ф1), than the rotor is made of bronze (Бр ОСН-Ю-2-3), or vice versa.

Bushes of the fair-sized pumps are the only parts made of bronze. The rotors are made of the steel (12ХН3А).

Rotors made of bronze Бр ОФ10-1 are used with the port plate made of steel 20Х. Have been cemented, the port plate hardness reaches 55...60 HRC.

To reduce the wear out, the end faces of bronze parts are covered with silver, indium with a sublayer of lead or with lead.

To reduce the friction and improve the dirt collection resistance, the parts are covered with a thin layer of silver.

The pistons are of steels providing the minimal buckling and high hardness of the surface: ХВГ (55 – 60 HRC), ШХ-15 (62 – 64 HRC).

The pistons working in the cylinder barrel are produced of beryllium bronze (Бр Б2).

4 CENTRIFUGAL PUMPS

4.1 General information

Centrifugal pumps (CFP) are a sub-class of dynamic axisymmetric work-absorbing turbomachinery. Centrifugal pumps are used to transport fluids by the conversion of rotational kinetic energy to the hydrodynamic energy of the fluid flow. The rotational energy typically comes from an engine in GTE. The fluid enters the pump impeller along or near to the rotating axis and is accelerated by the impeller, flowing radially outward into a diffuser or volute chamber (casing), from where it exits.

Advantages of centrifugal pumps are:

– a centrifugal pump is very simple because of direct conversion of the motor to rotational energy;

– they don’t require any valves or many moving parts;

– their output is very steady and consistent (without hydraulic shock);

– they are very small and light compared to other types of pumps that create the same output;

– there is a possibility to move at high speeds with minimal maintenance;

– easy to drive it with turbine;

– they have high reliability and durability.

Disadvantages of centrifugal pumps are:

– relatively poor suction power (should be primed);

– cavitation hazard.

These pumps are widely used in aircraft and GTE fuel systems as transfer and booster pumps. Besides CFP are applied to supply fuel in the ATJE afterburning chambers, and in TPA (turbo-pump assembly) of LPRE (liquid propellant rocket engine) centrifugal pumps are used as the main ones.

Before starting CFP cavities must be primed (filled with working fluid). Like most pumps, a centrifugal pump converts rotational energy (often from an engine) to energy in a moving fluid. A portion of the energy goes into kinetic energy of the fluid. Fluid enters axially through eye of the casing, is caught up in the impeller blades, and is whirled tangentially and radially outward until it leaves through all circumferential parts of the impeller into the diffuser part of the casing. The fluid gains both velocity and pressure while passing through the impeller. The doughnut-shaped diffuser, or scroll, section of the casing decelerates the flow and further increases the pressure.

Discharge (outlet) device collects the liquid leaving the impeller, and transform kinetic energy of a stream to a pressure head (energy of pressure). Thus, in the discharge exhaust velocity partially transforms to pressure.

Suction (inlet) pipe serves for a fluid supply to impeller eye with a definite average velocity c_0. Thus it is necessary to provide the most uniform velocity distribution, and in some cases – a definite twist of a stream.

The pressure at the inlet of impeller eye p_{in} must exceed the saturation vapor pressure p_s of working fluid by the value of cavitation margin $\Delta p_{cav.min}$, providing cavitation-free operation of the pump:

$$p_{in} \geq p_s + \Delta p_{cav.min}.$$

The value of a cavitation margin depends on the design of the pump, its purpose and parameters. For example, for low pressure pumps (0.1…0.15 MPa) and middle-pressure pumps (transfer and booster pumps installed in tanks of planes) cavitation margin is

$$\Delta p_{cav.min} = 0.01 - 0.025, \text{ MPa}.$$

For the fuel centrifugal pumps of an engine, that are booster pumps (BPE) for the main high-pressure pump of the engine (MPE) cavitation margin is

$$\Delta p_{cav.min} = 0.06…0.08, \text{ MPa}.$$

Effective way of the pump cavitation properties improving is installing the *axial (screw) pump* which creates an additional pressure in front of the pump impeller. The screw pump, besides, creates an initial hydrodynamic twist of fluid that reduces its relative speed at the inlet of impeller blades. As a result, the local underpressure on blades reduces therefore the suction head of the pump increases.

4.2 Nomenclature of centrifugal pumps

The layout of the simple one-stage centrifugal pump is shown in Fig. 4.1. The process liquid enters the suction nozzle 1 and then into the eye (center) of a revolving device known as an impeller 2. When the impeller rotates, it spins the liquid sitting in the cavities between the vanes 3 and case outward and

provides centrifugal acceleration. The potential energy (static pressure), and kinetic energy of liquid (its absolute speed) increase. The stator section of a centrifugal pump, after flow exits the impeller, is usually a diffuser 4. Here absolute speed of liquid decreases and pressure increases. The simple diffuser consists of the flat disks making its walls, and is known as vaneless. A vane diffuser is a set of stationary vanes 5 (in fig. 4.1 they are shown by a dashed line) that surround the impeller. The purpose of the vane diffuser is to increase the efficiency of centrifugal pump by allowing a more gradual expansion and less turbulent area for the liquid to reduce velocity. The diffuser vanes are designed in a manner that the liquid exiting the impeller will encounter an ever increasing flow area as it passes through the diffuser. This increase in flow area causes a reduction in flow velocity, converting kinetic energy into flow pressure. After the diffuser liquid enters the volute (spiral shape casing) 6. Due to the gradually increasing cross sectional area volute collects all the liquid reducing its velocity and increasing the pressure. The liquid leaves the volute to a discharge pipe and then streams to hydraulic system.

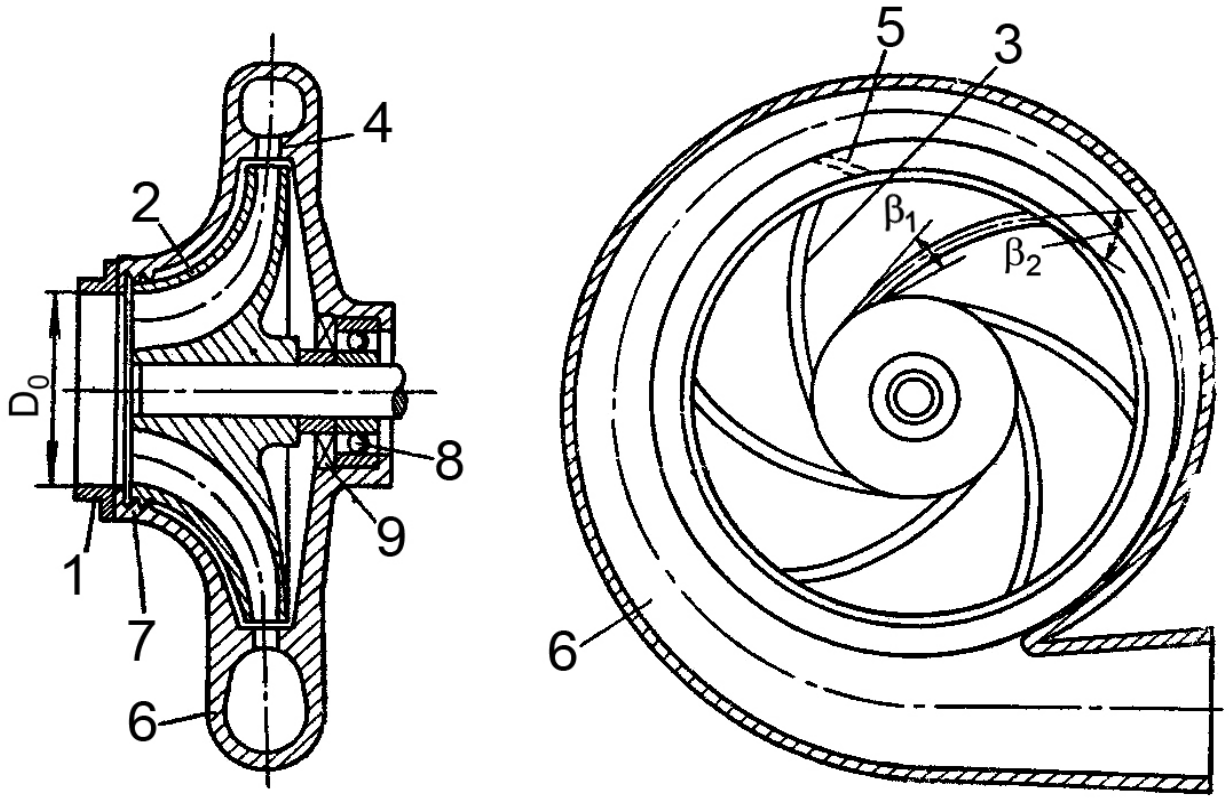

Fig. 4.1 – The centrifugal pump configuration:
1-suction pipe; 2-pump impeller; 3-blades; 4-diffuser; 5-diffuser vanes;
6– volute; 7-front seal; 8-shaft bearing; 9-bearing seal

Seals 7 (see Fig. 4.1) reduce a liquid overflowing from a cavity with high pressure (a diffuser) to a cavity with low pressure (impeller eye inlet).

Centrifugal pumps can be generally designed with the axial, spiral and double-face inlet, one - and multistage. The choice of an axial or spiral inlet depends on operational conditions of the pump and the engine. A double-face inlet is used for pumps with high flow rates to reduce the inlet velocity therefore to improve the cavitation properties of the pump. Centrifugal pump containing two or more impellers is called a multistage centrifugal pump. The impellers may be mounted on the same shaft or on different shafts. For higher pressures at the outlet, impellers can be connected in series. For higher flow output, impellers can be connected parallel.

4.3 The basic parameters of the pump

For calculation of the pump and an evaluation of its main properties the most important are the following basic parameters:

1. A *volume flow rate* of liquid through the pump Q_p. The mass fuel flow rate (found in thermo-gas dynamic calculation of an engine) determines Q_p for the booster fuel pump, taking into account a safety factor K:

$$Q_p = K \cdot G_f / \rho_f .$$

2. *Pump pressure head*. The necessary feed pressure defines pressure created by the pump. Feed pressure for the booster fuel pump is defined by the value of a necessary suction head of MPE p_{in}^{MPE}. It is necessary to subtract pressure of the liquid at the inlet of the pump p_{in} from this pressure.

Thus, the pressure difference created by the pump is

$$\Delta p_p = p_{in}^{MPE} - p_{in}$$

and pump head is

$$H = \Delta p_p / \rho_f .$$

3. *Pump efficiency*. Losses in the pump and its full efficiency η_p are characterized by three efficiencies – volumetric η_v, hydraulic η_h and mechanical η_m.

The *volumetric efficiency* defines the amount of the liquid flowing from a cavity of a high pressure back into a cavity of low pressure, and the value of leakages of the liquid from a cavity of a high pressure through seals. Thus,

$$\eta_v = \frac{Q_p}{Q_0},$$

where Q_0 - a volume flow rate of the liquid through a pump impeller.

The value η_v depends on a design of the pump and discharge pressure. For impellers of the semiclosed type η_v = 0.75 - 0.9; for impellers of the enclosed type η_v = 0.85 - 0.95.

The *hydraulic efficiency* characterizes the value of hydraulic losses of a pressure in the pump. These losses are a sum of the losses due to stall and shock of a stream at the impeller's eye, at the inlet of the diffuser, at the inlet of the volute and in the discharge pipe, and losses due to a liquid friction on walls of channels. The hydraulic efficiency represents the relation of the existing pressure head created by the pump H, to a theoretical pressure head H_T, i. e.

$$\eta_h = \frac{H}{H_T}.$$

Depending on a design of the pump and its dimensions and also on the quality of the path surface

$$\eta_h = 0.8 - 0.95.$$

Product $\eta_v \cdot \eta_h$ is the internal efficiency of the pump η_{in}.

The mechanical efficiency η_m characterizes power losses for friction in bearings, seals, and also a wheel friction losses by friction at the external walls

of the wheel. The value of mechanical losses differs a lot depending on the pump design. For aircraft pumps

$$\eta_m = 0.9 - 0.95.$$

Full efficiency of the pump

$$\eta_p = \eta_v \cdot \eta_h \cdot \eta_m .$$

The full efficiency defines a part of a useful power N_f (used for liquid pressurizing) in all spent power N_p, i. e.

$$\eta_p = \frac{N_f}{N_p}.$$

Average value of full efficiency for modern pumps is 0.5 … 0.85.

3. Useful power

$$N_f = Q_p \Delta p_p .$$

The required power for a pump driving due to losses is more than the useful power. Taking into account all types of losses the required power is:

$$N_f = \frac{Q_p \Delta p_p}{\eta_p}.$$

6. *The specific speed* is defined as "the speed of an ideal pump geometrically similar to the actual pump, which when running at this speed will raise a unit of volume, in a unit of time through a unit of head". Specific speed is an index number correlating pump flow, head and speed at the optimum efficiency point. It classifies pump impellers with respect to their geometric similarity. This index is important when selecting impellers for different conditions of head, capacity and speed. Usually, high head impellers have low specific speeds and low head impellers have high specific speeds.

Low-specific speed radial flow impellers develop hydraulic head principally through centrifugal force. Pumps of higher specific speeds develop head partly by centrifugal force and partly by axial force. An axial flow or propeller pump with a maximum specific speed generates its head exclusively through axial forces. Radial impellers are generally low flow/high head designs whereas axial flow impellers are high flow/low head designs.

The specific speed is a dimensionless complex following from the theory of pumps similarity. Generally

$$n_s = 20.2 \cdot n \cdot \sqrt{Q_p} \Big/ H^{3/4},$$

where n - rotation speed of the pump shaft, rpm.

The *specific speed* is constant for all similar pumps, and for the same pump doesn't change with the change of the rotation speed.

4.4 Classification of centrifugal pumps

For centrifugal pumps (CFP) the following classification is accepted:

1. By the specific speed:

– low-speed (n_s = 40 - 80);

– average (normal) rapidity (n_s = 80 - 140);

– high-speed (n_s = 140 - 300).

The specific speed shows a geometrical shape of an impeller meridional section (Fig. 4.2). When n_s is small – meridional section of an impeller is narrow and long. With n_s increasing the flow path extends, the relation b_2/D_2 increases, diameters of a discharge and a suction become closer, the relation D_2/D_0 decreases and an impeller gradually turns from the radial in diagonal, and then - into an axial type.

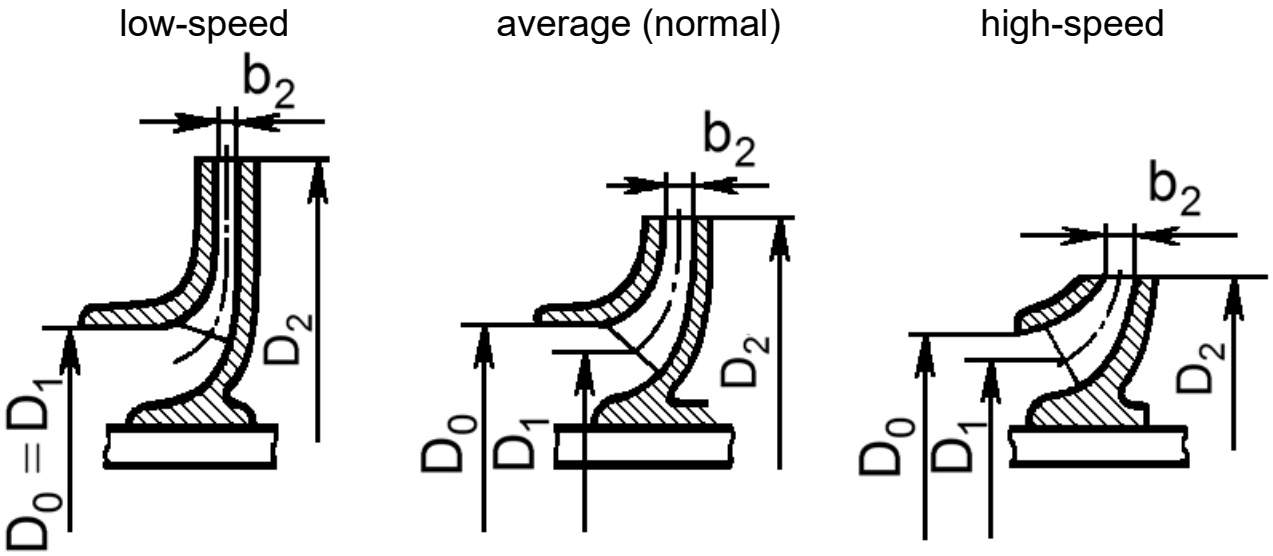

low-speed	average (normal)	high-speed
n_s = 40 - 80	n_s = 81 - 140	n_s = 141 - 300
$D_2/D_0 \approx 2.5$	$D_2/D_0 \approx 2$	$D_2/D_0 \approx 1.4$ - 1.8
$b_2/D_2 \approx 0.04$	$b_2/D_2 \approx 0.08$	$b_2/D_2 \approx 0.1$ - 0.2

Fig. 4.2 – Dependence between impeller shape and specific speed

According to the formula, when rotation speed is constant the higher value n_s corresponds to high flow rate and low pressure. The Q_p increasing and Δp_p reducing leads to increasing in cross section of the impeller path (width) and to size loss of outlet diameter of an impeller. Thus, at great values n_s the impeller duct will be short and wide. With n_s reducing the duct is narrowed, and the relation D_2/D_0 increases.

Aviation pumps, as a rule, have rather low volume flow rate Q_p and low value n_s (not more than 60). Thus, practically all impellers of aviation CFP can be referred to as the low-speed ones.

2. By *impeller design* (Fig. 4.3)*:*

– enclosed;
– semi-open;
– open.

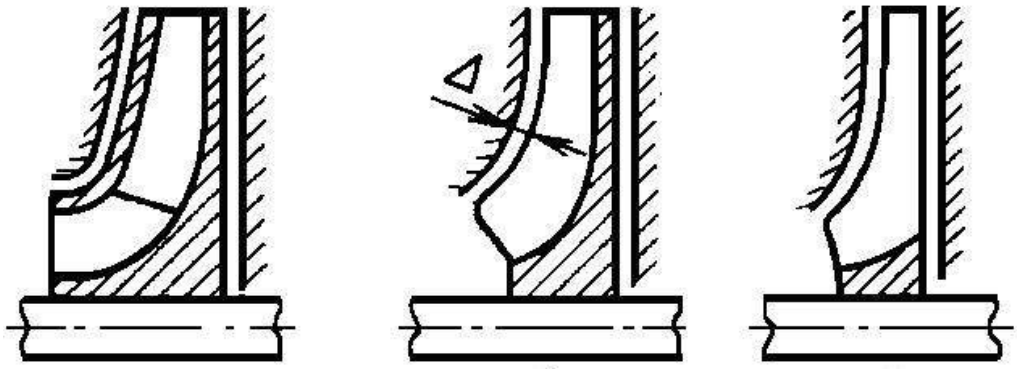

a b c

Fig. 4.3 – Types of centrifugal impellers:
a – enclosed; b – semi-open; c – open

The first two types are applied more often as their efficiency and cavitation performance are better. Open impellers have losses due to overflowing of a liquid through an axial clearance Δ from one side of blade to another. Semi-open and open impellers should have small axial clearance because the clearance increase results in the efficiency fall.

3. By *blades arrangement*:

– forward-facing vanes;
– radial vanes;
– backward-facing vanes.

Impellers with the forward-facing vanes have the highest efficiency. Impellers with backward-facing vanes have the highest pressure ratio.

Impellers with radial blades are the simplest and are inexpensive in manufacturing.

4. By the type of CFP drive:

– with a direct drive from the engine (MPE);
– with the electric drive (ElCFP);
– with an air-operated turbodrive (ATDCFP);
– with a hydraulic drive:
– hydro turbine (HTCFP);
– hydro motor (HMCFP).

5. By the arrangement on the plane:

– inner-tank (the drive of the pump and suction pipe are in a tank, and the pump case with the impeller and discharge – out of a tank);

– out-of-tank (only a suction pipe of the pump is in a tank);

– main (located in pipeline between a tank and the ultimate consumer);

– caisson (the version of inner-tank) for pumping of fuel from a caisson - tanks (entire pump, including discharges, is in a tank).

4.5 Velocity diagram at the inlet of the impeller and the arrangement of the blades

The fuel flows into the impeller eye (Fig. 4.4) with a velocity

$$c_0 = \frac{Q_0}{\frac{\pi}{4} \cdot \left(D_0^2 - d_{hb}^2 \right)},$$

where D_0 and d_{hb} are the outer diameter of the inlet and impeller hub diameter, respectively.

In preliminary calculations the c_0 is considered to be directed along the axis of the pump, not taking into account the possible flow twist (e.g., in a screw booster pump).

The meridional velocity component of the liquid at the blade inlet:

$$c_{1m} = \frac{Q_0}{F_1},$$

where F_1 - the cross sectional area – the surface of revolution. Its generating line is normal to the meridional component of the velocity (see Fig. 4.4).

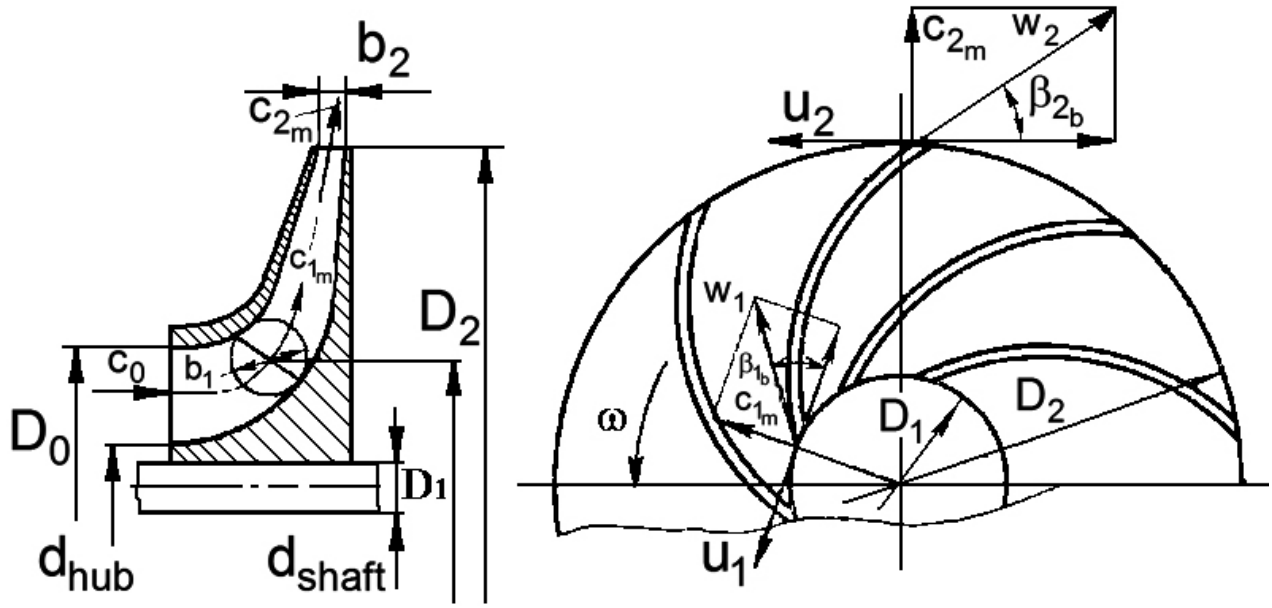

Fig. 4.4 – A flow path of a centrifugal pump impeller

Taking into account blocking of the flow path with blades

$$F_1 = \pi \cdot D_1 \cdot b_1 \cdot \psi_1,$$

where D_1 - the average diameter of the blade inlet edge;

b_1 - the width of the inlet;

$\psi_1 < 1$ - the factor of flow path blocking with blades at the inlet.

According to the diagram in Fig. 4.5

$$\psi_1 = \frac{t_1 - s_1}{t_1} = 1 - \frac{\delta_1 \cdot z_1}{\pi \cdot D_1 \cdot sin(\beta_{1b})},$$

where δ_1 - the thickness of the blade at the inlet to the impeller;

z_1 - number of blades;

t_1 - pitch of the blades;

β_{1b} - the blade installation angle at the inlet.

The value of ψ_1 strongly depends on the size of the pump. For the large LRE pumps ψ_1 = 0.85 - 0.9. For small aviation pumps ψ_1 can be significantly lower, so to reduce flow path blocking at the inlet a significant thinning of the blades is allowed.

The edge of the blades may be parallel to the impeller axis under some angle to it. It is much easier to make blades with edges parallel to the axis of the pump, at the place where the turn of the liquid has been almost completed. The diameter of the inlet at the edge of the blade D_1 is often made equal to the diameter of the impeller inlet D_0 (see Fig. 4.4).

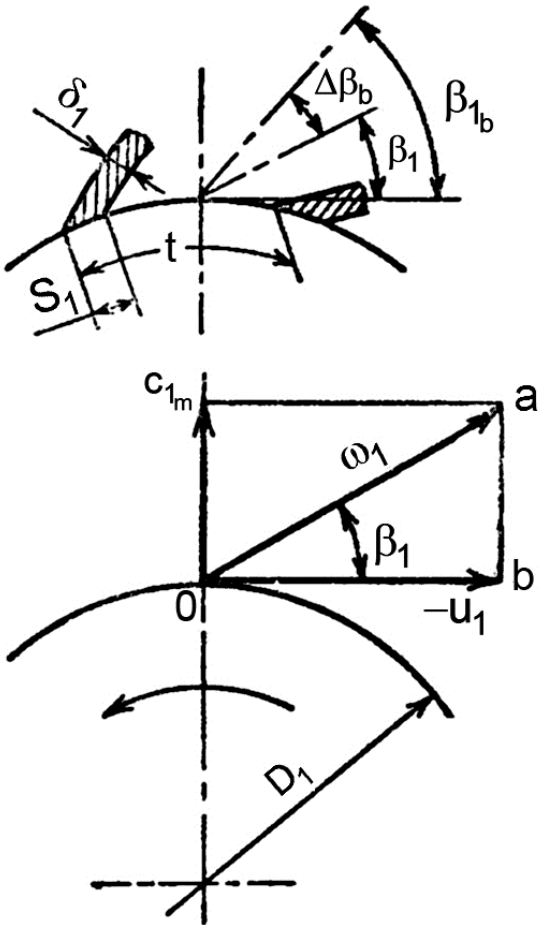

Fig. 4.5 – The velocity diagram at the impeller eye

However, such edges arrangement excludes the inlet part of the impeller from energy transferring to the fluid. Sometimes the blades are made longer and begin from the inlet part of the impeller. The impeller with such blades has better cavitation performance. At the same time to ensure a smooth fluid flow the blade should have complex-shaped surface of double curvature along the

whole edge (as a rotating *inlet guide vanes* of centrifugal compressor in GTE).

Entering the impeller the fluid gets a definite velocity relatively to impeller, called as a relative velocity w. At any point of the impeller its value is the vector difference of the meridional velocity c_m and the circumferential velocity u $\left(\vec{w} = \vec{c} - \vec{u}\right)$. For example, at the inlet of the blade the circumferential speed of the impeller

$$u_1 = \frac{\pi \cdot D_1 \cdot n}{60}.$$

The value of the relative velocity at the inlet can be calculated from the equation

$$w_1 = \sqrt{c_{1_m}^2 + u_1^2}\ .$$

Its direction is determined by the angle that is measured from the negative direction of the circumferential velocity, and

$$tg\,\beta_1 = \frac{c_{1_m}}{u_1}.$$

Fig. 4.5 shows the velocity diagram at the inlet of the blade. It is represented as a triangle *Oab* and therefore is often called as the velocities triangle.

To make the flow enter the impeller without shock, i.e. with minimal losses, the relative velocity of the flow must correspond to the shape of the impeller inter-blade channel. As the pumps operating experience shows, the impeller works better when the blade inlet angle β_{1b} is a little higher than the angle β_1.

Thus, at the impeller inlet blade is bent against the rotation direction at an angle β_{1b} so that the angle of attack of the blade inlet edges $\Delta\beta_{1b}$ is positive

$$\Delta\beta_{1_b} = \beta_{1_b} - \Delta\beta_1 > 0\,,$$

usually $\Delta\beta_{1_b} = 5...15°$.

If the front edge has a large inclination, the different points of this edge have different circumferential velocity u, and the angle $\Delta\beta_{1_b}$ will vary respectively. The pressure drop on the blade inlet is proportional to the square of relative velocity w_1. In order to prevent cavitation, it is desirable that the velocity w_1 to be as less as possible.

From the triangle of velocities it rises that w_1 depends on the c_{1_m} and u_1. And according to the expressions for c_{1_m} and u_1 with increasing the impeller inlet diameter D_0 and hence D_1 a meridional velocity c_{1_m} decreases and the circumferential velocity u_1 increases (Fig. 4.6). Obviously, you can find the most optimum inlet diameter D_0^{opt} that corresponds to minimum value of w_1.

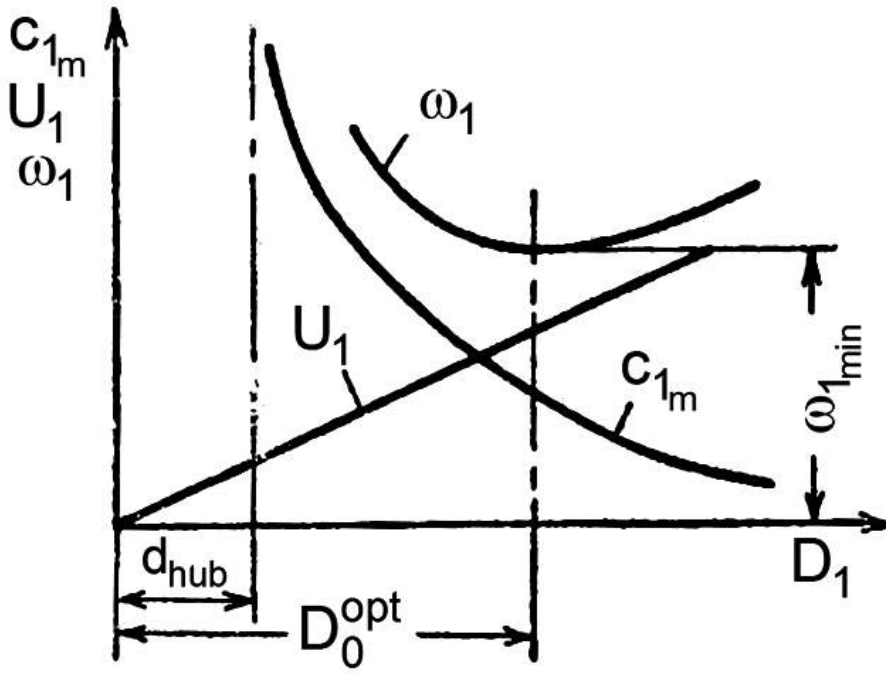

Fig. 4.6 – The changes in velocity as a function of the impeller inlet diameter

If we analyze the condition of minimum pressure drop at the blade inlet we get the equation to define the equivalent diameter. This equation is called 1st Rudnev's formula

$$D_{1e} = (4.4...5)\sqrt[3]{\frac{Q_0}{n}}, \text{ m},$$

where $D_{1e} = \sqrt{D_0^2 - d_{hb}^2}$ is the inlet equivalent diameter.

4.6 Velocity diagram at the outlet of the impeller

Let's consider the velocity diagram at the impeller outlet (Fig. 4.7) where the liquid flow has a definite velocity w_2 relative to the impeller in the inter-blade channel. This velocity can be calculated using the equation of the fluid flow through the impeller channel. The axis of the channel, and hence the flow axis (if the flow coincides with the channel axis), directed relatively to the impeller under the angle of the blades at the outlet of the impeller β_{2b}, measured from the negative direction of the circumferential velocity in the direction of rotation.

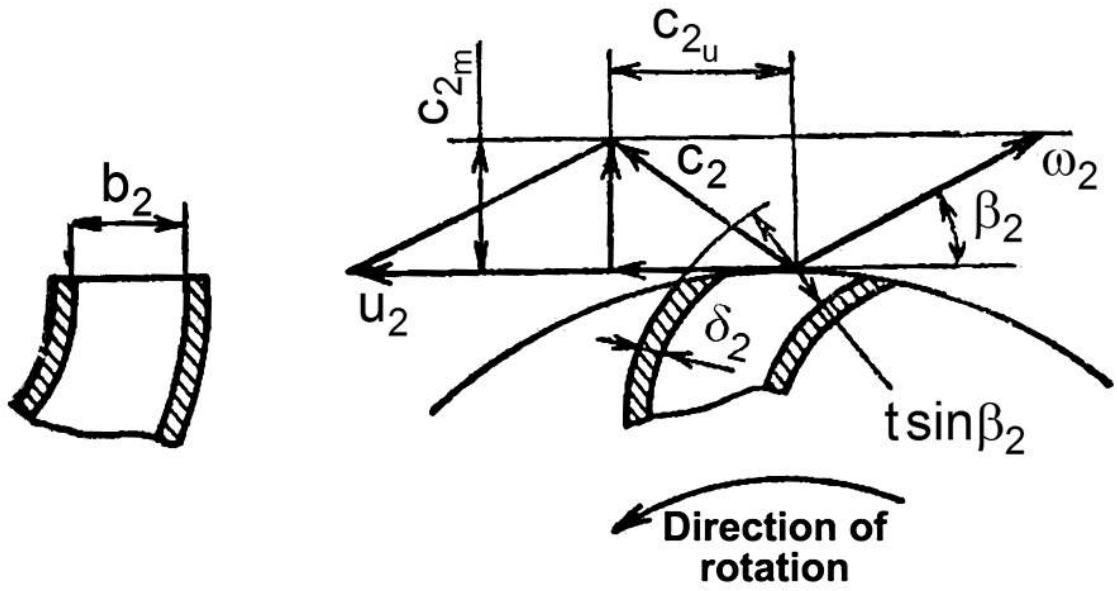

Fig. 4.7 – The velocity diagram at the impeller outlet

The cross sectional area of the channel is equal to the product of the impeller width b_2 and expression $t_2 \cdot sin\,\beta_{2b}$, that is the second cross-sectional dimension of the channel perpendicular to the flow axis.

For the whole impeller the outlet cross-sectional area is $t_2 \cdot z_2 \cdot b_2 \cdot sin\,\beta_{2b}$, but as $t_2 \cdot z_2 = \pi \cdot D_2$, then the cross-sectional area is $\pi \cdot D_2 \cdot b_2 \cdot sin\,\beta_{2b}$.

Therefore, taking into account blocking the flow path with blades at the outlet the relative velocity is

$$w_2 = \frac{Q_0}{\pi \cdot D_2 \cdot \psi_2 \cdot b_2 \cdot sin\,\beta_{2b}},$$

where $\psi_2 < 1$ - the factor of blocking the flow path with blades at the outlet.

As well as for inlet of the impeller

$$\psi_2 = 1 - \frac{\delta_2 \cdot z_2}{\pi \cdot D_2 \cdot sin\,\beta_{2b}},$$

where δ_2 - the thickness of the blade at the outlet of the impeller.

The factor of blocking the flow path with blades at the outlet is 0.93 - 0.97. The direction of the velocity w_2 approximately coincides with the direction of the channel axis, i.e. with the inclination of the blade outlet β_{2b}.

Besides the relative velocity w_2 the outlet flow also has a circumferential velocity of the impeller tip – u_2. The same flow velocity will remain after leaving the impeller due to inertia. The absolute flow velocity at the outlet c_2 is equal to the geometric sum of these two velocities.

The projections of the absolute velocity c_2 on the circumferential velocity direction c_{2u} (circumferential component of the absolute velocity) and on the radius of the impeller – c_{2m} (the meridional component of the absolute velocity) are of great importance in the pump calculations.

Taking into account blocking of the flow by blades at the outlet, meridional velocity is

$$c_{2m} = w_2 \cdot sin\,\beta_{2b} = \frac{Q_0}{\pi \cdot D_2 \cdot b_2 \cdot \psi_2}.$$

The pump impellers are typically designed so that the velocity c_{2m} is equal to or little lower than c_{1m}.

Circumferential component of the absolute velocity c_{2u} can be calculated based on the fact that in any direction the sum of component projections is a resultant projection. Projection of circumferential flow velocity u_2 on the tangential direction is equal to itself, and the projection of the relative velocity

$$-w_2 \cdot cos\beta_{2b} = -\frac{c_{2m}}{tg\beta_{2b}},$$

whence from the velocity diagram (see fig. 4.7) we obtain the relation

$$c_{2u} = u_2 - \frac{c_{2m}}{tg\beta_{2b}}.$$

4.7 Theoretical head of a pump

Theoretical pressure head created by centrifugal pump can be calculated from Euler equation

$$H_{th\infty} = u_2 \cdot c_{2u\infty} - u_1 \cdot c_{1u},$$

where $H_{th\infty}$ - the pressure head generated by the impeller with an infinite number of blades;

c_{1u} - circumferential component of the absolute velocity at the inlet.

Since the inlet flow twist in circumferential direction (i.e. velocity c_{1u}) ceteris paribus reduces the pump pressure, the flow should come the impeller radially to ensure c_{1u} equal to zero. Then the formula of the theoretical head turns into the main pump design equation

$$H_{th\infty} = u_2 c_{2u\infty}.$$

This pressure head consists of increasing the static pressure of the liquid and the dynamic pressure due to increasing its absolute velocity.

Since $u_2 = \frac{\pi \cdot D_2 \cdot n}{60}$ and a value of c_{2u} is proportional to u_2 (because $u_2 \gg \frac{c_{2m}}{tg\beta_{2b}}$), the theoretical pump head will depend on the square of the tip speed, i. e.

$$H_{th\infty} = k_p \cdot u_2^2 = k_p \left(\frac{\pi \cdot D_2 \cdot n}{60} \right)^2,$$

where k_p < 1 - the coefficient determined by the design of the pump.

The last formula shows that for a given impeller size pressure is proportional to the square of the speed, and at a given rotation speed is proportional to the square of the impeller diameter.

Using the Euler's formula, it is necessary to put there the actual velocity c_{2u}, which fluid has at the outlet of the impeller. According to the outlet velocity diagram we assume that the stream in the impeller strictly follows the profile of the blades. However, this situation is possible only in theory, when the infinite number of infinitely thin blades are placed on the impeller. At a finite number of blades only the flow near the blade surface (in the direction of the impeller movement), follows its profile. More distant from the blade fluid have an outlet angle β_2 smaller than the angle β_{2b} by the lag angle $i = \Delta\beta_2$ (Fig. 4.8). For this reason (see Fig. 4.7) at the same value of the w_2 velocity c_{2u} for distant flow is smaller, and the pressure head is also smaller.

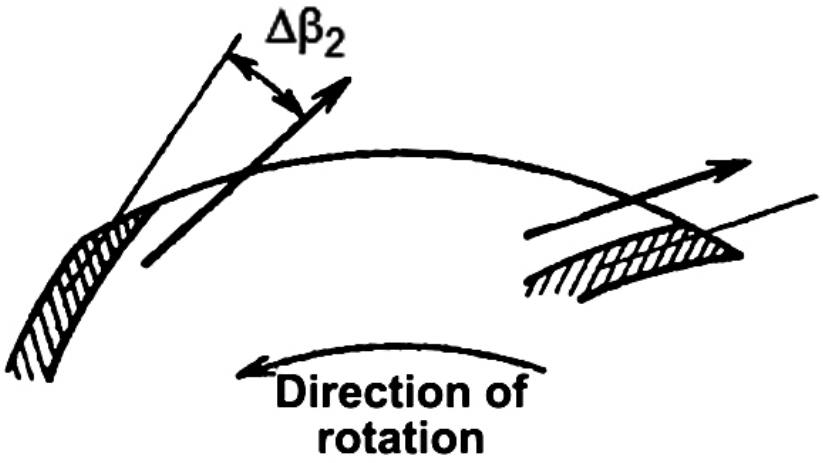

Fig. 4.8 – The flow lag angle $i = \Delta\beta_2$

By averaging the pressure head through the entire flow, overall theoretical pressure head created by the impeller with a finite number of blades H_{th} is less than the pressure that would have created by the impeller with an infinite number of blades $H_{th\infty}$. Relation between these pressures is determined by the ratio

$$H_{th} = \frac{H_{th\infty}}{1+p},$$

where p - is a factor which takes into account the pressure fall due to a finite number of blades; the greater the pressure fall, the higher the p.

The value of p can be calculated by the approximate formula

$$p = 2 \cdot \frac{\varphi}{z_2} \cdot \frac{1}{1-\left(D_1/D_2\right)^2}.$$

The value of p and, consequently, the pressure fall will be greater the smaller the number of blades z_2 and the shorter the channel between the blades (the higher ratio D_1/D_2). The value of φ takes into account the processing quality and the value of the outlet blade installation angle. For the centrifugal impellers this ratio is

$$\varphi = \left(0.55 - 0.68\right) + 0.6 \sin \beta_{2b}.$$

The pressure head fall due to the finite number of impeller blades doesn't increase the work or power necessary for the impeller rotation. It is because if the impeller does not quite twists the flow, then the energy of incomplete twist is not taken by the flow from the impeller. Thus, head losses due to the finite number of blades need only change in the impeller size or increasing rotation speed (increasing of u_2), but does not lead to loss of work and should not be considered in impeller efficiency factors.

As it seen from the formula for the impeller theoretical pressure head, it depends on the velocity diagram at the outlet of the pump. Velocity diagram significantly depends on the value of the angle β_{2b}.

4.8 Cavitation in centrifugal pumps

Cavitation (cold boiling) is the formation of vapor cavities in a liquid – i.e. small liquid-free zones ("bubbles" or "voids") – that are the consequence of forces acting upon the liquid. It usually occurs when a liquid is subjected to rapid changes of pressure that cause the formation of cavities where the pressure is relatively low. When subjected to higher pressure, the voids implode and can generate an intense shock wave.

Cavitation is a significant cause of wear in some engineering contexts.

Collapsing voids that implode near to a metal surface cause cyclic stress through repeated implosion. This results in surface fatigue of the metal causing a type of wear also called "cavitation".

The most cavitation hazard in a centrifugal pump is at the impeller blade inlet edge where the full pressure of the fluid is minimal (pump has not given the energy to the liquid yet) but the absolute and relative flow velocities are still great.

The high relative velocity at the inlet to the blade is the reason of the reduced pressure zone at the rear side of the blade (Fig. 4.9), i. e. of a cavitation. In addition, the non-uniform field of absolute velocities at the inlet of the impeller causes additional pressure drop in the zones, where the velocity is higher than the average.

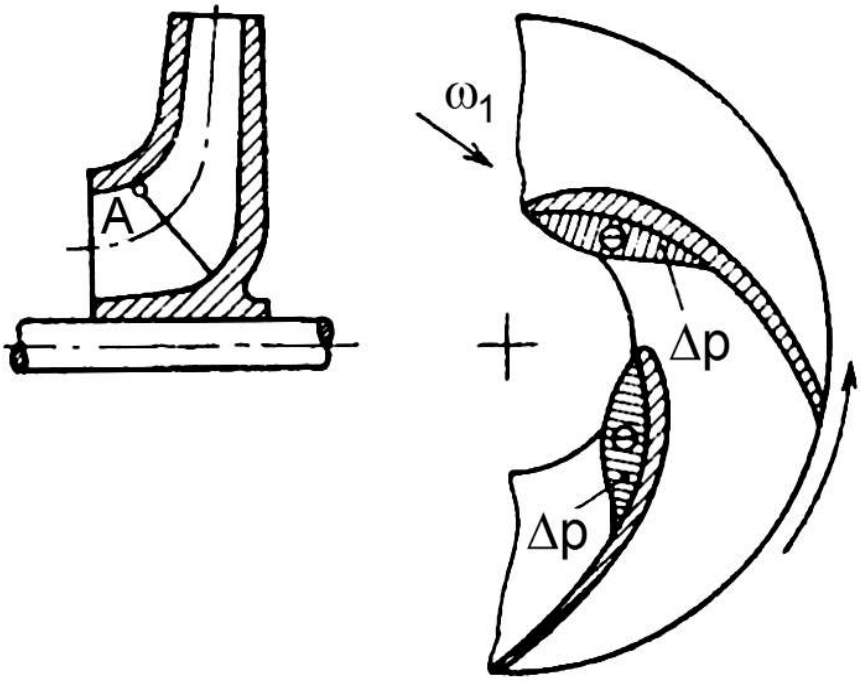

Fig. 4.9 – The low pressure field in the flow around pump blades

Cavitation-free operation condition

$$p_{in} > p_s + \Delta p_{cav.min},$$

or

$$p_{in} - p_s > \Delta p_{cav.min}.$$

Value $p_{in} - p_s$ represents the pressure difference, which can be still used for increasing the flow velocity without cavitation, and is called as positive suction head.

Ceteris paribus, increase of the pump rotation speed n and flow rate Q_0 results in increasing the relative and absolute flow velocities and, consequently, increasing the cavitation hazard. With the n and the Q_0 growth the cavitation on the blades occurs under lower inlet pressure.

As a result of the cavitation, the volume supplied by the pump, is filled with vapor, the pressure head and the flow rate of supplied liquid decrease. That's why cavitation is unacceptable in aviation pumps.

Change in pressure head during cavitation is described by the so-called cavitation performances.

There are two types of performances: stall performances (Fig. 4.10, a, b), i. e. the pressure head H dependence on the inlet pressure p_{in} (or difference $p_{in} - p_s$), and cavitation performances, which express the dependence between the limiting inlet pressure $p_{in.min}$ (below which cavitation takes place) and the rotation speed n and flow rate Q_0. Stall performances are obtained as a results of the test for a given pump flow rate and rotation speed.

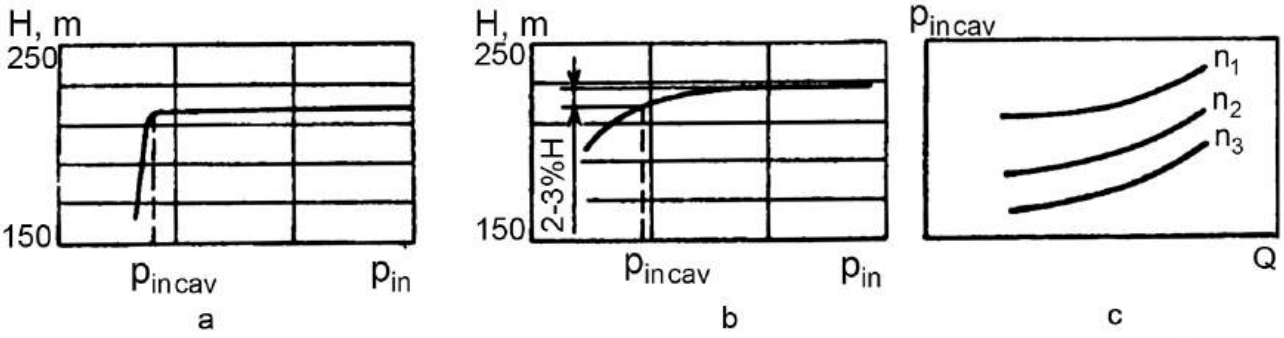

Fig. 4.10 – Cavitation performances:
a, b - stall performances; c - cavitation performances

The limiting inlet pressure $p_{in.min}$ (below which cavitation takes place) is a pressure that results in a pressure head drop of 2 – 3 %. Cavitation performances $p_{in.min} = f(n, Q)$ are based on a series of tests (Fig. 4.10, c). Cavitation properties of the pump can be precisely defined only experimentally.

When calculating the pump, one of the main task is to determine the maximum allowable rotation speed from the cavitation free operation condition

under a given inlet pressure and flow rate. From the condition of the cavitation-free operation

$$p_{in} - p_s > \Delta p_{cav.min}$$

and making the analysis of the $\Delta p_{cav.min}$ components, one obtain formula for calculating the maximum allowable pump rotation speed (2-nd Rudnev's formula)

$$n = \frac{C_{cav}}{31.2\sqrt{Q_0}} \Delta H_{cr}^{3/4}, \text{ rpm.}$$

Here C_{cav} = 800…1100 m/s – cavitation specific speed;

$$\Delta H_{cr} = \frac{p_{in} - p_s(T)}{\rho} + \frac{c_0^2}{2} - \Delta H_{res} \text{ – cavitation margin,}$$

where $p_s(T)$ – saturated vapor pressure of fluid under the definite inlet temperature, Pa;

c_o – flow velocity at the pump inlet 2 - 3 m/s;

ΔH_{res} – cavitation reserve 20 - 30 J/kg.

Specific cavitation speed (critical cavitation factor) is determined experimentally and describes the pump cavitation quality, i.e. the degree of pump tendency to cavitation under low p_{in}. The first time this factor was proposed by S.S. Rudnev, so it is often called as the Rudnev factor. For conventional pumps C_{cav} = 800...1100 m/s. For impellers with high anti-cavitation properties of special shape and special blade profiling, C_{cav} can reach 2000...2200 m/s. Using the axial or screw pump as a booster (which is one of the main method to prevent cavitation), the C_{cav} value increases up to 3000...3100m/s. Screw booster pump not only increases the pressure of the liquid, but also creates a twisted flow, thus reduces the relative velocity of the fluid at the pump inlet. Two - or three - start screws are usually used; pressure

head of a screw pump is 3 - 20% of the total head.

Pump anti-cavitation properties depend on the design (the number and the length of the blades, the angle of attack, the use of double-inlet, the use of oversized impellers), as well as the thermodynamic properties of the fuel being supplied.

5 FUEL SPRAY NOZZLES

5.1 General

Fuel atomization is the process of liquid transformation in the great number of small droplets. The fuel atomization increases the ratio between the liquid entire surface and its volume making the fuel evaporate faster. The fuel atomization and its evaporation are the key aspects of the combustion chamber (CC) operation.

There are many types of the fuel spray nozzles (next – fuel nozzle).

The degree of atomization mostly depends on a pressure drop, a spray cone, radian and circumferential flow distribution at different distances from the orifice.

The pressure drop for the satisfactory atomization is approximately 0.1-0.15 MPa. For the high-quality atomization, the pressure drop is recommended to be within the range 6-12 MPa.

The air/fuel mixture preparing starts from the fuel atomization. The FSN are arranged in the combustor dome in the frontal part of the flame tube. The fuel nozzle may fall into four categories: pressure fuel nozzle, pressure-swirl fuel nozzle, air-atomizing fuel nozzle, vaporizing fuel nozzle.

All existing nozzles implement two atomization principles. The first principle is called centrifugal, the second – spray. The spray nozzles discharge the fuel through the cylindrical orifice (Fig. 5.1). The spray range of the spray nozzle is substantial. These nozzles suite most of all for the preliminary sizing. They are used because they are of the simpler construction and their production cost is much lower. These nozzles find their use in the afterburners of the aircraft engines. The temperature of the gas flowing through the afterburner is very high, therefore the vaporization makes no problems. The typical spray angle (2α) of these nozzles is 10-15°.

The swirl fuel nozzles implement the centrifugal atomization principle. They are widely used in the propulsion engineering. The operation of the swirl fuel nozzle is shown in Fig. 5.2.

The fuel nozzle is a unit consisting of a swirl chamber that ends with the orifice. The tangential channels feed the swirl chamber with the high pressure fluid. When the fuel gets to the orifice from the swirl chamber, it intensively rotates. Finally the heavily swirled spray leaves the orifice.

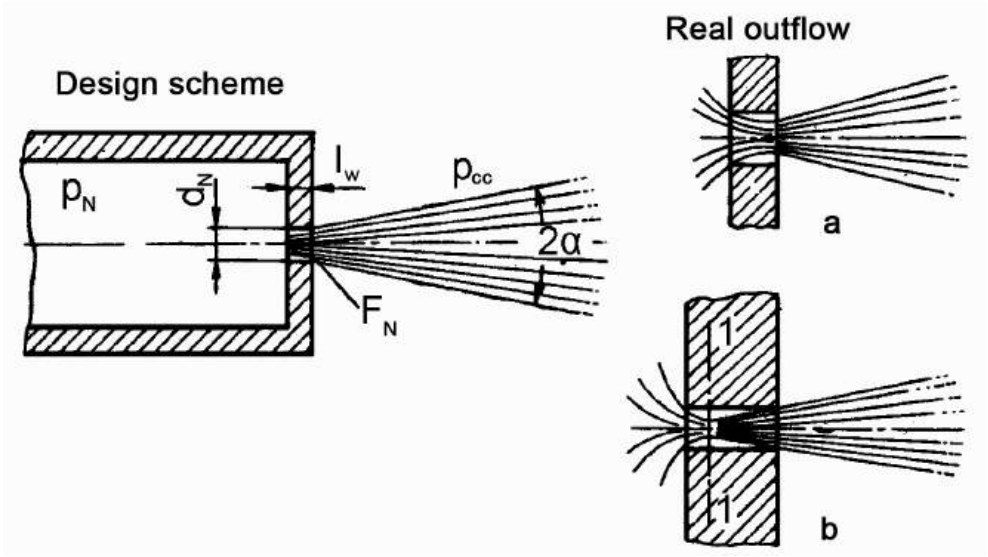

Fig. 5.1 – The spray nozzle scheme:
a - the short nozzle; b - the long nozzle

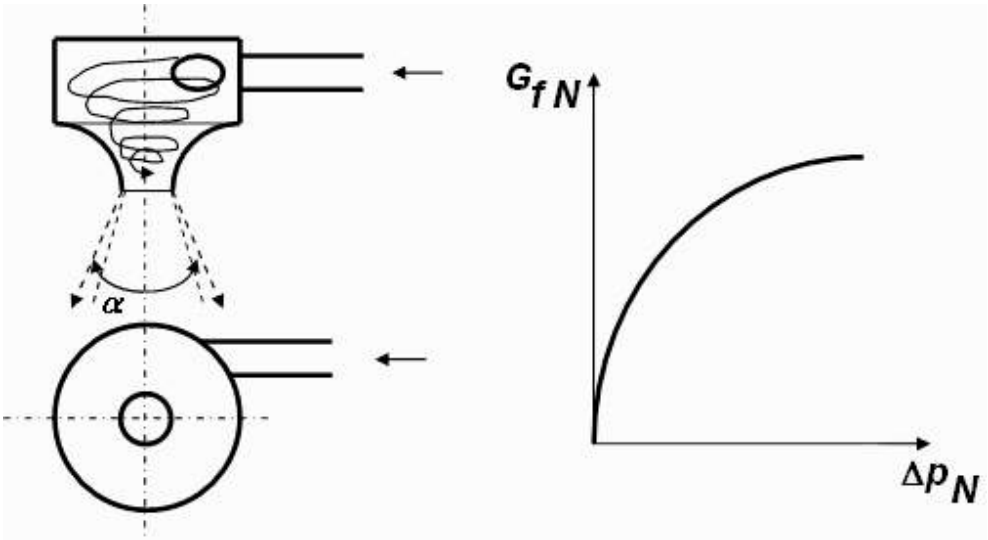

Fig. 5.2 – Fuel nozzle operation

Being acted by the aerodynamic and mass forces, the annular stream at the nozzle discharge rapidly expands and forms the hollow cone (the spray cone). Next, the spray cone becomes thinner and finally breaks out to small droplets. The latest ones are mixed well with the twisted by the flame stabilizer primary air.

A spray cone is characterized with the spray angle, which in its turn depends on how intensively has the fuel been swirled.

The spray cone is characterized by the spay angle, which is within the range $2\alpha = 40 - 120°$. The higher values correspond to a greater swirl intensity.

The main problem that is assigned to the designers developing a new fuel spray nozzle is an atomization quality. This is an especially hard task for the

gas turbines because they are multimode objects. The main issue is that fuel flow rate is proportional to the squared root of pressure drop. Hence, to decrease the fuel flow rate 40 times, the pressure drop must be reduced 1600 times. Simple analysis shows that the pressure drop at the idle mode must be 0.004-0.006 MPa in case of the 6-9 MPa nominal pressure drop. This is not sufficient for any atomization. The other problem is that the spray cone remains almost constant at different modes, but it is preferable to decrease it at the low modes.

A duplex nozzle is the nozzle with two fuel feeding channels. The inner channel is called pilot. It is of a lower diameter. The fuel flow passing through the pilot channel is relatively small. The fuel is supplied through both channels at the nominal and higher modes (Fig. 5.3). Opposite to the simplex nozzle, the duplex one atomizes the fuel efficiently at all modes. It also provides the required spray angles at the idle mode. This is achieved by the proper design of a pilot channel.

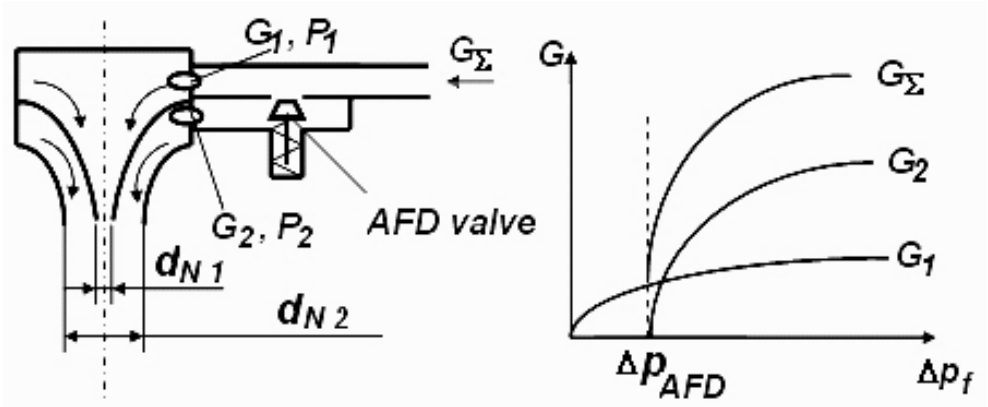

Fig. 5.3 - Operation of the duplex two-orifice fuel nozzle

5.2 Analysis and design

Equation of the liquid flow rate through the fuel spray nozzle

Let us consider the 1D inviscid flow. In this case, the ideal secondary flow rate is calculated as

$$G_{N\,id} = \rho F_N c_{a\,id},$$

where $G_{N\,id}$ is an ideal flow rate;

F_N is a cross-sectional area of the nozzle orifice discharge;

$c_{a\,id}$ is an axial velocity at the orifice discharge;

ρ is a fluid density.

The velocity is determined from the Bernoulli`s equation for the incompressible fluid

$$p_{in} = p_g + \frac{\rho c_{a\,id}^2}{2},$$

where p_{in} is the pressure at the nozzle inlet;

p_g is the pressure in the combustion chamber or in the another cavity with the considered nozzle.

Let us substitute the axial velocity at the orifice discharge from the Bernoulli`s equation to the fuel flow rate equation.

$$G_{N\,id} = F_N \sqrt{2\rho \Delta p_N},$$

where $\Delta p_N = p_{in} - p_g$ is the pressure drop at the nozzle.

A flow factor is the ratio of the real flow rate through the nozzle to the ideal one. It is evaluated as

$$\mu_N = \frac{G_N}{G_{N\,id}},$$

whence the real flow is

$$G_N = \mu_N F_N \sqrt{2\rho \Delta p_N}.$$

5.3 Spray nozzle

The flow is discharged as a single stream or some streams (Fig. 5.4). These spray nozzles may be of the different design and hence discharge the flow in different ways. The spray nozzle is usually designed to provide the attached flow (see fig. 5.4, c, d). The transfer from the attached flow to the separated flow in these nozzles is affected by numerous factors, such as the inlet conditions (radial velocity component), the geometrical parameters, the pressure drop, temperature and pressure of the fluid, the pressure and the temperature in the discharge cavity (the cavity to which the fluid is discharged), the chamfers and the roundings, surface quality, and many others.

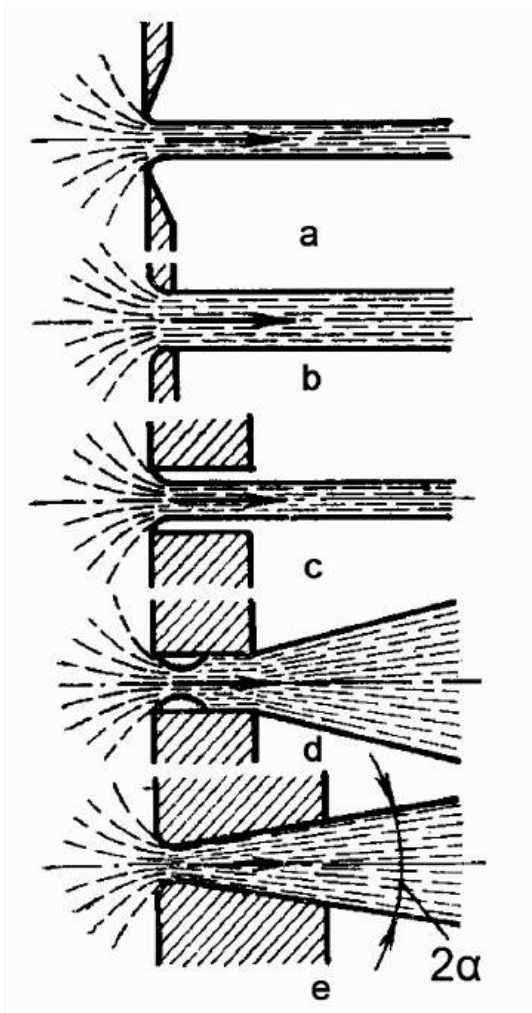

Fig. 5.4 – Examples of the fluid injection:
a – a sharp end orifice;
b - a rounded end orifice;
c – a sharp end orifice with the great length to diameter ratio;
d – a separated flow orifice;
e - Venturi tube

The flow in the nozzle depends on the length to diameter ratio (l/d) (see Fig. 5.4). If the inlet orifice has the sharp edges and the l/d ratio is less than 1.5, then the flow is unstable. This happens because the confuser portion (see Fig. 5.4, c) is not looped or is looped at different distances from the orifice discharge (this depends on the arbitrary factors).

If $l/d > 1.5$ then the flow is loop and stable (see Fig. 5.4, d). In this case, the hydraulic resistance can be evaluated by the well-known formulas. The used formula depends on the flow mode. The relation $\mu_N = f(Re, l/d)$ has been deduced from the analytical relations and the experimental data. The example of such relation is presented in Fig. 5.5. This graph describes the experimental data well enough.

If the nozzle channel has a bottleneck where the flow moves at the high speed and the low pressure, then the cavitation may originate in case l/d ratio is greater than 1.5. The flow narrows in case of the sharp inlet to the nozzle or the conical portion with the apex angle more than 20°). The cavitation causes the reduction of the flow coefficient. However, if the nozzle inlet edge is

rounded, the flow path has no conical portions with the apex angle more than 20° and the relative length of the conical portion exceeds 1.5, then the cavitation is rear and its effect is insignificant.

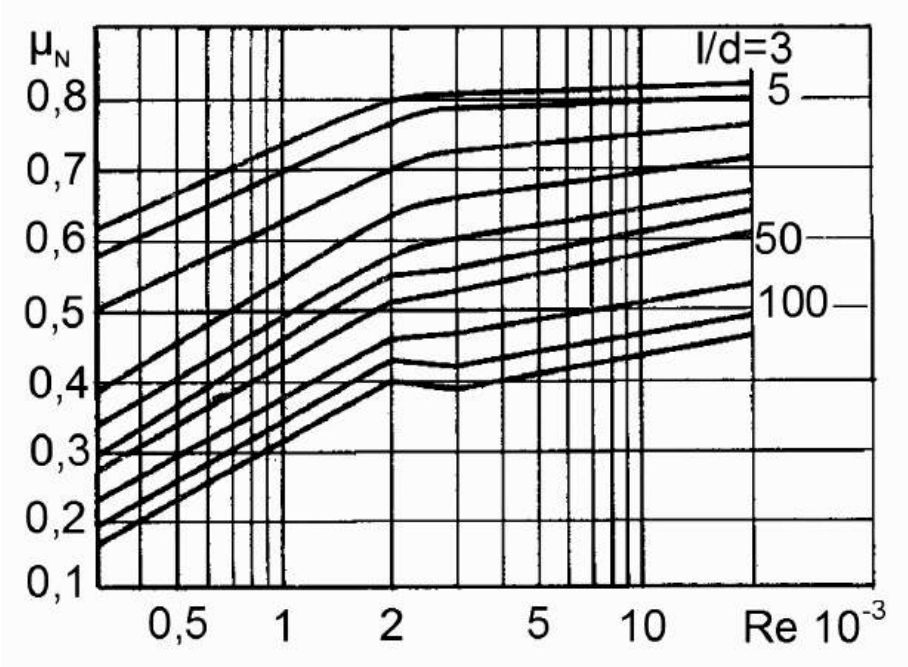

Fig. 5.5 – Dependence of the flow factor vs Reynolds number at different l/d ratios

The nozzles that are under the development may have different l/d ratios, diameter of the fuel nozzle (3-6 mm), flow factors (0.65-0.85), spray angle $(2\alpha = 10 - 15°)$.

5.4 Swirl fuel nozzle

Simplex fuel nozzle

Such parameters of the simplex fuel nozzle as the spray angle, the flow factor, the droplet size vary within the wide range at the constant pressure drop. They mostly depend on the geometrical parameters of the fuel nozzle. This enables an opportunity for the designer to simply affect the mixing.

Operation of the swirl fuel nozzle is different from the spray fuel nozzle operation. The fluid is supplied to the swirl fuel nozzle (Fig. 5.6) through the tangential channels 3. That is why, the angular momentum relative to orifice axis at the swirl fuel nozzle inlet is not zero. The fluid flows through the nozzle and rotates at the same time. The rotation generates the considerable centrifugal force. Hence, being acted by the centrifugal force, the stream

transforms to thin film cone. This thin film is called the spray cone. Next, the centrifugal force demolishes the film and forms the small droplets. The droplets scatter straight. Their trajectories are tangential to their previous trajectories.

Let us consider the theoretical bases of the simplex swirl fuel nozzle for the ideal fluid. The swirl nozzle we consider has a single tangential channel.

Let us suppose that the mass of the fluid entering the swirl chamber is concentrated at the tangential channel axis (see Fig. 5.6). Then the fluid velocity c_{in} in the tangential channel is equal to the circumferential velocity at the swirl chamber inlet. Let us designate the inlet radius of the fluid rotation around the nozzle axis as R_{in}.

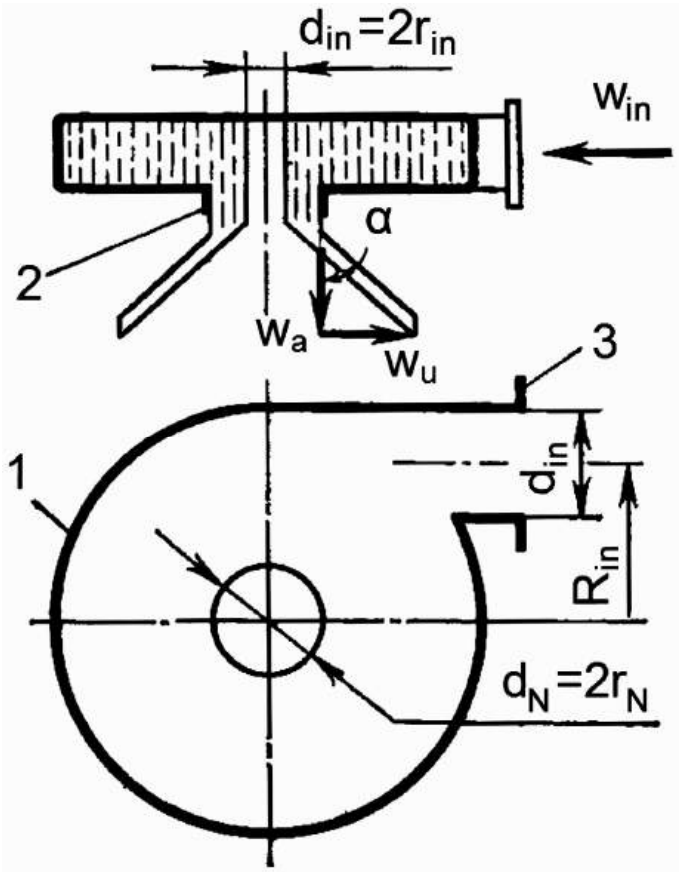

Fig. 5.6 – The design scheme of the swirl fuel nozzle

In case of the ideal nozzle (no friction in the channels and no local resistances), the flow through the swirl nozzle obeys the angular momentum conservation law:

$$c_{in}R_{in} = c_u r;$$

$$p_{in} = p_g + \frac{\rho c_a^2}{2} + \frac{\rho c_u^2}{2} \text{ or } \Delta p_N = \frac{\rho c_a^2}{2} + \frac{\rho c_u^2}{2},$$

where c_a and c_u are axial and circumferential components of the fluid particle;

p_g is a static pressure at the orifice outlet;

r is a radius of the particle rotation relative to swirl nozzle axis.

Let us analyze the momentum conservation laws. It is obvious that as the radius of the particle rotation approaches zero $(r \to 0)$, the circumferential component of the velocity approaches the infinity $(c_u \to \infty)$. The pressure of the fluid approaches the great negative value, which makes no physical sense. In fact, the pressure decreases only to the pressure in the discharge cavity (in case this cavity is a combustion chamber, then pressure is equal to p_g). The cavity part, where pressure is equal to the pressure at the discharge cavity is not filled with the fluid. This cavity rotates forming the vortex of r_v radius. Hence, the closer stream flows to the orifice axis, the greater axial component of the velocity becomes. It reaches the extreme value at the boundary of the gas vortex.

The gas vortex occupies the whole swirl chamber height. That is why the fluid outflows only through the small annular area next to the orifice wall. So, the parameter, which characterizes the ratio of area filled with fluid to the entire orifice area is called effective area ratio.

$$\varphi = F_{fluid} \big/ F_N = 1 - r_a^2 \big/ r_N^2 ,$$

where r_N is a fuel nozzle orifice.

The distribution of the axial component of the flow velocity at the fuel nozzle orifice discharge obeys the condition $c_a^2 \big/ 2 = const$, i. e. axial component of the particle velocity at the orifice discharge is the same for all particles and is radius independent.

Following the mass conservation law for the nozzle inlet and the orifice discharge, we get

$$c_{in} \cdot i \cdot f_{in} = c_a \cdot \varphi \cdot \pi \cdot r_N^2 ,$$

where f_{in} is an area of the single channel at the nozzle inlet, i is the number of the channels.

Let us set the relation between c_a and c_{ua}. Following the mass conservation law we get

$$c_{ua} = A\frac{\varphi}{\sqrt{1-\varphi}}c_a,$$

where $A = \frac{\pi \cdot R_{in} \cdot r_N}{i \cdot f_{in}}$.

The nondimentional parameter A depends on the geometrical parameters. It is of the great importance in the design and the analysis of the swirl fuel nozzle. This parameter is called geometrical composite parameter.

Using the expression for the flow factor μ_n, one obtains

$$\mu_N = \frac{G_N}{G_{N\,id}} = \frac{c_a}{c_{a\,id}}\varphi,$$

whence $\mu_T = 1\Big/\sqrt{1/\varphi^2 + A^2/(1-\varphi)}$.

To obtain the flow factor μ_N you should know the effective area ratio φ, which depends on the gas vortex size. Many approaches to the fuel nozzle design regard that there must be an optimal diameter of the gas vortex that provides the maximum output at some available head. The effective area ratio φ in this case corresponds to the extreme flow factor μ_N. Let us differentiate the considered above equation to get the extreme ratio between the geometrical composite parameter and the effective area ratio:

$$A = (1-\varphi)\Big/\sqrt{\varphi^3/2}.$$

If we substitute the expression for the flow factor formula, we will finally obtain:

$$\mu_N = \sqrt{\varphi^3/(2-\varphi)}.$$

The latest equation and the equation for $A = A(\varphi)$ prove that the flow factor μ_N of the swirl fuel nozzle and the effective area ratio φ are constant at different operational modes (this statement runs only for the inviscid and incompressible fluid). They depend only on the geometrical composite parameter.

Let us determine the spray angle (2α) of the swirl fuel nozzle. It depends on the ratio between the circumferential and axial components of the particle velocity (Fig. 5.7):

$$tg\alpha = c_u / c_a .$$

As $c_a = const$ and c_u varies, so α varies along the orifice discharge radius. It increases when attaining to the axis. Therefore, the stream leaving the orifice has the shape of a hollow cone.

To facilitate the calculations, the designers usually use the averaged spray angle α_{av}. This angle is determined by some averaged $c_{u\,av}$. The $c_{u\,av}$ is determined at the mean radius, which is calculated as $r_m = (r_a + r_N)/2$. Finally, the formula for α_{av} calculation is

$$tg\alpha_{av} = \frac{2\mu_N}{\sqrt{\left(1+\sqrt{1-\varphi}\right)^2 - 4\mu_N^2 A^2}}.$$

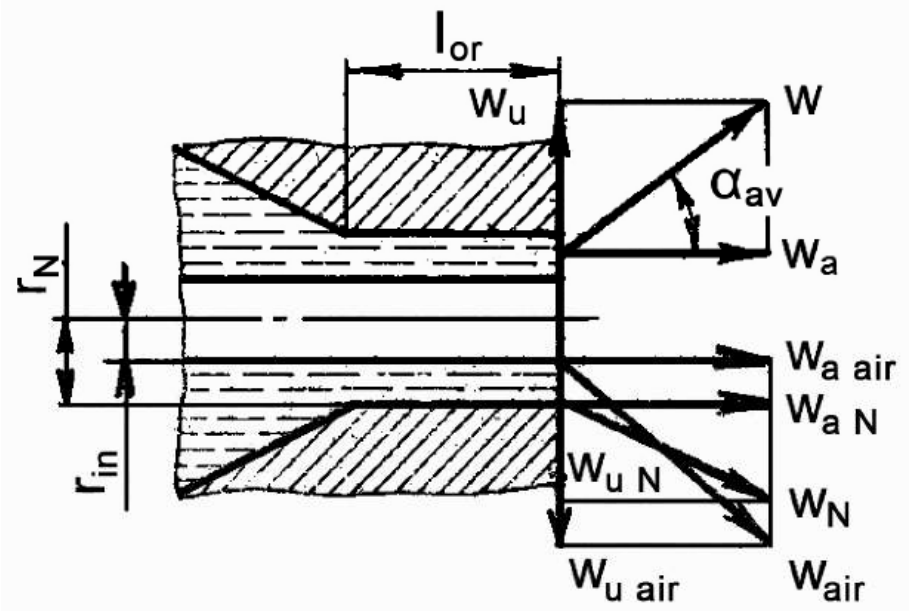

Fig. 5.7 – The velocity and the direction of the liquid particles at the orifice discharge

The dependence of μ_N, φ, and $2\alpha_{av}$ on the geometrical composite parameter are presented in Fig. 5.8.

To design the fuel nozzle, which spray cone is $2\alpha_{av} = 90 - 100^\circ$, its geometrical composite parameter must be within the range 3-5.

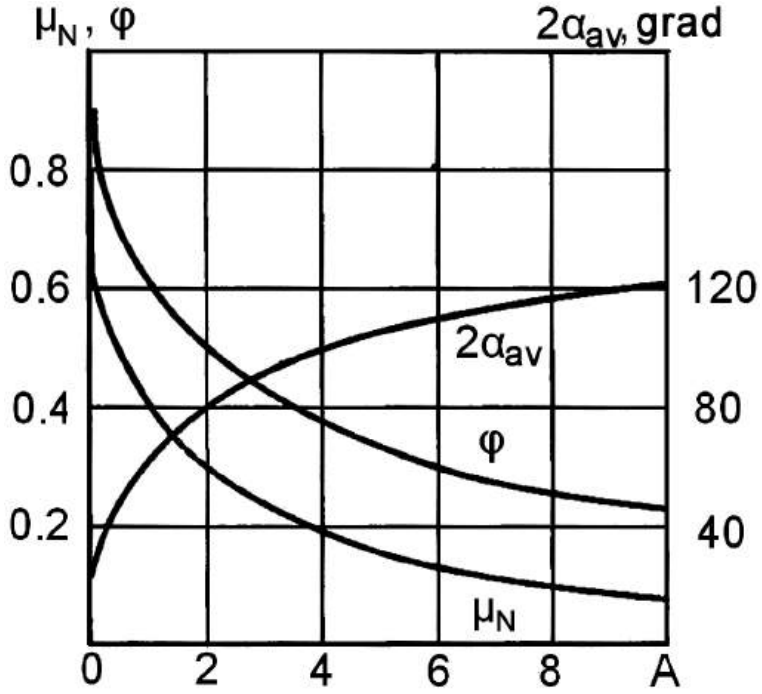

Fig. 5.8 – The dependences of μ_N, φ, and $2\alpha_{av}$ on the geometric composite parameter

The flow factor of such nozzles is 0.25-0.15, i. e. it is considerably less than of the spray nozzles. If the inlet channels are at an angle β to the axis to the orifice axis, then the composite geometrical parameter is calculated as

$$A = \frac{\pi R_{in} r_N}{i f_{in}} \sin\beta .$$

When the fluid is viscous, the flow factor and the averaged spray cone change due to friction forces. Friction makes the swirling effect less intense and, consequently, reduces the circumferential velocity component and at the same time increases the axial velocity. The atomization of more viscose fluids (the flow factor μ_N is high) happens at lower averaged spray cone angle $2\alpha_{av}$.

The simplest of the standard methods to consider the viscosity is to introduce the so-called equivalent composite geometrical parameter of the nozzle

$$A_e = \frac{\pi R_{in} r_N}{i \cdot f_{in} + \frac{\pi\lambda}{2} R_{in}\left(R_{in} - r_N\right)} sin\beta,$$

where λ is a friction factor, which is calculated as

$$lg\,\lambda = \frac{25.8}{\left(lg\,Re\right)^{2.58}} - 2.$$

The Reynolds number in the is determined as

$$Re = \frac{2\,G_N}{\rho \cdot \nu\sqrt{\pi \cdot i \cdot f_{in}}},$$

where ν is a kinematic viscosity at the given temperature.

The tangential channels interconnect the pre-swirl chamber with the swirl chamber. This is essential to make the fluid move tangent to a swirl chamber wall. These channels have the definite length. In case of the short tangential channels, the flow does not have time enough to take the right direction. It turns to the swirl chamber axis. Thus, the momentum becomes less and the flow factor becomes more compared to the one deduced before. The averaged spray cone angle $2\alpha_{av}$ also becomes less. The relative inlet duct length $\overline{l}_{in} = l_{in} \Big/ \left(2\sqrt{f_{in}/\pi}\right)$ (where l_{in} is the inlet duct length) should be at least 1.5-2. The number of the tangential channels may vary from 2 to 8. The swirl chamber is considered normal when the condition $H \le 2R_{in}$ (where H is a swirl chamber height) is followed. Longer swirl chambers have lower circumferential components of the velocity because of the friction. The friction also lead to the bigger flow factor and low averaged spray cone angle. The friction affects in the same manner at great R_{in}/r_N ratio. The recommended maximum R_{in}/r_N is 2.5.

Numerous experimental data show that the flow conditions in the nozzle make almost no effect on the flow factor. They also prove that the mentioned conditions make a very small effect on the spray cone angle. Usually the recommended ratio of $l_N/2r_N$ is about 0.25.

5.5 Duplex fuel nozzle

Fuel gets to the duplex nozzle through two manifolds in a definite proportion. Usually the pilot channel supplies the idle fuel. The main channel supplies the fuel at the above idle operational modes. Both channels operate simultaneously at the maximal, the cruise and other modes. Hence, the relation between the fuel flow rates through the pilot and through the main channel can be expressed as

$$G_{main} = G_{fuel} - G_{fuel\ idle},$$

where G_{main} and $G_{fuel\ idle}$ are secondary fuel flow rates through main and pilot channels respectively.

As you already know, the nozzles can be simplex or duplex. The duplex nozzles with the pilot channel arranged inside the main channel are the most interesting for being considered (Fig. 4.9).

The analysis of the duplex fuel nozzle is very similar to the simplex fuel nozzle analysis. Designers must make sure that the radius of the gas vortex formed by the main channel is greater than the outer radius of the pilot nozzle.

The spray cones of the pilot orifice and the main orifice can intersect each other, be in the contact with each other or do not interact with each other. The case depends on the geometrical parameters of the channels, mutual positioning of the orifices and the ejection velocities of the fuel flows. The duplex nozzle can be considered as a set of two simplex nozzles. The nozzle parameters are set to make the spray cones intersect each other at a quite short distance from the orifice discharge. The main channel is a swirl-type simplex nozzle. The pilot nozzle is inside the gas vortex of the r_{vort} radius formed by the main channel. The outer radius of the pilot nozzle is equal to r_{outer}, which is greater than the inner radius for a wall thickness (0.5-0.8 mm).

5.6 Some aspects of the duplex fuel nozzle

The analysis of the duplex fuel nozzle is very similar to the simplex nozzle analysis. Pilot and main channels are analyzed separately. Each channel is analyzed in the same manner to the simplex fuel nozzle. The fluid motion inside the fuel nozzle is presented in Fig. 5.9. The analysis order is similar to the considered above.

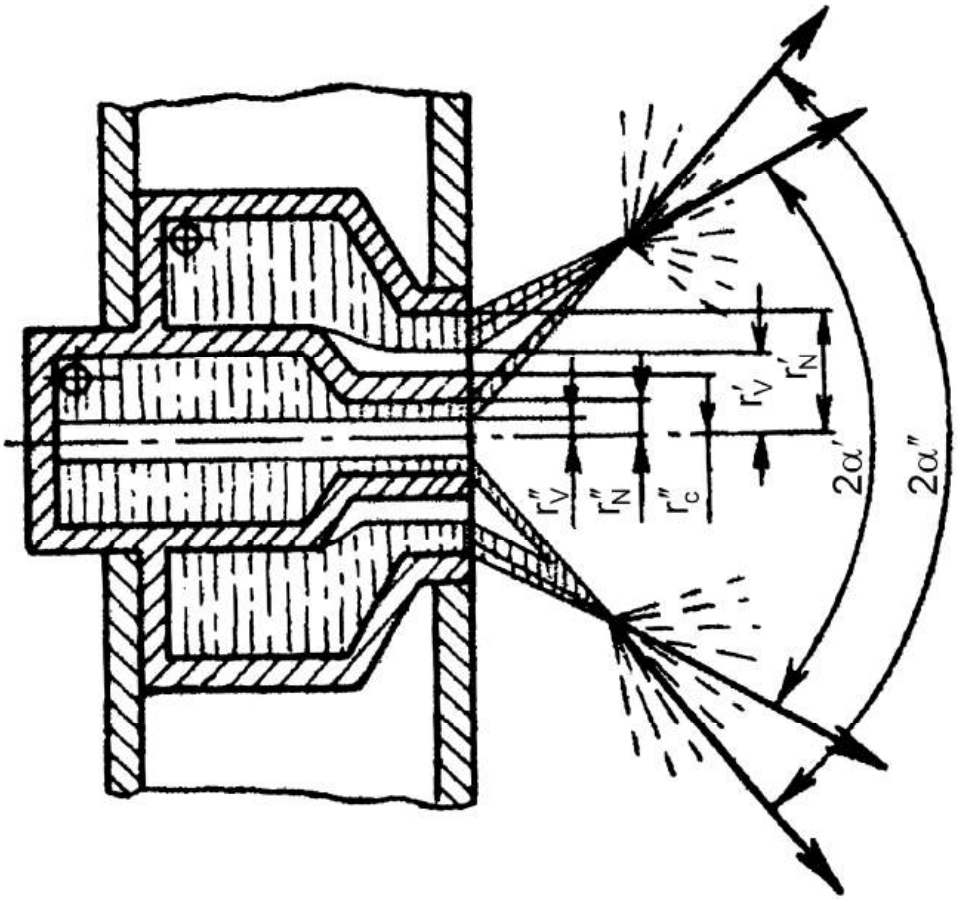

Fig. 5.9 – Duplex fuel nozzle

The initial data must be chosen to provide the geometrical composite parameter of the pilot channel being higher than that of the main channel $A'' > A'$. If the requirement is met, then the spray angle of the pilot channel is bigger than that of the main channel $(2\alpha'' > 2\alpha')$. This approach to the design provides better fuel atomization thanks to the fluid from the pilot channel intersection with the flow from the main channel.

There is another important aspect of the duplex nozzle analysis. The vortex radius of the main channel r_V' must be greater than the outer radius of the nozzle casing of the pilot channel r_c'', i. e.

$$r_V' > r_{cl}''.$$

If $r_V' \le r_{cl}''$ then the casing of the pilot channel blocks the portion of atomization volume of the main nozzle.

The outer radius of the orifice casing of the pilot channel can be calculated as

$$r''_{cl} = r''_N + \delta'',$$

where r''_N is the radius of the pilot channel orifice;

δ'' is a width of the orifice casing of the pilot channel (0.5…0.8 mm).

The vortex radius of the main channel is evaluated as

$$r'_{vort} = r'_N \sqrt{1 - \varphi'},$$

where φ' is a coefficient of “real” (not blocked) atomization volume of the main nozzle.

The coefficient φ' is determined from the graph (fig. 5.8) according to the known geometrical composite parameter of the main channel A'. If the condition $r'_{vort} > r''_{casing\ I}$ is not met then the fuel nozzle must be redesigned.

5.7 Fuel atomization by the fuel nozzles

The atomization of the fuel ejected by the fuel nozzle plays a key role in the combustion.

The fuel atomization can be considered as two consecutive processes. First, the fuel streams or vortex sheet, which is ejected through the fuel nozzle are split into the big droplets. The big droplets are next split into fine droplets (secondary atomization). Both processes are caused by the internal and external forces acting the droplets.

The external forces include the interaction force. It appears as a result of the droplet interaction with the environment. The interaction force is proportional to the squared relative speed of the fluid, an environment density and the squared droplet diameter. The external forces also include the force appearing at the mutual collision of the streams or droplets, or when the droplets strike the obstacle. An inertia, molecular forces and a turbulent friction are the internal forces.

The inertia appears because the fluid moves in the nozzle channels. It is proportional to the fluid density, its squared absolute velocity and squared characteristic size (e.g. diameter). Same to the external forces, the internal ones catalyze the atomization. The available turbulence also stimulates the atomization.

The internal molecular forces include a viscosity force originating between the fluid layers and a surface tension at the margin between the liquid and the gas. The viscosity force hampers the stream atomization by reducing the stream turbulence and absorbing the energy of the moving fluid. Surface tension intends to minimize the surface of the droplet volume, thereby hampering the stream atomization. The molecular forces become less intense at the high temperatures. The turbulence rate depends on a natural turbulence, the fuel nozzle design (disturbances at the fuel nozzle inlet, the channel surface roughness, etc.) and some other factors.

When the fluid experiences the internal and external forces, then the surface disturbances appear making the streams fall into the droplets. This process is schematically presented in Fig. 5.10, a, b. First, the continuous stream leaving the nozzle twists (see Fig. 5.10, a). Then nodes and bridges appear. Finally, the stream is demolished to the droplets.

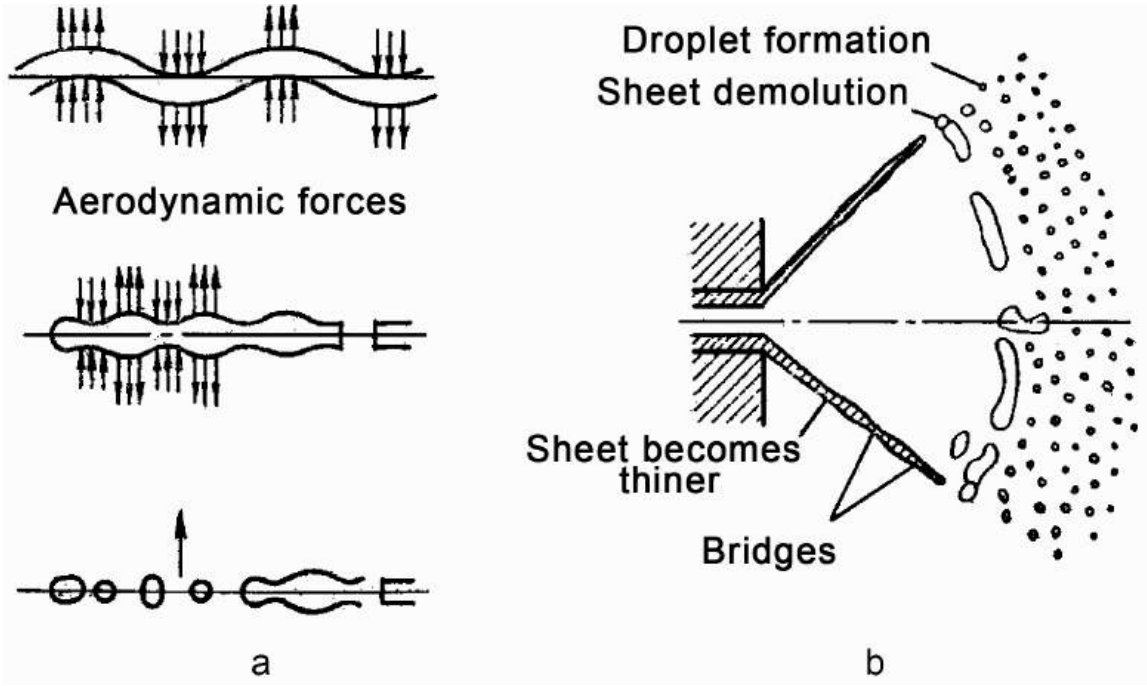

Fig. 5.10 – The continuous stream atomization in the spray nozzle (a) and the swirl nozzle (b)

The fuel atomization by the swirl nozzle corresponds to the engine operational mode (see Fig. 5.10, b), when the ejection speed is high and the fluid turbulence is intense. When the ejection speed is low and the turbulence is of the low intensity (e. g. a throttling mode), then the fluid leaving the swirl nozzle may remain continuous. The predominant surface tension at some distance from the orifice pulls the sheet together in a spiral wisp. Next, the

pressure drop increases, making the internal forces, the inertia and the external force increase too. These forces cause the hollow cone formation. It is next demolished at some distance from the fuel nozzle. It has been experimentally proved that the nature of the fuel ejection from the fuel nozzle largely depends on the pressure drop. When pressure drop is low, then the fuel flows out of the nozzle in the form of the unstable and disordered flow of the droplets. If the fuel pressure at the orifice discharge increases, then it forms there a cone near the orifice. It is bubbled because of the surface tension. At the further increase of the discharge pressure, the inertia prevails over the surface tension, and the bubble discloses taking the form of a tulip with ragged edges. The sheet decays into the relatively large droplets at the tulip`s edges. Then the curved surface of the cone is flatten to form of a conical shape vortex sheet. The shroud is thinned at the distance from the nozzle discharge orifice. It becomes unstable and breaks up into trickles, and then – into drops, to form a uniform hollow spray cone (Fig. 5.11).

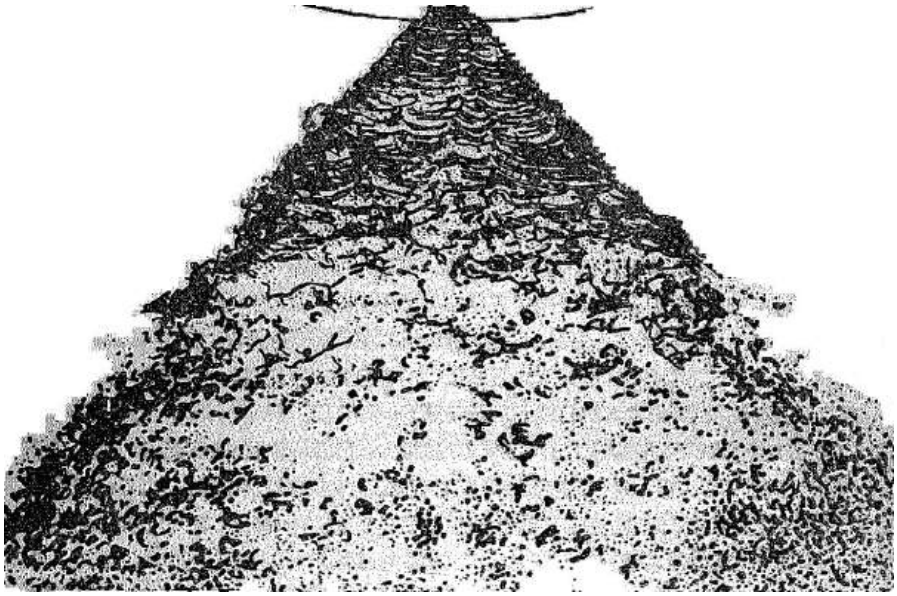

Fig. 5.11 – Photo of a spray torch by the swirl nozzle

Parameters to characterize the atomization quality are a fineness, a homogeneity, a spray cone shape and its range. The fineness is usually characterized by the droplet size, formed after the trickle break up. The homogeneity of the vortex sheet is determined by the droplet size variation range. The smaller the difference between the maximum and minimum diameters of the atomized fuel droplets is, the greater the uniformity is. To assess the fineness and the homogeneity of the spray, you will need to know the fluid distribution, the droplet size and the fluid spray spectrum. The droplet

sizes are used to calculate the evaporation rate, to analyze the droplet motion, to determine the mixing conditions and the qualitatively assess the operation of different elements of the mixing system.

The spray cone spectrum is obtained experimentally. The experimental results are represented in a graph format; the horizontal axis represents the droplet diameter and the vertical axis – the relative mass of the droplets, which diameters are less than the current diameter on the horizontal axis. Such graph is shown in fig. 5.12.

The atomization fineness is characterized by an average droplet size. Different researchers intend different meaning to the average droplet size.

Engineers often use the so-called median diameter, which is determined from the condition that the relative mass of the droplet with a diameter less than or equal to the median one, is 0.5 (see Fig. 5.12). The median diameter of the droplet d_m is usually within the range of 25-250 μm (swirl nozzles), 200-500 μm (spray nozzles). The median diameter of the ejected by nozzle (A = const) droplet significantly depends on the pressure drop and the fluid viscosity. The pressure drop determines the speed at the orifice discharge.

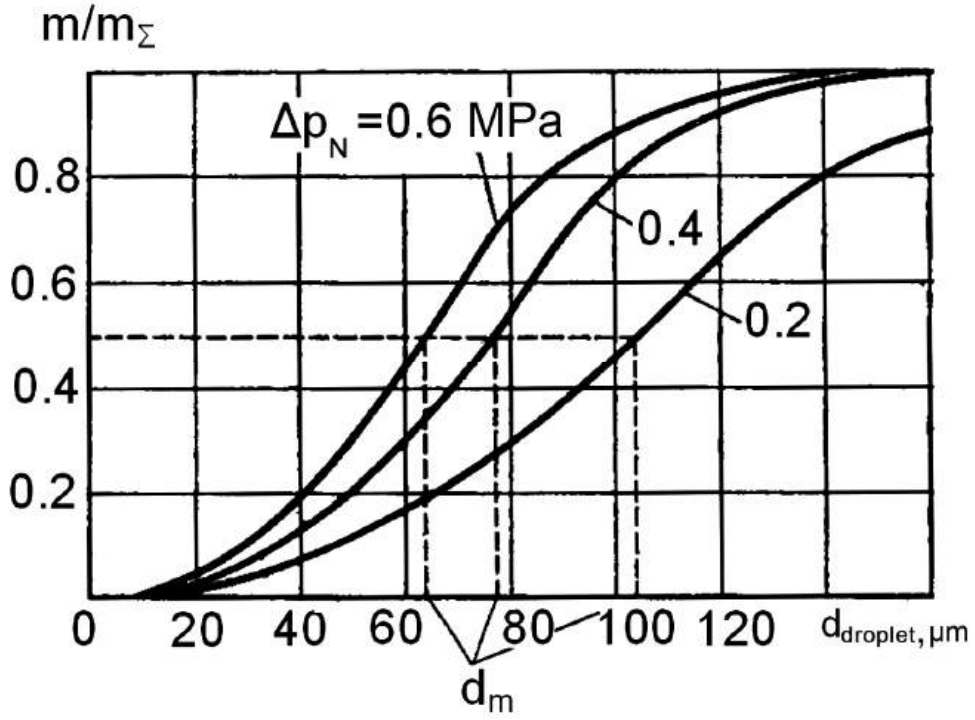

Fig. 5.12 – Mass curves of the liquid distribution of a swirl fuel nozzle

The effect of the pressure drop on the median droplet diameter is shown in Fig. 5.12. The median diameter decreases with the increase of the pressure drop (at first – quickly, then – slowly). The atomization of the viscose fluid is

less fine at the same pressure drop. The droplets of the fluid ejected into the dense environment have less mean diameter. Such parameters of the atomization as a spray cone shape and its range are associated with the fineness and the homogeneity. Thus, the desire to obtain a great spray cone angle thanks to the changes made in the structural parameters reduces μ_N. This means that the sheet leaving the orifice will become less thick. This gives the finer atomization. The spray range becomes low both because of the big spray cone angle and because of an increased surface of the spray cone. The resistance of the environment is proportional to the spray cone surface. It also affects the spray range.

The important characteristics of the atomization process are a fluid distribution on the radius and along the circumference of the fuel cone (Fig. 5.13, 5.14). In most cases, the nozzles do not provide a uniform distribution of the fuel in the cone.

The Fig. 5.13 contains the diagrams of the flow rate to an area on the radius of the fuel cone for the two distances from the orifice discharge.

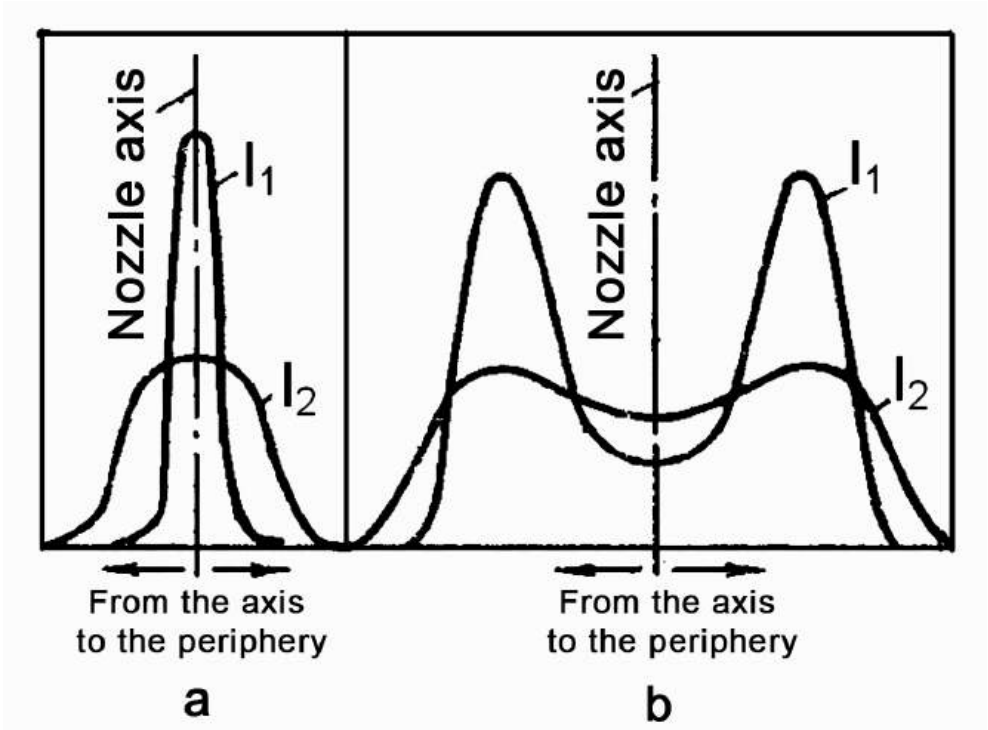

Fig. 5.13 – The diagram of the fuel flow rate to an area on the radius of the fuel cone dG_f/dF from two distances from the orifice discharge $(l_2 > l_1)$:
a – spray nozzle; b – swirl nozzle

Typically, the spray nozzle (see Fig. 5.13, a) has the maximum flow rate near the axis. Opposite to the spray nozzle, the swirl one (see Fig. 5.13, b) has

peaks distant from the axis and minimum values near the axis. The distribution is caused to the spray cone form of the corresponding nozzles. The fuel flow rate to an area diagrams become smoother at some distance from the orifice.

The non-uniform circumferential distribution (Fig. 5.14) mainly depends on the nozzle construction, for example, on the disclosure of the nozzle R_{in}/r_N and the number of the input channels.

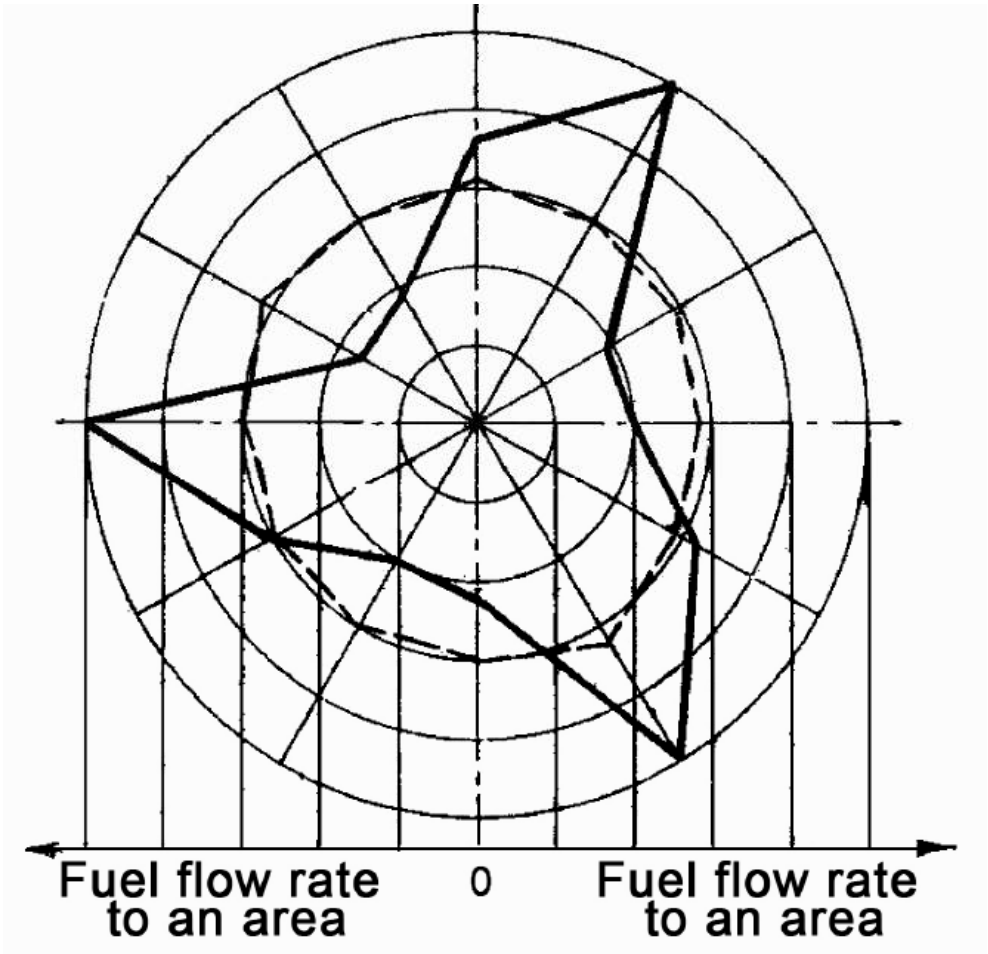

Fig. 5.14 – The fuel flow rate to an area diagrams of the swirl nozzle; the number of the input channels is 3:

—— R_{in}/r_N = 0,83, - - - - R_{in}/r_N = 1,62

BIBLIOGRAPHY

1. Авиационные силовые установки. Системы и устройства [Текст] / Н. Т. Домотенко, А. С. Кравец, Г. А. Никитин и др. – М. : Транспорт, 1976. – 312 с.

2. Системы авиационных двигателей [Текст] : учеб. пособие / С. В. Безуглый, С. В. Епифанов, А. И. Скрипка, Б. Я. Хмелик. – Х. : Нац. аэрокосм. ун-т «Харьк. авиац. ин-т», 2008. – 74 с.

3. Проектирование систем силовых установок самолетов [Текст] : консп. лекций / С. В. Епифанов, В. Д. Пехтерев, А. И. Рыженко и др. – Х. : Нац. аэрокосм. ун-т им. Н. Е. Жуковского «Харьк. авиац. ин-т», 2011. – 512 с.

4. Скубачевский, Г. С. Авиационные газотурбинные двигатели. Конструкция и расчет деталей [Текст] / Г. С. Скубачевский. – М. : Машиностроение, 1981. – 552 с.

5. Агрегаты систем авиационных двигателей [Текст] : учеб. пособие / С. В. Безуглый, А. И. Скрипка, Б. Г. Нехорошев, Б. Я. Хмелик. – Х. : Нац. аэрокосм. ун-т им. Н. Е. Жуковского «Харьк. авиац. ин-т», 2007. - 90 с.

6. Безуглый, С. В. Конструкция топливных форсунок авиационных двигателей [Текст] : учеб. пособие / С. В. Безуглый, В. Е. Костюк, И. Ф. Кравченко. – Х. : Нац. аэрокосм. ун-т им. Н. Е. Жуковского «Харьк. авиац. ин-т», 2008. - 49 с.

7. Безуглый, С. В. Плунжерные насосы. Конструкция и проектирование [Текст] : учеб. пособие / С. В. Безуглый, А. И. Скрипка. - Х. : Нац. аэрокосм. ун-т им. Н. Е. Жуковского «Харьк. авиац. ин-т», 2010. – 80 с.

8. Безуглый, С. В. Центробежные насосы авиационных двигателей [Текст] : учеб. пособие / С. В. Безуглый. – Х. : Нац. аэрокосм. ун-т им. Н. Е. Жуковского «Харьк. авиац. ин-т», 2006. - 27 с.

9. Безуглый, С. В. Шестеренные насосы. Конструкция и проектирование [Текст] : учеб. пособие / С. В. Безуглый, А. И. Гаркуша, В. С. Чигрин. – Х. : Нац. аэрокосм. ун-т им. Н. Е. Жуковского «Харьк. авиац. ин-т», 2009. – 48 с.

10. Bezuglyi, S. Components of Aircraft Power Plant Systems [Text]: lect. summary / S. Bezuglyi, F. Sirenko, M. Shevchenko. – Kharkov: National Aerospace University «Kharkov Aviation Institute», 2016. – 100 p.

Навчальне видання

Безуглий Сергій Володимирович
Сіренко Фелікс Феліксович
Шевченко Максим Володимирович

АГРЕГАТИ СИСТЕМ АВІАЦІЙНИХ СИЛОВИХ УСТАНОВОК

(Англійською мовою)

Редактор Н. В. Котляр
Технічний редактор Л. О. Кузьменко

Зв. план, 2016
Підписано до друку 24.10.2016
Формат 60х84 1/16. Папір офс. № 2. Офс. друк
Ум. друк. арк. 5,8. Обл.-вид. арк. 6,5. Наклад 70 пр. Замовлення 268.
Ціна вільна

Видавець і виготовлювач
Національний аерокосмічний університет ім. М. Є. Жуковського
«Харківський авіаційний інститут»
61070, Харків-70, вул. Чкалова,17
http://www.khai.edu
Видавничий центр «ХАІ»
61070, Харків-70, вул. Чкалова, 17
izdat@khai.edu

Свідоцтво про внесення суб'єкта видавничої справи
до Державного реєстру видавців, виготовлювачів і розповсюджувачів
видавничої продукції сер. ДК № 391 від 30.03.2001